THE UNIVERSITY OF CHICAGO

THE DYNAMICS OF RAPID ADAPTATION TO OCEAN ACIDIFICATION IN THE MEDITERRANEAN MUSSEL

A DISSERTATION SUBMITTED TO
THE FACULTY OF THE DIVISION OF THE BIOLOGICAL SCIENCES
AND THE PRITZKER SCHOOL OF MEDICINE
IN CANDIDACY FOR THE DEGREE OF
DOCTOR OF PHILOSOPHY

DEPARTMENT OF ECOLOGY AND EVOLUTION

BY
MARK C. BITTER

CHICAGO, ILLINOIS
AUGUST 2020

DEDICATION

For my Mom and Dad, who have provided unwavering support, guidance, and love during my time on this Earth.

TABLE OF CONTENTS

LIST OF FIGURES

LIST OF TABLES

ACKNOWLEDGMENTS

Throughout the completion of this thesis I received extensive intellectual, logistical, financial, and emotional support for which I am especially grateful.

I would first like to thank my thesis committee – Cathy Pfister, Marty Kreitman, Marcus Kronforst, John Novembre, and Tim Wootton. I found the unique combination of expertise within my committee a critical attribute to the design, implementation, and effective completion of my thesis research. I would particularly like to acknowledge my advisor, Cathy Pfister, for extensive academic and professional guidance throughout this process, her enthusiastic support of my ambitious projects, and the model she sets as an academic and community member.

My thesis research was done in collaboration with an exceptional group of scientists, each of whom I am privileged and honored to have worked with. I thank Lydia Kapsenberg for her critical contributions to every aspect of my work, from proposal writing, to (very) long hours in the lab, to generating papers I am incredibly proud of. Jean-Pierre Gattuso generously provided the laboratory setting for my experiments, and provided substantial guidance throughout project planning, experimentation, and manuscript preparation. Angelica Miglioli and Samir Alluoiane provided extensive logistical support during each of the overly ambitious experiments I designed, and the projects would not have been possible without them. I would also like to thank Graeme Bell and Soo Young Park for their critical assistance with the quantitative PCR analyses presented in the final chapter of this thesis.

The community of scientists at the University of Chicago provided an incredibly fruitful environment for the development of my ideas. I value the numerous conversations regarding the conceptual, statistical, and computational components of my work with Trevor Price, Joe Marcus, Arjun Biddanda, Dan Rice, and Nick Van Kurren. Additionally, I would like to acknowledge current and past members of the Pfister and Wootton labs – John Park, Katherine Silliman, Brooke Weigel, Natasha Ershova, Dan Smith, Khashiff Miranda, Amy Henry, Simon Lax, Nicole Bitler, Sara Jackrell, Orissa Moulton, and Courtney Stepian. These sup-

portive and intelligent individuals provided conversation and advise during numerous lab meetings and field seasons.

My fellowship support was provided by the NSF Graduate Research Fellowship Program (Grant No. 1746045) and the Department of Education (Grant No. P200A150101). Research funding was provided by the France and Chicago Collaborating in the Sciences (FAACTS) Program, NSF Ocean Sciences Grant (No. 1521597) to Lydia Kapsenberg, The University of Chicago Hinds Fund, and The University of Chicago Department of Ecology and Evolution.

Finally, I sincerely thank my family and friends for the overwhelming love and support they provided throughout the completion of this thesis.

ABSTRACT

Global climate change has intensified the need to assess if, and how, natural populations adapt to abrupt shifts in their environment. While the tempo of adaptation in natural systems has been the subject of historical debate, recent studies using genome-wide sequencing approaches have indicated that evolution may occur more rapidly than previously anticipated. Such studies, however, have largely observed these processes in the context of model systems, and the extent to which these patterns will hold in ecologically-relevant species subject to the dramatic environmental perturbations associated with global change is unclear. Accordingly, this thesis investigates the capacity for, and mechanisms by which, the Mediterranean mussel, *Mytilus galloprovincialis*, may rapidly adapt to expected declines in global seawater pH. Reductions in seawater pH constitute a global change stressor impacting marine species globally, with anticipated impacts altering the structure and services of numerous ecological communities. Due to its experimental tractability, as well as its ecological and economic importance, *M. galloprovincialis* has become a model-species for exploring the physiological and morphological impacts of low pH seawater. Yet, the extent to which evolution may offset observed phenotypic consequences is unknown. To address this knowledge gap, the present thesis explores the following: (i) the processes shaping and maintaining variation in low pH tolerance across the native range of *M. galloprovincialis*; (ii) the extent to which the standing variation within natural populations can facilitate the magnitude of evolution necessary for persistence under global change conditions; and (iii) the molecular basis of low pH adaptation in marine bivalves and beyond. The presented results elucidate how contemporary gradients in pH variability shape distinct patterns of low pH plasticity across natural populations. Furthermore, my findings demonstrate that the standing variation within natural populations is sufficient for rapid adaptation to even extreme reductions in seawater pH. Lastly, I provide mechanistic links between the molecular mechanisms influenced by shifts in the external seawater pH environment and fitness-related abnormalities observed in *M. galloprovincialis*, a finding that likely explains observed low pH sensitivity

across a broad range of marine metazoans. This thesis lends to our conceptual understanding regarding the dynamics of rapid adaptation in natural populations, while explicitly informing the management of an ecologically and economically important marine species as global change progresses.

INTRODUCTION

The current rate of anthropogenic greenhouse gas emissions is without precedent in human history. Release of carbon dioxide (CO_2) via the burning of fossil fuels and industrial processes contribute approximately 78% to these emissions, and roughly half of all CO_2 emissions since the pre-industrial era have occurred in the last 40 years (Edenhofer *et al.*, 2014). As a result, Earth's climate system is undergoing rapid and complex changes. For example, terrestrial ecosystems are experiencing atmospheric warming and dynamics shifts in precipitation patterns, while oceanic habitats are becoming warmer, deoxygenated, and acidified (Edenhofer *et al.*, 2014). The rapid rate of environmental change is expected to induce the emergence of novel climatic conditions throughout Earth's terrestrial and marine surfaces by the end of this century, posing extensive threats to the persistence of species globally (Williams *et al.*, 2007). A fundamental challenge for scientists is to forecast how species will respond to these unprecedented shifts in the environment as a means to both predict the structure and function of natural communities as global change progresses, and effectively mange the myriad services these systems provide.

Broadly, global change is expected to elicit three fundamental responses from natural populations: (1) migration to regions of more favorable environmental conditions, (2) adaptation to the novel environmental conditions, or (3) extinction. While a global redistribution of species in response to warming has already been observed in a number of both terrestrial and marine taxa (Sunday *et al.* 2012), such patterns may not hold for all global change stressors and taxa. Specifically, a simple poleward expansion will not be effective for stressors lacking latiudinal gradients. Furthermore, the life history of some species may dramatically reduce their ability to disperse at a rate sufficient to track favorable environments (Fig. 1.2). In cases in which migration is impeded, species persistence will hinge upon adaptation to the rapidly changing environment (Hoffmann and Sgrò, 2011).

The extent to which genetic adaptation may allow species to avoid extinction as a result of global change has received extensive debate in recent decades. Long-standing population

genetic theory posits that evolution via natural selection is most effective when it occurs gradually, on the timescale of millennia (Bell, 2010). This dogma, however, has become fundamentally challenged by recent insights from next-generation sequencing approaches. Specifically, studies that have combined natural population censuses with genome-wide scans of variation have demonstrated that evolution can indeed occur rapidly, and on ecological timescales (Bergland *et al.*, 2014; Campbell-Staton *et al.*, 2017). Such rapid evolutionary processes predominately occur via the fixation of genetic variation already maintained within populations, thus forgoing the waiting time associated with the rise and fixation of an adaptive *de novo* mutation (Messer *et al.*, 2016). While this work has demonstrated that the tempo of adaptation via standing variation is likely sufficient to keep pace with environmental change, a fundamental question remains – To what extent can the standing variation within natural populations facilitate the magnitude of evolution necessary for species persistence under the conditions expected as a result of global change? The present thesis addresses this fundamental question within the context of global declines in seawater pH and an ecologically an economically important marine bivalve.

The world's oceans sequester approximately one third of all anthropogenic CO_2 emissions, driving a global decline in seawater pH termed ocean acidification. While ocean pH has varied throughout Earth's history, the current rate of pH decline is unprecedented in the past 55 million years. Global-mean seawater pH has dropped 0.1 units (log-scale) since the pre-industrial era, and is expected to drop an additional 0.3-0.4 units by the end of the century (Hönisch *et al.*, 2012). Lab-based studies have revealed largely deleterious effects of expected pH conditions on a range of marine taxa (Kroeker *et al.*, 2013). These effects are most pronounced in shell forming species, such as corals, urchins, and mussels, as ocean acidification induces changes to seawater carbonate chemistry that impede the formation of calcium carbonate exoskeletons (Kroeker *et al.*, 2013). While the phenotypic consequences of ocean acidification are now well characterized, the extent to which evolution will offset these consequences, mitigating expected alterations to global marine community structure

and function, remains largely unresolved (Sunday *et al.*, 2014).

The Mediterranean mussel, *Mytilus galloprovincialis*, has been the subject of extensive research into the physiological and morphological impacts of ocean acidification. These efforts are in large part motivated by the species' ecological importance in shallow coastal habitats, as well as its economic value as a globally harvested aquaculture species (Gazeau *et al.*, 2014a). Reductions in seawater pH affect *M. galloprovincialis* across all life-history stages, though these effects are most pronounced during larval growth and development. Specifically, ocean acidification conditions reduce larval shell size and induce a series of morphological abnormalities that become lethal during the shell-growing period (Kapsenberg *et al.*, 2018; Kurihara *et al.*, 2008). In this thesis, I assess the potential for, and mechanisms by which, *M. galloprovincialis* may adapt to ocean acidification.

In response to a shift in the environment, an individual genotype may alter its physiology, morphology, or behavior as a compensatory mechanism, a phenomenon termed phenotypic plasticity (Scheiner, 1993). Phenotypic plasticity is expected to serve as the initial response of species faced with environmental change, while variation in the plastic response will likely be a fundamental driver of evolutionary responses to global change (DeBiasse and Kelly, 2016; Whitehead and Crawford, 2006). Chapter 1 of this thesis explores how contemporary gradients in seawater pH across the native range of *M. galloprovincialis* shape population-level variation in low pH plasticity. Specifically, I combined high-resolution oceanographic monitoring with a laboratory-based experiment to link differences in habitat pH fluctuation dynamics to gene expression plasticity in two populations of *M. galloprovincialis*. Through this, I demonstrate how spatiotemporal gradients in pH drive the divergence of low pH plasticity across populations, a mechanism maintaining adaptive variation that could drive evolution to ocean acidification. Additionally, I use these results to confirm recent theoretical findings by demonstrating a depression of phenotypic plasticity in environments exhibiting high amplitude, and low predictability, environmental fluctuations.

In Chapter 2 I investigate the extent to which the variation currently present within *M.*

galloprovincialis populations will facilitate rapid adaptation to the extreme low pH conditions expected as a result of ocean acidification. To accomplish this, I conducted an extensive laboratory-based experiment in which I tracked changes in phenotypic and genetic variation of a diverse larval population throughout development in an ambient and extreme low pH treatment. Phenotypic data demonstrated that low pH-induced declines in shell-size are, in part, compensated for by natural selection during the shell-growing phase. Genomic data indicated that natural populations currently harbor substantial variation to adapt to ocean acidification, and that genotypes exhibiting the fastest shell growth in ambient conditions are genetically distinct from the fastest growers in low pH conditions. Ultimately, the data presented in this chapter call for maintaining variation within natural populations as an effective means to bolster species resilience to future global change.

Finally, Chapter 3 aims to develop a mechanistic understanding of the molecular basis of low pH adaptation. By leveraging data generated in Chapter 2 with a novel transcriptomics and real-time quantitative PCR analysis, I identify candidate genes involved in the *M. galloprovincialis* low pH response. I then assess the capacity for these candidates to evolve using a combination of selection coefficient computation and the identification of genotype-environment interactions. Finally, I provide direct links between the core molecular pathways in which these candidate genes operate and the observed morphological abnormalities driving *M. galloprovincialis* mortality in low pH seawater. Through this, I demonstrate the importance of calcification-independent processes in low pH adaptation, thus helping to explain pH sensitivity across a broad range of marine metazoans.

In concert, the chapters of this thesis elucidate the processes producing and maintaining environmentally relevant variation within natural populations, and how this variation works to fuel rapid evolution in response to abrupt shifts in the environment. The focus of this work on a foundational marine species facilitates the direct application of these results to the sustainable harvesting of coastal marine species as global change progresses.

CHAPTER 1

HABITAT PH FLUCTUATION DYNAMICS SHAPE THE PLASTIC RESPONSE TO OCEAN ACIDIFICATION

1.1 Abstract

Phenotypic plasticity is expected to facilitate the persistence of natural populations as global change progresses. The attributes of fluctuating environments that favor the evolution of plasticity have received extensive theoretical investigation, though empirical validation of these findings is still in its infancy. Here, we combine high-resolution environmental data with a laboratory-based experiment to explore the influence of habitat pH fluctuation dynamics on the plasticity of gene expression in two populations of the Mediterranean mussel, *Mytilus galloprovincialis*. We linked differences in the magnitude and predictability of pH fluctuations in two habitats to population-specific gene expression profiles in an ambient and stressful pH treatment. The results presented demonstrate population-based differentiation in gene expression plasticity, whereby mussels native to a highly variable, and less predictable, habitat displayed reduced phenotypic plasticity between pH treatments, via an elevation of baseline expression at stress response loci in the benign environment. This work validates recent theoretical findings on evolution in fluctuating environments using an ecologically important marine bivalve, and further suggests that populations inhabiting regions exposed to frequent, and unpredictable, stressful conditions may exhibit reduced plasticity as global change progresses.

1.2 Introduction

The ubiquity of environmental variability has motivated decades of theoretical and empirical work aimed at determining the mechanisms facilitating the persistence of natural populations in fluctuating environments (Lewontin and Cohen, 1969). One such mechanism is pheno-

typic plasticity – generally defined as the ability of a single genotype to alter its phenotype in response to a change in environmental conditions (Scheiner, 1993). Early theoretical models primarily focused on how the relative rates of change in the environment and strength of stabilizing selection shape plasticity, broadly demonstrating that highly heterogeneous environments over space and/or time select for the evolution of plastic phenotypes (Gomulkiewicz and Kirkpatrick, 1992; Scheiner, 1993; Via and Lande, 1985). Empirical work has provided general support for theoretical expectations, identifying elevated plasticity within populations inhabiting environments that are more variable relative to a reference (Kingsolver and Wiernasz 1991; Kingsolver and Huey 1998; Schaum *et al.* 2013; Kenkel and Matz 2016). However, specific attributes of environmental variability that have been shown in theory to dictate whether or not plasticity is adaptive remain untested experimentally. Such validation is of increasing concern as global change progresses and plasticity, if present, may serve as the initial response of populations to the associated directional shifts in the environment (Hoffmann and Sgrò, 2011; Seebacher *et al.*, 2015).

One attribute of variable environments that warrants empirical investigation is the predictability of fluctuating selection pressures, and how it affects the evolution of phenotypic plasticity (Scheiner 1993; Bonamour *et al.* 2019). Predictability may arise directly via a highly autocorrelated environment, or indirectly through habitat cues in which a second environmental variable correlates strongly with the agent of selection (Reed *et al.*, 2010). For example, the predictable aerial emergence in coastal marine habitats due to ebbing tides are associated with a pre-emptive shift in thermal physiology to cope with anticipated changes in temperature (Connor and Gracey, 2011). Recent theoretical models have shown the dramatic costs associated with switching phenotypes in response to an unreliable cue, and the tendency of highly unpredictable environments to depress plasticity and ultimately favor a fixed-phenotypic strategy, such as bet-hedging (Bonamour Suzanne *et al.*, 2019; Botero *et al.*, 2015; DeWitt *et al.*, 1998; Moran, 1992; Reed *et al.*, 2010; Scheiner and Holt, 2012; Tufto, 2015, 2000). Though predictability is logistically challenging to manipulate in the laboratory,

one recent study used experimental evolution of an RNA virus to demonstrate that less autocorrelated environments favored increased stress tolerance (Wieczynski *et al.*, 2018). Such lab-based results must be interpreted with caution, however, as experimental evolutionary approaches may not replicate patterns of plasticity observed in nature (Kellermann *et al.*, 2015). Accordingly, the present study leveraged a natural gradient in fluctuating selection pressures to test the influence of fluctuation magnitude and predictability on phenotypic plasticity in an ecologically important marine bivalve subject to a global change stressor.

The global decline in seawater pH, termed ocean acidification, is a consequence of increasing atmospheric carbon dioxide emissions and poses extensive threats to marine systems. Laboratory-based studies assessing its expected biological effects have mounted over the past two decades, demonstrating a range of largely deleterious developmental, physiological, and morphological responses across taxa (Kroeker *et al.*, 2013). While the majority of such studies have imposed static pH treatments in order to quantify these effects, oceanographic monitoring approaches have demonstrated the dynamic nature of contemporary pH fluctuations across marine habitats (Wootton, Pfister, and Forester 2008; Hofmann *et al.* 2011; Wootton and Pfister 2012; Kapsenberg and Hofmann 2016). This variability is pronounced in coastal environments, where local abiotic (e.g. upwelling) and biotic (e.g. photosynthesis and respiration) processes can drive substantial differences in pH regimes across scales of meters to hundreds of kilometers. Though regional differences in low pH exposure have been shown to broadly drive differentiation in pH tolerance across populations for some marine species (Hofmann *et al.* 2014; Vargas *et al.* 2017; Kapsenberg *et al.* 2017a; Kapsenberg and Cyronak 2019), these studies have not explicitly linked various attributes of pH variability to observed patterns of divergence.

A coastal species that has both ecological and economic value and is sensitive to ocean acidification is the Mediterranean mussel, *Mytilus galloprovincialis*. Reductions in seawater pH negatively impact *M. galloprovincialis* across life-history stages (Gazeau *et al.* 2014; Kapsenberg *et al.* 2018), though recent evidence suggests that natural populations harbor

substantial genetic variation to adapt to ocean acidification (Bitter *et al.*, 2019). Along the southern coast of France, populations of *M. galloprovincialis* are distributed throughout habitats that vary appreciably in the dynamics of fluctuating selection pressures. Specifically, shallow water lagoons in the region have limited mixing with the open Mediterranean Sea, increasing the influence of localized atmospheric and biological processes on the water bodies and driving dramatic fluctuations in abiotic conditions (Plus *et al.*, 2003). In contrast, populations persisting along the open coastline are exposed to water masses that are more reflective of the greater Mediterranean Sea, and therefore experience less dramatic environmental variability. While patterns of oceanic circulation (Berline *et al.*, 2014) and preliminary population genetic analysis (Quesada *et al.*, 1995) suggest high-levels of genetic connectivity between coastal and lagoon populations, evidence of local adaptation within high gene flow marine systems has recently accrued (Sanford and Kelly, 2011). Accordingly, we leveraged the high variability of the lagoons and relative stability in the open coastal habitats to explicitly test theoretical predictions regarding how exposure to, and predictability of, stressful pH conditions influence plasticity. We utilized transcriptome-wide changes in gene expression as the metric of plasticity, as shifts in gene expression are a fundamental cellular response of an organism to a change in its environment (López-Maury *et al.*, 2008), and variation in gene regulation is an heritable trait driving evolution across populations and species (Whitehead and Crawford, 2006). Additionally, assays of gene expression may identify shifts in organismal physiology that are undetectable via the examination of macroscopic traits, and have become increasingly utilized to characterize the physiological consequences of expected climate change conditions (DeBiasse and Kelly, 2015).

The aims of this study were to: (1) conduct high-frequency oceanographic monitoring of a coastal and lagoon habitat for one year to assess differences in the magnitude and predictability of stressful pH events at each site, (2) assess how observed differences in each habitat's pH fluctuation dynamics impact the gene expression profiles of native *M. galloprovincialis* individuals within in an experimentally-imposed benign and stressful pH treatment, and

(3) determine how the magnitude of pH-stress response, and therefore phenotypic plasticity, varied between a coastal and lagoon population. Our hypotheses are illustrated in Figure 1.1, which depicts patterns of gene expression for each population in a benign and stressful pH treatment as a reaction norm – a commonly used model of phenotypic plasticity in which a genotype's (or population's mean) phenotype is plotted as a function of an environmental gradient. The slope of this relationship provides a proxy for the degree of phenotypic plasticity, and our results are discussed in light of this model (Via and Lande, 1985). We tested the hypothesis that the lagoon population would exhibit elevated expression of stress-response loci in the benign pH treatment, and a reduced magnitude of gene expression change between pH treatments. Our empirical findings support the theoretical expectations illustrated in Figure 1.1, suggesting that population-based differences in phenotypic plasticity are indeed shaped by contemporary gradients in environmental variability.

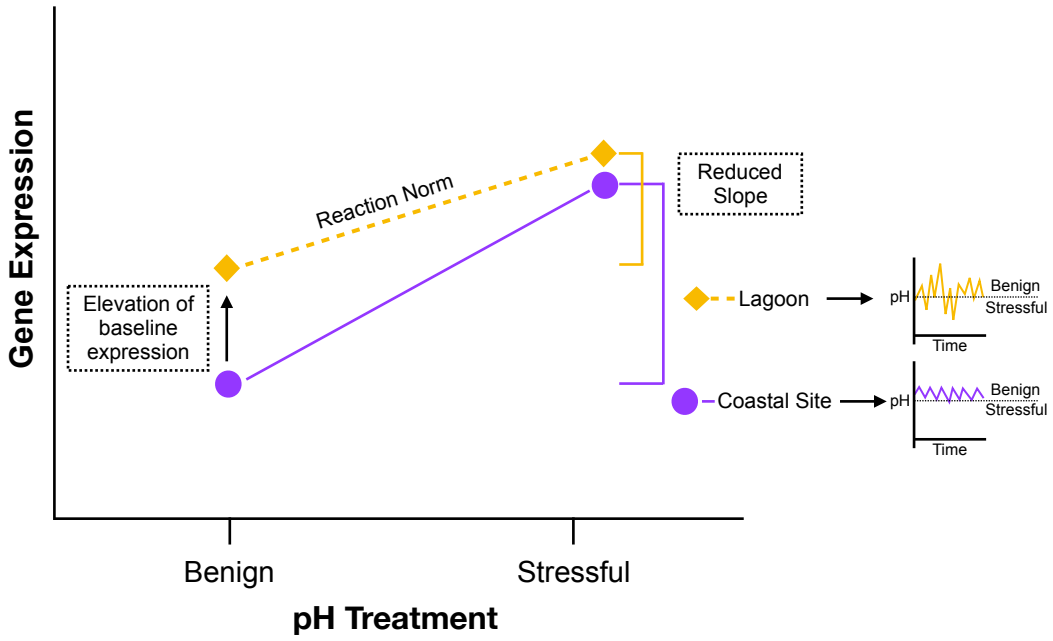

Figure 1.1: Conceptual overview depicting predictions of how environmental fluctuation magnitude and predictability shape patterns of phenotypic plasticity. The gene expression values of the lagoon (orange diamonds) and coastal (purple circles) populations are illustrated in a benign and stressful pH treatment. Lines connecting gene expression values indicate the reaction norm, the slope of which indicates the expected amount of pH-stress plasticity for each population. The lagoon population, which experiences an elevation in the magnitude, and a reduction in the predictability, of pH fluctuations, is expected to exhibit an increase in baseline expression of stress response genes in the benign pH treatment, and a reduced magnitude of gene expression plasticity in response to the stressful treatment. Note that this schematic ignores direction, and simply considers total amount of gene expression change.

1.3 Methods

1.3.1 Study site descriptions and environmental monitoring

The two Mediterranean populations of *M. galloprovincialis* utilized in this study inhabited the Bay of Villefranche-sur-Mer (hereafter referred to as the coastal site, Environment Observable Littoral buoy at 43.682^{o}N, 7.319^{o}E) and the Thau Lagoon (hereafter referred to as the lagoon 43.4158^{o}N, 3.6888^{o}E), locations separated by 300 km of coastline and exposed to unique oceanographic features that influence local environmental exposures. The coastal site is a south-facing inlet with steep bathymetry resulting in steady mixing with the Mediterranean Sea (De Carlo *et al.*, 2013). The lagoon is one of a series of shallow water lagoons along the Southern coast of France, with a mean depth of approximately 4 m and intermittent mixing with the Mediterranean Sea via two narrow channels (Plus *et al.*, 2003).

Autonomous oceanographic monitoring of the coastal site was conducted between September 2016 and August 2017 using SeaFET pH sensors (Martz *et al.*, 2010, 2010) and Seabird Electronic (SBE25) profilers with 60-minute sampling frequencies. Sensors were deployed on a buoy submerged to 2 m in a total water depth of 80 m. Detailed sensor deployment and quality control methodology are reported previously, with an estimated error in pH_T of 0.01 units (Kapsenberg *et al.* 2017b). Monitoring of the lagoon site was conducted between October 2016 and June 2017 using SeaFET pH and SBE37 sensors with twenty-minute sampling frequencies. For pH, SeaFET data were calibrated using SeaFET temperature data (0.004 units pH_T error; Kapsenberg and Hofmann 2016) and multiple field collected pH reference samples per deployment (Bresnahan *et al.*, 2014). Open cell titration was used to determine total alkalinity necessary to calculate *in situ* pH (Dickson *et al.*, 2007). Spectrophotometric measurements of pH samples were performed on discrete samples using m-cresol indicator (Dickson *et al.*, 2007) with an accuracy of 0.006 units pH_T (determined by Kapsenberg *et al.* 2017b). Based on 13 reference samples, spatio-temporal mismatch error of the reference sampling was 0.014 units pH_T (following calculations in Kapsenberg and Hofmann 2016).

The final estimated standard uncertainty of pH data from the lagoon is 0.016 units pH_T. For SBE37, data quality was compared against a calibrated SBE 25+ for temperature and measurements.

Time-series data were compared between sites to determine differences in seawater pH fluctuation magnitude and predictability. Specifically, the hydrogen ion concentration of all pH observations at each site were calculated and used to determine the mean and range of pH values exhibited at the coastal and lagoon sites. Differences in the distribution of pH values observed for each site were compared using a Kolmogorov-Smirnov (KS) test, and differences in the variance of pH at each site were tested using Hartley's maximum F-ratio test (F_{max}) (each performed in R v. 3.6.1).

The predictability of pH fluctuations at each site was assessed using a combination of time-series autocorrelation, spectral, and environmental correlation analyses. The temporal autocorrelation of pH at each site was computed across hourly and daily-lag intervals using the *acf* function in R. For the daily interval, the daily average pH value for each site was used to compute the lag-1 through lag-28 autocorrelations. The hourly and daily intervals provided scales of predictability that are relevant to the study species, and indicated the relative influence of photosynthesis/respiration (24-h) and tidal cycles (14 and 28 d) on pH fluctuation dynamics at each site. Spectral analysis was further used to identify the predominant pH periodicity at each site (*spectrum* function in R). Lastly, differences in cue reliability of pH fluctuations at each site were assessed by computing Pearson's correlation coefficient between pH and temperature across the observation periods (*cor* function in R). pH and temperature can co-vary in coastal marine habitats (Cyronak *et al.*, 2019), and though we lack direct demonstration of coastal species utilizing temperature as a cue for changes in pH, differences in the correlation of these parameters between sites is likely demonstrative of differences in the suite of additional abiotic variables (e.g. oxygen) that may serve as cues for shifts in seawater pH for this species.

1.3.2 Animal collection

Adult *M. galloprovincialis* individuals were collected via SCUBA diving from the coastal site on 14 October 2016. Mussels were collected from a subtidal mooring in 5 m of water, located within 10 m of the oceanographic sensors. Mussels were transported dry (in netted bags) by boat to the Laboratoire d'Océanographie in Villefranche-sur-Mer, France (LOV), where they were kept in aerated flow-through seawater tank at 16^{o}C. Adult *M. galloprovincialis* individuals were collected from the lagoon on 11 October 2016. Mussels were collected by hand from the underside of a floating dock in approximately 0.5 m water within 10 m of oceanographic sensors. Individuals were placed in a cooler chilled with ice and transported dry by motor vehicle to LOV, where they were stored in a flow-through seawater container at 16^{o}C. Common garden conditioning (described below) began 3 and 7 d after the coastal and lagoon population collections, respectively.

1.3.3 Experimental design

The experiment consisted of two phases: (1) an initial common garden conditioning of 6 weeks, followed by (2) a pH treatment exposure of 5 d, after which mussels gill tissue was sampled for transcriptomic analysis. The common garden conditioning aimed to remove the effects of recent environmental history on individual gene expression profiles, and the subsequent 5-day exposure to stable pH treatments was utilized to elicit an acclimatized transcriptomic response to the experimental benign and stressful pH treatments (Thompson *et al.*, 2012). The benign pH treatment corresponded to the average condition observed at both study sites throughout the oceanographic monitoring period (pH_T = 8.1). The stressful pH treatment (pH_T = 7.7) reflected a value known to induce physiological stress on the species (Kapsenberg *et al.* 2018), and which was occasionally observed at the lagoon, but never at the coastal site (Fig. 1.3C).

For common garden conditioning, fifty adult mussels from each population, ranging in size from 50 to 70 mm, were placed in a single, 43.8 L flow-through seawater tank (flow

rate 7.8 L h^{-1}). To prevent mussels from aggregating and mixing between populations, individuals were kept in 625 cm^2 mesh bags that were spread evenly throughout the tank (5 individuals/bag). The temperature of the common garden was maintained at 16.3 (0.4) ^{o}C. For the first two weeks of conditioning, the mussels were fed 15 mL of Microfeast pz-20 (Salt Creek Inc). During the remainder of common garden conditioning, the mussels were fed a combination of 8 mL Shellfish Diet 1800 and 8 mL Iso 1800 (Reed Mariculture). Feeding took place three times per week during the duration of the common garden conditioning. Temperature, salinity (Metler Toledo SevenEasy Conductivity), and pH within the common garden were monitored throughout the conditioning period using discrete sampling. Total alkalinity was measured using the methods described above. Aragonite saturation and pCO2 were computed using the pH and AT measurement and the *seacarb* package in R (Gattuso *et al.*, 2016) with dissociation constants K_1 and K_2 (Lueker *et al.*, 2000), K_f (Perez and Fraga, 1987), and K_s (Dickson, 1990). Results of common garden conditions are presented in Table S1.

Following common garden conditioning, a subset of mussels from each population were randomly selected and transferred to a pH manipulation system to assess population-specific responses to a benign (pH_T = 8.1) and stressful pH level (pH_T = 7.7). The experimental system was a flow-through seawater pH-manipulation system described by (Kapsenberg *et al.* 2017c). Briefly, seawater within the system was pumped from 5 m depth in the Bay of Villefranche, filtered to 0.35 μm and UV-sterilized, and maintained at a constant temperature of 15.5^{o}C. Seawater pH was controlled in four header tanks using a glass pH electrode feedback system (IKS aquastar) and pure CO_2 gas addition and constant CO_2-free air aeration. Two header tanks were used per treatment to account for potential header tank effects. Each header tank distributed water at a rate of 8 L hr^{-1} into two, replicate 8 L treatment buckets (N = 4 replicates per treatment), resulting in equal pH exposure across replicates (Table S1). Honeywell Durafet pH sensors were deployed in each header tank and one downstream replicate bucket to continually monitor temperature and pH throughout the course of the

experiment (see Kapsenberg *et al.* 2017c for calibration methods). pH accuracy of Durafet calibration was 0.01 units pH_T. Samples for AT and salinity were obtained from the header tanks daily (Table S1).

Ten individuals from each population were distributed between two independent replicate buckets per treatment (N = 5 individuals per bucket, N = 10 individuals per population per treatment), for a total of 5 d. At the end of the exposure period, all individuals within each replicate bucket were removed and gill tissue was sampled within ten minutes. Sampling of each replicate bucket was randomized and dissections of individuals were completed within 1.5 h. Gill tissue (volume 0.1-0.2 mL) was stored in 1 mL of RNAlater stabilization solution. The samples were maintained at room temperature for 24 h to allow the stabilization solution to permeate the tissue samples. Samples were then transferred to a -80^{o}C freezer pending RNA isolation (as per manufacturer's recommendations).

1.3.4 RNA isolation and sequencing

Total RNA was isolated using the PureLink RNA Mini Kit with on-column DNase treatment as per the manufacturers instructions for purification from animal tissue. Quality of extraction via Bioanalyzer indicated extremely high quality extracts with RNA Integrity Numbers ranging between 9.8-9.9. Prior to library preparation, the quantity of all extracts was determined using a Qubit. 500 ng of total RNA per sample was used for 3' mRNA sequencing with the QuantSeq FWD kit (Lexogen) (Moll *et al.*, 2014). 3' RNAseq, also known as TagSeq, only sequences a single fragment for each transcript, allowing for shorter sequencing reads and lower sequencing depth than traditional RNAseq. By only sequencing a single fragment, this method also eliminates the need for length bias correction in estimating transcript abundances, and has been shown to provide more accurate estimates of transcript abundances than standard RNAseq (Lohman *et al.*, 2016). Sequencing library quality was assessed using a Bioanalyzer HS chip, and the 40 libraries were multiplexed and sequenced on a single lane of Illumina HiSeq 4000 at the University of Chicago Genomics

Core Facility, yielding an average of 6.4 million 50-bp single end reads per sample. Raw sequencing reads were mapped to a *M. galloprovincialis* reference transcriptome containing 151,320 non-redundant transcripts (Moreira *et al.*, 2015) using bowtie2 (Langmead and Salzberg, 2012), and yielded an overall alignment rate of 75.6 percent. A custom Perl script written by Misha Matz (available at https://github.com/z0on/tag-based_RNAseq) was used to count the number of reads mapping to each unique transcript in the reference. The resulting matrix consisted of observed counts of all transcripts for each individual, and was used for all analyses exploring population differentiation and pH-stress plasticity. As it is possible that multiple transcripts in this matrix are potentially isoforms originating from the same gene, the term "transcript expression" (instead of "gene expression") is utilized throughout the remainder of this chapter.

1.3.5 Identifying population-specific patterns of transcript plasticity and genetic differentiation

Differences in transcript expression were used to (1) assess patterns of population-specific responses to each pH treatment, (2) explore the extent to which observed population-differentiation could be related to habitat pH fluctuations and predictability and (3) determine how pH plasticity differed between the two populations. The R package *DESeq2* and associated protocols (Love *et al.*, 2014) were used to normalize and filter transcript counts, as well as to compute the $\log_2$-fold change (LFC) in expression of each transcript using a generalized linear model and a series of defined contrasts. For each contrast, transcripts were filtered such that the count of each transcript was <10 across all samples and >25 reads mapped to at least two individuals. First, we quantified population differentiation by computing LFCs between populations for both the benign and stressful pH conditions, using the coastal population transcript counts as the reference in the comparison. A total of 12,809 transcripts passed filtering for the comparison of the populations in the benign pH treatment, and a total 12,733 transcripts passed filtering for the comparison of the popula-

tions in the stressful pH treatment. Second, we quantified differences in the magnitude of the pH-stress response (i.e., plasticity) by computing LFC's for each population independently between pH treatment, using the benign pH treatment transcript counts as the reference for each comparison. A total of 12,927 transcripts passed filtering for the quantification of the coastal population's pH plasticity, and a total of 12,674 transcripts passed filtering for the quantification of the lagoon population's pH plasticity. Lists of differentially expressed transcripts generated for all comparisons were defined as those transcripts exhibiting an LFC with a Benjamini-Hochberg false discovery rate corrected p-value <0.1 (Love *et al.*, 2014). The distribution of LFCs were visualized with volcano plots using the *EnhancedVolcano* package in R. Overrepresented gene ontologies (GO) for each comparison were identified using the GO enrichment analysis method, and associated scripts, provided by Wright *et al.* 2015. Briefly, this method takes into consideration the full distribution of LFCs to identify GO categories that are significantly enriched within up or down regulated genes using the Mann-Whitney U Test and a false discovery rate threshold of 0.1 (Wright *et al.*, 2015).

To visualize and further quantify the differentiation of the populations in each treatment, Principal Component Analysis (PCA) was conducted on the 500 transcripts displaying greatest variance across individuals in each transcript counts matrix (Love *et al.*, 2014). PCA was run using the plotPCA function in *DESeq2* on a log2 normalization of the count data. An ANOVA was then conducted to test for population-based differences along PC1 in each treatment. We then explored the extent to which transcriptome-wide patterns of differentiation between populations in the benign treatment were predominantly driven by each population's native pH environment. To accomplish this, a list of pH-responsive transcripts was defined as those transcripts differentially expressed between pH treatments in either population. If habitat pH variability were a predominant driver of the differentiation of each population's gene expression profile, these pH-responsive loci were expected to exhibit elevated divergence between populations relative to all other transcripts differentiating the populations.

Figure 1.2: Species exhibiting sessile life-history stages, such as *M. galloprovincialis* and the two *Homo sapien* individuals pictured above, will need to rapidly adapt to persist as global change progresses.

A permutation analysis of variance test (PERMANOVA) with 999 permutations was used to compare the LFC distribution of these pH-responsive loci (N = 29) to the LFC distribution of all transcripts differentially expressed between populations in the benign treatment (N = 231).

The total magnitude of pH-stress response was compared between populations to generate reaction norms of individuals from the coastal and lagoon sites and thereby determine whether plasticity differed between populations (Fig. 1.1). Only transcripts that passed filtering in the analysis of each populations low pH response were considered (n = 11,358 total transcripts). Population-based differences in the distribution of LFC of these transcripts was assessed using a two-sided Kolmogorov-Smirnov (KS) test in R. Subsequently, a PERMANOVA was used to identify significant differences in the magnitude of LFC across all transcripts between populations. This analysis was conducted across all transcripts for which the absolute value was computed (i.e., independent of direction of transcript expression change), as well as independently for up (n = 2,934) and down-regulated transcripts (n = 2,529). Each PERMANOVA was run with 999 permutations and using the *RVAideMemoire* package in R) (Hevré 2017).

Finally, we computed transcriptome-wide F_{ST} as a proxy for the level of gene flow occurring between the lagoon and coastal populations. Specifically, using the same filtered and trimmed reads from which transcript counts were generated, we identified 385,718 single nucleotide polymorphisms (SNP) using *mpileup* in Samtools (Li *et al.*, 2009). These SNP's were winnowed to a total of 26,097 after filtering using VCFTools and the following specifications: minor allele frequency = 0.05, minimum SNP Quality >30, minimum mean depth = 10, and maximum missing data = 0.9 (Danecek *et al.*, 2011). The software OutFLANK was then used to compute the mean F_{ST} across all variants using a sample size bias correction (Whitlock and Lotterhos, 2015).

1.4 Results

1.4.1 Site-specific patterns of pH fluctuation dynamics

While the mean pH value observed at each site was comparable – the coastal population experienced an average pH_T of 8.07 (N = 8,045; 12 month observation period) and the lagoon population experienced an average pH_T of 8.11 (N = 16,992; 9 month observation window) (Fig. 1.3A-B), distinct differences in the magnitude and predictability of the pH fluctuations were observed between sites. Specifically, there was a dramatic increase in the range of observed pH values at each site, whereby the bay environment exhibited a range pH values between 7.96-8.16 and the lagoon site exhibited pH values between 7.47-8.39. Additionally, a significant difference in the distributions of observed pH values (D = 0.459, $p<0.001$) and variance across pH values (F = 5.27, $p<0.001$), was detected between sites (Fig. 1.3C). The temporal autocorrelation of pH was elevated in the coastal site across all lags of both the hourly (Fig. 1.3D) and daily-intervals (Fig. S1). Spectral analysis identified a predominant signature of diurnal variability at each site (Fig. S2). The coefficient of correlation between pH and temperature was dramatically reduced in the lagoon (R^2 = -0.17) relative to the coastal site (R^2 = -0.90), though the relationship between these abiotic variables was significant at each site (coastal: t = -180.86, $p<0.001$; lagoon: t = -22.63, $p<0.001$) (Fig. S3). This observed reduction in pH temporal autocorrelation and correlation between pH and temperature demonstrate a reduction in predictability in the lagoon habitat.

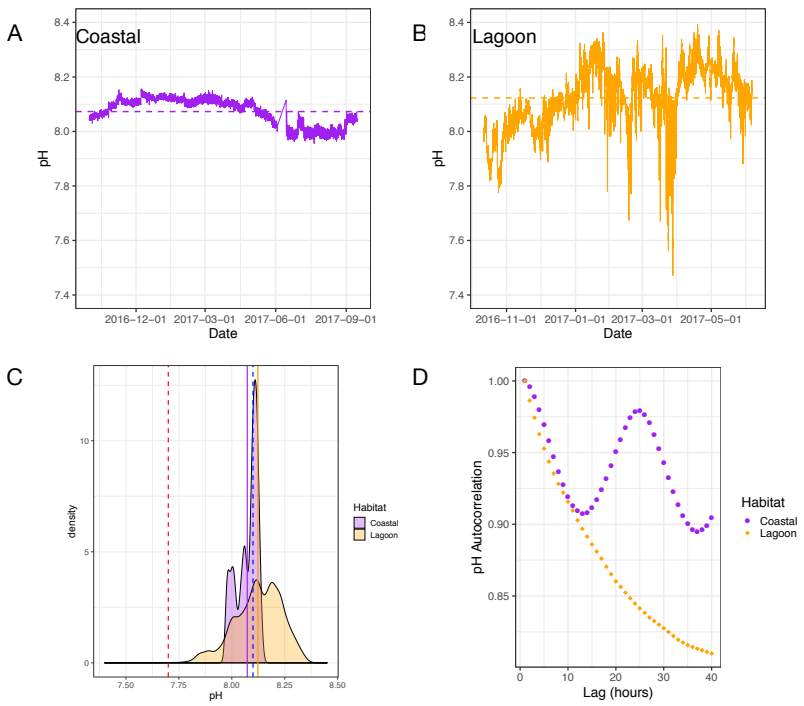

Figure 1.3: Time-series pH data collected at the (A) coastal and (B) lagoon habitats, with dashed lines indicating mean pH values across observation window. The distribution of pH values observed during the pH-monitoring period at each site (C), where solid vertical lines indicate mean pH at the coastal (purple) and lagoon sites (orange). Dashed vertical lines indicate experimentally imposed benign (blue) and stressful (red) pH treatments. In (D) the temporal autocorrelation in the pH time-series is shown using hourly lag intervals for each habitat.

1.4.2 Population differentiation in benign and stressful pH conditions

Using the coastal population transcript expression profile as a reference, a total of 260 transcripts were differentially expressed between populations in the benign treatment (171 up-regulated, and 89 down-regulated), while only 93 transcripts were differentially expressed between populations in the low pH treatment (55 up-regulated, 38 down-regulated). PCA indicated that the molecular phenotypes of the coastal and lagoon populations were signifi-

cantly differentiated in the benign pH treatment ($F_{1,18} = 13.8$, $p = 0.002$; Fig 1.4C), but not the stressful pH treatment ($F_{1,18} = 0.6$, $p = 0.458$; Fig. 1.4D). Volcano plots demonstrated a relative enrichment of transcripts up-regulated in the lagoon population in both the benign and stressful pH treatment, as indicated by the increased density of transcript points in the upper-right corner of Figures 1.4C & 1.4D. GO enrichment analyses identified 54 ontologies overrepresented in the population-differentiation in benign conditions, including a suite of metabolic and biosynthetic pathways (Fig.'s S4 S5).

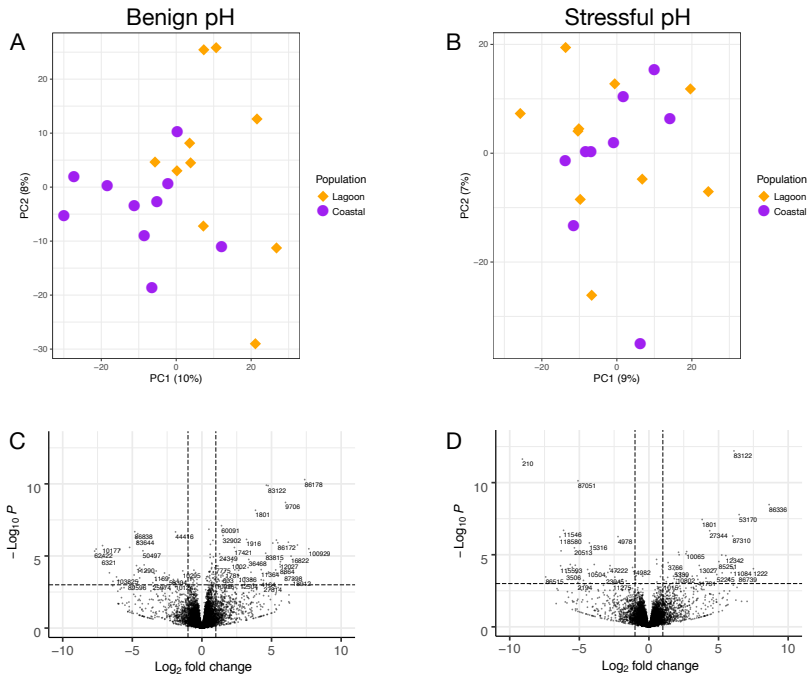

Figure 1.4: Patterns of differentiation between the coastal and lagoon populations after five days of exposure to benign (left panel) and stressful (right panel) pH treatments. Principal component analysis of normalized $\log_2$-fold-change data between populations in benign (A) and stressful pH conditions (B). Volcano plots depicting transcript expression change and p-value distributions in benign (C) and stressful (D) pH conditions. Transcripts that are labeled exhibited a log2-fold-change >2 and FDR-corrected $p$value <0.05.

Lastly, transcripts responding to pH were significantly more diverged than all other tran-

scripts differentiating populations in benign conditions ($F_{1,258} = 13.62$, $p = 0.001$) (Fig. 1.5). This suggests that the observed differentiation between the coastal and lagoon population is indeed linked to habitat pH exposures.

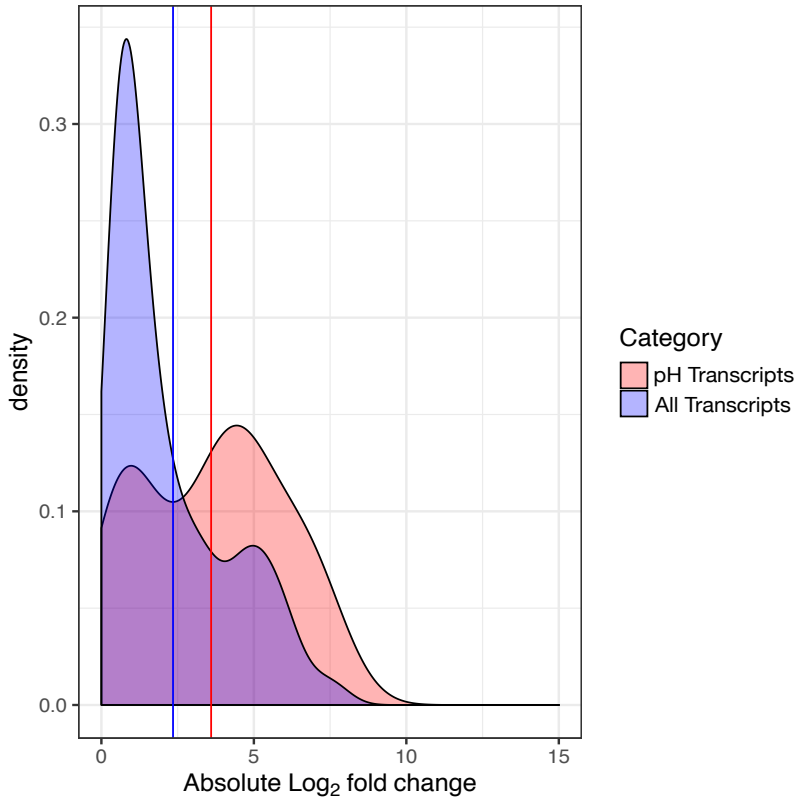

Figure 1.5: Overlaid absolute $\log_2$-fold-change distributions of pH-responsive transcripts (red) and all other transcripts differentiating populations in the benign treatment (blue) ($F_{1,258} = 13.62$, $p = 0.001$). Solid lines correspond to mean expression differences between populations at pH-responsive transcripts (red) and mean expression difference at all other transcripts (blue).

The computed mean transcriptome-wide F_{ST} was 0.003, indicating low genetic differentiation, and high levels of gene flow, between the lagoon and coastal populations.

1.4.3 Population-based differences in pH plasticity

Each population exhibited significant changes in transcript expression in response to the low pH exposure: 57 differentially expressed transcripts (26 up and 31 down-regulated) were identified in the coastal population and 49 differentially expressed transcripts (16 up and 41 down-regulated) were identified in the lagoon population. GO enrichment analyses indicated that metabolic process pathways dominated each population's low pH response (Fig.'s S7 S8).

The observed $\log_2$-fold change (LFC) distribution generated from each population's pH-stress response was distinct (D = 0.059, p<0.001) (Fig. 1.6C), and the total magnitude of LFC across all transcripts was significantly greater in the coastal population, indicating reduced plasticity in the lagoon population ($F_{1,22714}$ = 25.4, p= 0.001) (Fig. 1.6D). When segregated by LFC direction, the magnitude of response of the coastal population was significantly greater for down-regulated ($F_{1,5056}$ = 4.12, p= 0.043), but not up-regulated transcripts ($F_{1,5866}$ = 2.05, p= 0.13) (Fig. 1.6D).

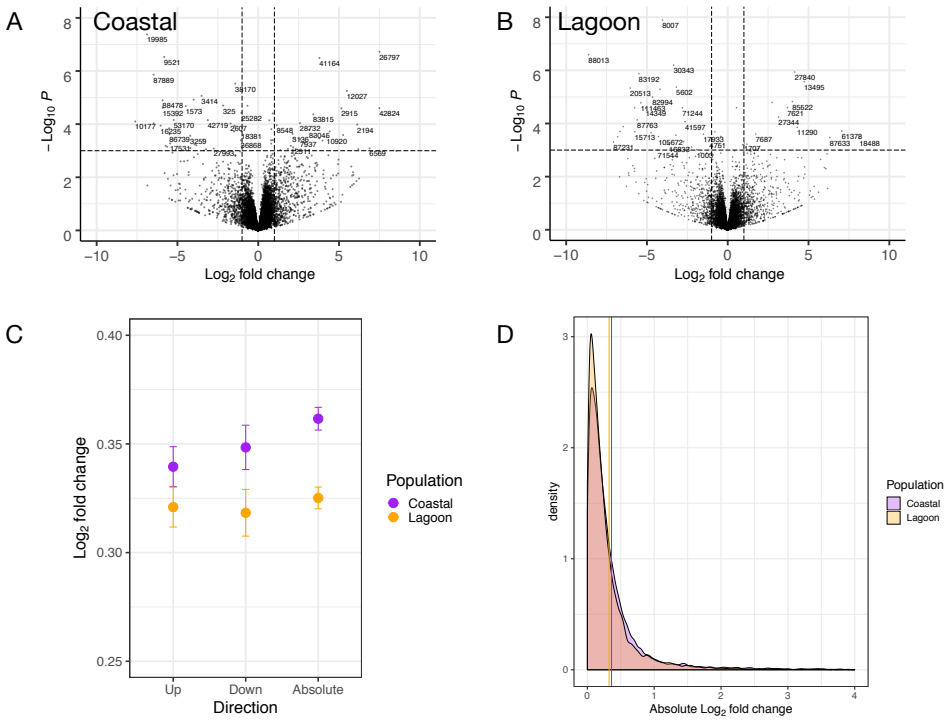

Figure 1.6: Observed differences in transcript expression plasticity between the coastal and lagoon populations. Volcano plots depicting transcript expression and p-value distributions between pH treatments for individuals native to the coastal (A) and lagoon (B) habitats. Transcripts that are labeled exhibited a log2-fold-change >2 and FDR-corrected *p*value <0.05. (C) Observed differences in the distribution of absolute transcript expression change transcripts in the coastal (purple) and lagoon (orange) populations (D = 0.059, $p<0.001$). (D) Differences in up ($F_{1,5866} = 2.05$, $p= 0.13$), down ($F_{1,5056} = 4.12$, $p= 0.043$), and absolute ($F_{1,22714} = 25.4$, $p= 0.001$) transcript expression of individuals from the coastal and lagoon sites in response to the stressful pH conditions.

1.5 Discussion

Environmental variability plays a dominant role in shaping the ecology and evolution of species across marine and terrestrial habitats. This study leveraged high frequency monitor-

ing of seawater pH to document the fine-scale and dynamic nature of pH fluctuations within coastal ecosystems, and explored the extent to which it drives divergence and shapes unique patterns of phenotypic plasticity between populations. The results presented both inform emerging theory and the mechanisms underlying species resilience to future climate change.

1.5.1 Local differences in pH variability within the Northwest Mediterranean Sea

While a consistent decline in mean pH has been documented in the northwest Mediterranean Sea (Kapsenberg *et al.* 2017b), our high frequency monitoring of a lagoon and open coastal location demonstrates the dynamic nature of coastal carbonate chemistry across a small portion of a species biogeographic range. The dramatic pH fluctuations observed within the lagoon are driven by the shallow depth and limited mixing with the Mediterranean Sea, which both act to increase the relative influence of local weather patterns, biology, and benthic processes on seawater conditions (Waldbusser and Salisbury, 2014). These processes ultimately elevate the magnitude, and depress the predictability, of pH fluctuations in the lagoon relative to the coastal site. These oceanographic data suggest that individuals from the lagoon more frequently encounter stressful pH conditions, and that the pH fluctuations are dramatically more unpredictable than those experienced by the coastal population. Though we additionally identified subtle differences in mean pH values across the observation windows between sites, this may be driven by the early termination of oceanographic monitoring at the lagoon site. Specifically, this precluded monitoring during the mid-summer months within the lagoon habitat, the period during which the coastal site exhibited its lowest pH values (Fig. 1.3). Ultimately, these data robustly demonstrate that natural populations of the species currently persist across dramatic differences in pH variability regimes within the Mediterranean Sea.

While documentation of differences in pH variability at similar spatial scales have been previously been reported in coastal environments (Wootton and Pfister 2012; Kapsenberg and

Hofmann 2016), this is the first account, to our knowledge, to explicitly quantify differences in the predictability of pH fluctuations occurring on a timescale that is biologically-relevant for some coastal marine species and life stages (Kapsenberg *et al.* 2018; Kapsenberg and Cyronak 2019). Recent efforts have sought to explore how global change will alter the dynamics of climate change stressor variability (Bindoff *et al.* in 2019), furthering the need to understand which aspects of environmental variability shape the responses of natural populations to these stressors.

1.5.2 Population differentiation in benign and stressful pH conditions

The molecular phenotypes of the populations were significantly diverged in the benign pH treatment after six weeks of common garden conditioning. This finding demonstrates that observed differences in environmental exposure history indeed shape distinct gene expression profiles under the average pH condition experienced within the region. Our GO enrichment analysis indicated that this differentiation was dominated by metabolic pathways, suggesting that differences in stressful environmental conditions shaped the molecular phenotype of each population in the benign environment (DeBiasse and Kelly, 2015). Time-series data from the lagoon indicated that the site not only exhibited greater pH variability, but also temperature variability (Fig. S8), another abiotic variable that induces physiological stress on the species (Anestis *et al.*, 2007; Lockwood and Somero, 2011). The presence of several biosynthetic pathways in the GO enrichment analysis, however, suggests that differences in pH exposure between habitats may still be an important driver of this differentiation. Specifically, biomineralization pathways have been repeatedly shown to respond to reductions in seawater pH across marine bivalves (Arivalagan *et al.*, 2017; Hüning *et al.*, 2016, 2012). This potential role of habitat pH in population-differentiation was corroborated by the elevated divergence of pH-responsive transcripts between the populations in the benign environment. These data ultimately suggest that in response to the elevated magnitude, and unpredictable-nature, of low pH stress, the lagoon population has elevated its baseline

expression of stress response loci during periods of benign pH conditions. Similar findings have been reported in coral populations exposed to extreme thermal fluctuations (Barshis *et al.*, 2013) and oyster populations exposed to recurrent low salinity events (Maynard *et al.*, 2018). These studies hypothesized that an elevation of baseline expression at stress-response loci limited the magnitude of response necessary to respond to the frequently stressful conditions, though the extent to which the predictability of the fluctuating selection pressures drove observed patterns was not explored in either study. Ultimately, our findings illustrate that contemporary spatial and temporal variability in pH throughout the Mediterranean may work to maintain phenotypic variation in stress tolerance across populations, which may facilitate rapid adaptation as ocean acidification progresses (Bitter *et al.*, 2019).

The increasing phenotypic similarity between populations in low pH was likely driven by the conserved molecular response present within the species to cope with this stressor. The observed pathways involved in each population's response have indeed been observed across a range of marine calcifying species (Kelly and Hofmann, 2013). Additionally, as the stressful pH conditions utilized in this study are more common in the lagoon habitat, it is possible that the individuals from the coastal site became more "lagoon-like" in their response to the change in the environment (Fig. 1.4). Furthermore, the lagoon population may in fact be persisting closer to its physiological limit of pH tolerance (Stillman, 2003), suggesting it may suffer from ocean acidification effects sooner than the coastal population as global change progresses.

1.5.3 pH fluctuation dynamics shape plasticity

Each population exhibited a significant physiological response to the reduction in seawater pH, as indicated by observed differential transcript expression between experimentally imposed pH treatments. GO enrichment analysis indicated each population's pH-stress response was dominated by metabolic pathways, consistent with the increasing body of work investigating the physiological response of marine bivalves to ocean acidification (DeBiasse

and Kelly, 2015; Hüning *et al.*, 2012). We leveraged data across all transcripts to robustly explore differences in reaction norm slope between populations. Through this, we observed that the magnitude of transcriptome response was significantly greater in the coastal population, indicating a relative reduction in reaction norm slope and depression of pH plasticity in the lagoon population (as illustrated in Fig. 1.1). The observed differentiation in the molecular phenotypes and the distinct reaction norm slope in each population suggest that the lagoon habitat favors an elevation of baseline expression with a muted plastic response at pH-stress response loci. A recent study using experimental evolution and the intertidal copepod, *Tigriopus californicus*, similarly demonstrated that increased thermal tolerance came at a loss of transcript plasticity (Kelly *et al.*, 2017). While we cannot rule out the influence of inter and trans-generational plasticity on the observed differentiation, this study adds to the increasing body of literature suggesting signatures of local adaptation within marine metapopulations subject to high levels of gene flow (Sanford and Kelly, 2011). Furthermore, these results indicate that populations locally adapted to regions with increased abiotic stress exposure may exhibit relatively limited phenotypic plasticity in responding to global change, thus relying on other responses, such as genetic adaptation, for persistence (Hoffman and Sgró 2011).

1.5.4 Concluding remarks

While observations broadly linking environmental variability to the evolution of phenotypic plasticity has mounted over decades and across systems (Kingsolver and Wiernasz 1991; Kingsolver and Huey 1998; Schaum *et al.* 2013; Kenkel and Matz 2017), empirical work has lagged behind the theoretical work in exploring how various attributes of variability promote or constrain plasticity. To date, most empirical approaches have used experimental-evolution in model systems to explicitly test theoretical predictions (Wieczynski *et al.*, 2018) or solely considered the magnitude and frequency of stressful conditions on patterns of plasticity (Barshis *et al.* 2013, Maynard *et al.* 2018). In light of this, our study leveraged a nat-

ural gradient in fluctuating selection pressures to highlight the potentially important role of fluctuation predictability in patterns of phenotypic plasticity across populations, thus supporting recent theoretical studies (Bonamour Suzanne *et al.*, 2019; Botero *et al.*, 2015). Furthermore, by exploring the response of an ecologically and economically valuable marine bivalve and its response to a global change stressor, we have demonstrated the fine-tuned nature of organismal physiology to localized differences in environmental variability. Further exploration into the generality of these findings across abiotic stressors and species is warranted, to both test theoretical predictions and better predict how species will cope with global change.

1.6 Author Contributions

Mark C. Bitter designed the study with inputs from Catherine A. Pfister, Lydia Kapsenberg, and Jean-Pierre Gattuso. MCB and LK conducted the experiments. MCB conducted molecular and computational analyses with assistance from Katherine Silliman. MCB wrote the chapter with inputs from CAP, LK, J-PG and KS.

CHAPTER 2

STANDING GENETIC VARIATION FUELS RAPID ADAPTATION TO OCEAN ACIDIFICATION

2.1 Abstract

Global climate change has intensified the need to assess the capacity for natural populations to adapt to abrupt shifts in the environment. Reductions in seawater pH constitute a conspicuous global change stressor that is affecting marine ecosystems globally. Here, we quantify the phenotypic and genetic modifications associated with rapid adaptation to reduced seawater pH in the Mediterranean mussel, *Mytilus galloprovincialis*. We reared a genetically diverse larval population in two pH treatments (pH_T 8.1 and 7.4) and tracked changes in the shell size distribution and genetic variation through settlement. Additionally, we identified differences in the signatures of selection on shell growth in each pH environment. Both phenotypic and genetic data show that standing variation can facilitate adaptation to declines in seawater pH. This work provides insight into the processes underpinning rapid evolution, and demonstrates the importance of maintaining variation within natural populations to bolster species' adaptive capacity as global change progresses.

2.2 Introduction

A fundamental focus of ecological and evolutionary biology is determining if and how natural populations can adapt to rapid changes in the environment. Recent efforts that have combined natural population censuses with genome-wide sequencing techniques have shown that phenotypic changes due to abrupt environmental shifts oftentimes occur concomitantly to signatures of selection at loci throughout the genome (Bergland *et al.*, 2014; Campbell-

1. A version of this chapter has been published as: Bitter, M.C., Kapsenberg, L., Gattuso, J.-P., Pfister, C.A., 2019. Standing genetic variation fuels rapid adaptation to ocean acidification. Nature Communications 10, 1-10.

Staton *et al.*, 2017; De Wit *et al.*, 2014; Rodríguez-Trelles *et al.*, 2013; Schiebelhut *et al.*, 2018; Umina *et al.*, 2005). These studies demonstrate the importance of standing genetic variation in rapid evolutionary processes (Barrett and Schluter, 2008), and challenge classical population genetic theory, which assumes that most genetic variation has a small effect on fitness and that selective forces alter this variation gradually over a timescale of millennia (Messer *et al.*, 2016). Though the mechanisms maintaining such significant levels of genetic variation in natural populations have been historically debated, recent population genomic surveys have begun to elucidate the role of spatially and temporally variable selection pressures in this process (Messer *et al.*, 2016). For example, environmental gradients in marine systems can maintain signatures of balanced polymorphisms between populations at multiple, putatively functional loci, even amidst high levels of gene flow (Bay and Palumbi, 2014; Gagnaire *et al.*, 2012; Pespeni and Palumbi, 2013; Silliman, 2019). While this variation has enabled the persistence of natural populations inhabiting contemporary and historic environmental variability, it is unclear whether it will facilitate the magnitude and rate of adaptation necessary for species persistence under the conditions expected as a result of global climate change (Hoffmann and Sgrò, 2011).

One pertinent threat facing marine species is ocean acidification, the global-scale decline in seawater pH driven by oceanic sequestration of anthropogenic carbon dioxide emissions (Hoegh-Guldberg *et al.*, 2014) . The current rate of pH decline is unprecedented in the past 55 million years (Hönisch *et al.*, 2012), and lab-based studies have shown negative effects of expected pH conditions on a range of fitness-related traits (e.g., growth, reproduction, and survival) across life-history stages and taxa (Kroeker *et al.*, 2013). Marine bivalves are one of the most vulnerable taxa to ocean acidification (Gazeau *et al.*, 2013; Thomsen *et al.*, 2015a), particularly during larval development (Kurihara, 2008). The ecologically and economically valuable Mediterranean mussel, *Mytilus galloprovincialis*, is an exemplary species for studying the effects of ocean acidification on larval development. Low pH conditions reduce shell size and induce various, likely lethal, forms of abnormal larval development (Kapsenberg L.

et al., 2018; Ventura *et al.*, 2016). Sensitivity to low pH, however, can vary substantially across larvae from distinct parental crosses, suggesting that standing genetic variation could fuel an adaptive response to ocean acidification (Kapsenberg *et al.*, 2018).

Here, we explored the potential for, and dynamics of, rapid adaptation to ocean acidification in *M. galloprovincialis*. We quantified the effects of low pH exposure on phenotypic and genetic variation throughout development in a single population of *M. galloprovincialis* larvae (Fig. 2.1). Larvae were reared in ambient and low pH and (i) shell size distributions were quantified on days 3, 6, 7, 14, and 26; (ii) the frequency of 29,400 single nucleotide polymorphisms (SNPs) across the species' exome was estimated on days 6, 26, and 43; and (iii) signatures of selection on larval shell size were determined in each treatment. To generate a starting larval population representative of the standing genetic variation within a wild population of *M. galloprovincialis*, 16 males were crossed to each of 12 females, hereafter referred to as founding individuals (N = 192 unique crosses). The resulting larval population was reared in an ambient (pH_T 8.05, N = 6 replicate buckets) and low pH treatment (pH_T 7.4-7.5, N = 6 replicate buckets). While the low pH treatment falls outside the range of annual variability the population currently experiences (pH_T 7.8-8.1)(Kapsenberg *et al.*, 2018), normal development of *M. galloprovincialis* larvae can occur at this pH (Kapsenberg *et al.*, 2018). We thus expected, *a priori*, that this value would effectively reveal the presence of variation underpinning low pH tolerance. Furthermore, while our low pH treatment falls below the expected 0.4 pH_T unit decline in global mean seawater pH by 2100(Hoegh-Guldberg *et al.*, 2014), marine species occupying unequilibrated coastal regions, such as the lagoon habitat of the study population, may periodically experience pH conditions that fall far below projected means during the next century (Melzner *et al.*, 2013).

Our results indicate substantial variation for low pH tolerance within *M. galloprovincialis*, and demonstrate that genotypes exhibiting elevated fitness in ambient conditions are distinct from those exhibiting elevated fitness in low pH conditions. In a broader framework, this study demonstrates a polygenic basis to a rapid adaptive response and suggests the

importance of maintaining variation within natural populations to bolster species resilience as global change progresses.

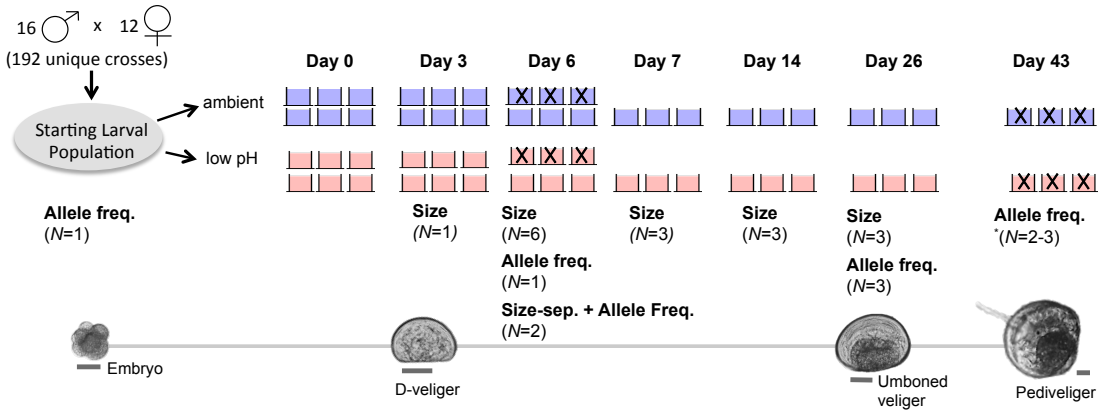

Figure 2.1: Experimental schematic. Pictures of larvae at key developmental points, cross design, and replication and sampling strategy throughout the experiment. Scale bar for larval pictures set at 50 μm. Blue and red buckets correspond to ambient and low pH treatments, respectively. Replicate buckets marked with an "X" were destructively sampled (i.e. all larvae removed/preserved) and thus absent from the experimental system on subsequent sampling days. *Allele frequency data from two replicate buckets in the ambient treatment was generated on day 43, as the third replicate bucket was sacrificed to optimize protocol for sampling settled larvae.

2.3 Methods

2.3.1 Larval Cultures

Mature *M. galloprovincialis* individuals were collected in September 2017 from the underside of a floating dock in Thau Lagoon (43.415°N, 3.688°E), located in Séte, France. Thau Lagoon has a mean depth of 4 m and connection to the Mediterranean Sea by three narrow channels. pH variability at the collection site during spawning season ranges from pH_T 7.80 to 8.10 (Kapsenberg *et al.*, 2018). Mussels were transported to the Laboratoire d'Océanographie

(LOV) in Villefranche-sur-Mer, France and stored in a flow-through seawater system maintained at 15.2^{o}C until spawning was induced.

Within 3 weeks of the adult mussel collection, individuals were cleaned of all epibiota using a metal brush, byssal threads were cut, and mussels were warmed in seawater heated to 27^{o}C (+12^{o}C of holding conditions) to induce spawning. Individuals that began showing signs of spawning were immediately isolated, and allowed to spawn in discrete vessels, which were periodically rinsed to remove any potential gamete contamination. Gametes were examined for viability and stored on ice (sperm) or at 16^{o}C (eggs). In total, gametes from 12 females and 16 males were isolated to generate a genetically diverse starting larval population. To produce pairwise crosses, 150,000 eggs from each female were placed into sixteen separate vessels, corresponding to the sixteen founding males. Sperm from each male was then used to fertilize the eggs in the corresponding vessel, thus eliminating the potential effects of sperm competition and ensuring that every male fertilized each female's eggs. After at least 90% of the eggs had progressed to a 4-cell stage, equal volumes from each vessel were pooled to generate the day 0 larval population (approximately 2 million individuals), from which the replicate culture buckets were seeded. 100,000 individuals were added to each culture buckets (N = 12, 18 embryos mL^{-1}). The remaining embryos were frozen in liquid nitrogen, and stored at -80^{o}C for DNA analysis of the day 0 larval population. Likewise, gill tissue was collected from all founding individuals and similarly stored for downstream DNA analyses. Larvae were reared at 17.2^{o}C for 43 days. Starting on day 4, larvae were fed 1.6 x 10^{8} cells of *Tisochrysis lutea* daily. Beginning on day 23, to account for growth and supplement diet, larvae diet was complemented with 0.2 µL of 1800 Shellfish Diet (Reed Mariculture) (days 23-28 and day 38) and approximately 1.6 x 10^{8} cells of *Chaetoceros gracilis* (days 29-37 and 39-41). Algae were added as a pulse to each experimental replicate, twice daily (early morning, late afternoon). As the system was flow through on days 0-26, the density of algae declined between consecutive pulses. The number of algae in each pulse was determined daily within the algal stock solution, and values reported above are the average

of daily algal additions. Evidence of food consumption by larvae was indicated by observed food in larval guts, as well as substantial growth of larvae throughout the experiment.

2.3.2 Larval sampling

We strategically sampled larvae throughout the experiment to observe phenotypic and genetic dynamics across key developmental events, including the trochophore to D-veliger transition (day 6), the shell growth period (days 4-26), and the metamorphosis from D-veligers to settlement (days 40-43). On day 6 of the experiment, larvae were sampled from three of the six replicate buckets per treatment. A subset of larvae (N = 91-172) from each bucket was isolated to obtain shell length distributions of larvae reared in the two treatments. The remaining larvae were separated by shell size using a series of six Nitex mesh filters (70 μm, 65 μm, 60 μm, 55 μm, 50 μm, and 20 μm; Fig. S10) and frozen at -80^{o}C. The smallest size group contained larvae arrested at the trochophore stage, and therefore unlikely to survive. The remaining five size classes isolated D-veligers from the smallest to the largest size. The shell length distribution of the larvae was used to inform, *a posteriori*, which combination of size classes would produce groups of the top 20% and bottom 80% of shell growers from each treatment. The relevant size groups from two replicates per treatment were then pooled for downstream DNA analysis of each phenotypic group. For the third replicate, *a posteriori*, all size groups were pooled in order to compute the allele frequency distribution from the entire larval population in each treatment on day 6. This sample was incorporated into analyses of remaining replicate buckets, which were specifically used to track shifts in phenotypic and genetic dynamics throughout the remainder of the larval period in each treatment.

Following size separation on day 6, the remaining replicate buckets (N = 3 per treatment) were utilized to track changing phenotypic and allele frequency distributions in the larval population through settlement. Larvae were sampled for size measurements on day 3 (N = 30-36 individuals), day 7 (N = 38-71 individuals), day 14 (N= 37-104 individuals), and day 26 (N = 49-112 individuals). Also on day 26, an additional 1,000 larvae per replicate were

frozen and stored at -80°C pending DNA analysis. Finally, on day 43, settled individuals were sampled from each bucket (settlement was first observed on day 40 in all buckets). Treatment water was removed, and culture buckets were washed three times with FSW to remove unsettled larvae. Individuals that remained attached to the walls of the bucket were frozen and stored at -80°C for DNA analysis.

2.3.3 Culture system and seawater chemistry

Larvae were reared in a temperature-controlled sea table (17.2°C) and 0.35 μm filtered and UV-sterilized seawater (FSW), pumped from 5 m depth in the bay of Villefranche. Two culture systems were used consecutively to rear the larvae, both of which utilized the additions of pure CO_2 gas for acidification of FSW. First, from days 0-26 the larvae were kept in a flow-through seawater pH-manipulation system. Briefly, seawater pH (pH_T 8.05 and pH_T 7.4) was controlled in four header tanks using a glass pH electrode feedback system (IKS aquastar) and pure CO_2 gas addition and constant CO_2-free air aeration. Two header tanks were used per treatment to account for potential header tank effects. Each header tank supplied water to three replicate culture buckets (drip rate of 2 L h^{-1}), fitted with a motorized paddle and Honeywell Durafet pH sensors for treatment monitoring (see Kapsenberg *et al.* 2017 for calibration methods).

On day 27 of the experiment, the flow-through system was stopped due to logistical constraints and treatment conditions were maintained, in the same culture buckets, using water changes every other day. For water changes 5 L of treatment seawater (70% of total volume) was replaced in each culture using FSW pre-adjusted to the desired pH treatment. Seawater pH in each culture bucket was measured daily, and before and after each water change.

All pH measurements (calibration of Durafets used from day 0-26 and monitoring of static cultures from day 27-43) were conducted using the spectrophotometric method and purified *m*-cresol dye and reported on the total scale (pH_T) (Dickson *et al.*, 2007). Samples for total

alkalinity (A_T) and salinity were taken from the header tanks every 2-3 days from days 0-26 and daily during the remainder of the experiment. A_T was measured using an open cell titration on Metrohhm Titrando 888 (Dickson *et al.*, 2007). Accuracy of A_T measurements was determined using comparison to a certified reference material (Batch 151, A. Dickson, Scripps Institution of Oceanography) and ranged between -0.87 and 5.3 μmol kg^{-1}, while precision was 1.23 μmol kg^{-1} (based on replicated samples, n = 21). Aragonite saturation and pCO_2 were calculated using pH and (A_T) measurements and the *seacarb* package (Gattuso *et al.*, 2016) in R with dissociation constants K_1 and K_2 (Lueker *et al.*, 2000), Kf (Perez and Fraga, 1987) and Ks (Dickson, 1990). Seawater chemistry results are presented in Tables S2-3.

2.3.4 Shell size analysis

Shell size was determined as the maximum shell length parallel to the hinge using brightfield microscopy and image analysis in ImageJ software. All statistical analyses were conducted in R (v. 3.5.3). As larval shell length data did not pass normality tests (Shapiro-Wilk test), shell-size was log-transformed to allow parametric statistical analysis. We tested the effect of day, treatment, and the interaction of the two using linear mixed effects models, with day and treatment as fixed effects and replicate bucket as a random effect (*lmer*). Effects of treatment and size class on log-transformed shell length from size-separated larvae were also analyzed using a linear-mixed effect model in which size class, treatment, and their interaction were fixed effects, while larval bucket was a random effect. Significance of the fixed effects were tested against a null model using a likelihood ratio test.

2.3.5 DNA extraction and exome sequencing

We implemented exome capture, a reduced-representation sequencing approach, to identify SNPs and their frequency dynamics throughout the course of the experiment. Exome capture targets the protein-coding region of the genome, and thus increases the likelihood

that identified polymorphisms that are in or near functional loci (Cosart *et al.*, 2011). Genomic DNA from each founding individual and larval sample was extracted using the EZNA Mollusc Extraction Kit, according to manufacturer's protocol. DNA was quantified with a Qubit, and quality was determined using agarose gel, Nanodrop (260/280), and TapeStation analysis.

Genomic DNA was hybridized to a customized exome capture array designed and manufactured by Arbor Biosciences (Ann Arbor, Michigan) and using the species transcriptome provided in Moreira *et al.* 2015. Specifically, in order to design a bait set appropriate for capture of genomic DNA fragments, 90-nucleotide probe candidates were tilled every 20 nucleotides across the target transcriptome contigs. These densely-tiled candidates were MEGABLASTed to the *M. galloprovincialis* draft genome contigs available at NCBI (GCAA_001676915.1_ASM167691v1_genomic.fna), which winnowed the candidate list to only baits with detected hits of 80 nucleotides or longer. After predicting the hybrid melting temperatures for each near-full-length hit, baits were further winnowed to those with at most two hybrids of 60^{o}C or greater estimated melting temperature in the *M. galloprovincialis* genome. This collection of highly specific baits with near-full-length hits to the draft genome were then down-sampled to a density of roughly one bait per 1.9 kbp of the final potential target space, in order to broadly sample the target while still fitting within our desired number of myBaits kit oligo limit. The final bait set comprises 100,087 oligo sequences, targeting 94,668 of the original 121,572 transcriptome contigs.

Genomic DNA from each sample was subject to standard mass estimation quality control, followed by sonication using a QSonica QR800 instrument and SPRI-based dual size-selection to a target modal fragment length of 350 nucleotides. Following quantification, 300 ng total genomic DNA was taken to library preparation using standard Illumina Truseq-style end repair and adapter ligation chemistry, followed by six cycles of indexing amplification using unique eight nucleotide dual index primer pairs. For target enrichment with the custom myBaits kit, 100 ng of each founder-derived library were combined into two pools of 14 li-

braries each, whereas 450 ng of each embryonic and larval-pool derived library were used in individual reactions. After drying the pools or individual samples using vacuum centrifugation to 7 μL each, Arbor followed the myBaits procedure (v. 4) using the default conditions and overnight incubation to enrich the libraries using the custom probe set. After reaction cleanup, half (15 μL) of each bead-bound enriched library was taken to standard library amplification for 10 cycles using Kapa HiFi polymerase. Following reaction cleanup with SPRI, each enriched library or library pool was quantified using qPCR, indicating yields between 30 and 254 ng each.

The captured libraries were sequenced at the University of Chicago Genomics Core Facility on three lanes of Illumina HiSeq 4000 using 150-bp, paired-end reads. The captured adult libraries were sequenced on an individual lane, while the twenty-two, pooled larval samples were split randomly between the remaining two lanes. Average coverage for founding individuals was 40x, while average coverage in pooled samples was 100x.

2.3.6 Read trimming and variant calling

Raw DNA reads were filtered and trimmed using Trimmomatic (Bolger *et al.*, 2014), and aligned to the species reference transcriptome provided in Moreira *et al.* using bowtie2 (Langmead and Salzberg, 2012). Variants in the founding individuals were identified using the Genome Analysis Toolkit's Unified Genotyper (Van der Auwera *et al.*, 2013). These variants were filtered using VCFTOOLs (Danecek *et al.*, 2011) with the following specifications: Minor Allele Frequency of 0.05, Minimum Depth of 10x, and a Maximum Variant Missing of 0.75. The resulting .vcf files provided a list of candidate bi-allelic polymorphisms to track at each time point, treatment, and phenotypic group in the larval samples. Accordingly, GATK's Haplotype Caller was used to identify these candidate polymorphisms within each larval alignment file, and the resulting .vcf was filtered using VCFTOOLs and the following specifications: Minor Allele Frequency of 0.01, Minimum Depth of 50x, and Maximum Depth of 450x. Only variants that passed quality filtering and were identified in all larval samples

(i.e. each day, treatment, and phenotypic group) were retained for downstream analyses. This process resulted in a candidate SNP list of 29,400 variants. Allele frequencies for each variant were computed as the alternate allelic depth divided by total coverage at the locus.

2.3.7 Allele frequency analysis

To explore how the allele frequency of the 29,400 SNPs changed in each environment throughout the course of the experiment, we used a combination of PCA, outlier loci identification tests, and a statistical test of genomic differentiation (F_{ST}). We visualized patterns of genetic variation throughout the experiment with PCA (*prcomp* function in R). Prior to PCA, the allele frequency matrix was centered and scaled using the *scale* function in R. Only larval samples that encompassed the full phenotypic distribution within a particular bucket were included in this analysis. In other words, the rows of the allele frequency matrix corresponding to larval samples that were selectively segregated based on shell size were removed, and PCA was run using the day 0 larval population and larval samples collected from each treatment on days 6, 26, and 43. A separate PCA was then implemented using allele frequency data from the day 0 larval population and all day 6 larval samples, which included discrete size groups from each treatment. This analysis thus explicitly examined a genomic signature of the individuals that were phenotypically distinct.

We next sought to identify the presence, number, and treatment-level overlap of genetic variants that significantly changed in frequency between larval samples. Specifically, Fisher's Exact Test (FET) and the Cochran-Mantel-Haenszel (CMH) test were used to generate probabilities of observed allele frequency changes, using the package *Popoolation* (Kofler *et al.*, 2011) in R. P-values for each SNP were converted to q-values in the R package *qvalue* (Storey *et al.*, 2019), and significant SNPs were identified as those SNPs with a q-value <0.01. As the CMH test computes probabilities for SNPs based on consistent changes among replicates, it is a powerful approach to identifying significantly changed SNPs when treatment replicates are available. Accordingly, this test was used identify significant allele frequency

changes between the day 0 larval population and the day 26 ambient and low pH treatment replicates (N = 3), the day 0 larval population and the settled individuals from ambient (N = 2) and low pH treatment replicates (N = 3), and between the top 20% and bottom 80% of growers in each treatment (N = 2). This test thus produced a single, significant SNP list for each treatment on days 26 and 43, as well as the size-separated day 6 larvae. As treatment replicates were not available the ambient and low pH larval population samples on day 6, an alternate contingency table test, FET, was used to obtain a list of significant SNPs for this day of sampling (with identical rank-based approach/multiple testing corrections as those used for the CMH tests). The resulting lists of significant SNPs for days 6, 26, and 43 were then compared to identify outlier loci for each treatment. Specifically, outliers were identified for each treatment as those loci containing significant SNPs on each sampling day (i.e. SNPs overlapping among a treatment's three significant SNP lists). As the buckets sampled on day 6 were independent cultures from those buckets sampled on days 26 and 43, this process leverages both multiple independent larval cultures and sampling days to obtain a robust outlier list for each treatment.

To provide a third, independent metric of genomic change in the larval population throughout the experiment, we computed the F_{ST} statistic for a series of comparisons. Specifically, we implemented a methods-of-moments estimator of F_{ST} from Pool-seq data in an analysis of variance framework, as described in Hivert *et al.* 2018 (*poolFStat* package in R). A global (exome-wide) F_{ST} statistic was computed pairwise between the day 0 larval population and the day 6 ambient and low pH larvae replicate buckets, day 26 ambient and low pH larvae replicate buckets, and settled individuals from all replicate buckets in ambient and low pH. F_{ST} was also computed to compare differentiation between phenotypic groups (top 20% and bottom 80% of growers) on day 6. As *poolFstatat* necessitates an approximation of population size, we parameterized the model using larval counts obtained on days 0 and 26, and estimates of larval population size for days 6 and 43. The population size in each replicate bucket on day 0 was 100,000 individuals, as larval counts were conducted on

the starting larval culture and an equal volume (containing 100,000 individuals) was added to each replicate bucket. To calculate population sizes on day 26, 200 mL of seawater was extracted from each replicate bucket, from which larvae were concentrated using a 70 μm mesh filter and subsequently photographed using brightfield microscopy. This mesh size was selected based on data obtained from the size selection of larvae (Fig. S9), and chosen to filter out D-veligers that had failed to grow, and therefore survive, beyond day 6. The number of photographed larvae on day 26 thus provided a proxy for the population size at this time point: population size was estimated to be 3,685, 2,090, and 1,183 in the ambient replicates and 2,503, 1,733, and 2,888 in the low pH replicates. These estimates suggest average mortality rates of 97.7% and 97.6% in the ambient and low pH conditions, respectively. These estimates are in accordance with previous studies that have similarly reported substantial mortality of marine bivalve larvae reared in laboratory settings (Fotel *et al.*, 1999; Lannan, 1980; Mallet *et al.*, 1985; Satuito *et al.*, 1994). Larval counts from day 26 were used to estimate a broad range of feasible population sizes on days 6 and 43. Specifically, given the observed population sizes on day 26 (reported above), F_{ST} was computed over large ranges of population sizes on day 6 (10,000-40,000 individuals) to encompass both linear and non-linear declines in population size throughout the growth period. While larval counts were additionally not conducted on day 43 (all larvae sampled on this day needed to be preserved for sequencing to ensure accurate allele frequency estimates), the larvae were observable to the naked eye at this time point. This allowed for the observations that there were: (1) no treatment specific patterns in the total number of settled larvae and (2) the number of settled larvae was greater than 100 but far less than 400 individuals at this time point. F_{ST} was thus computed using input pool sizes between 100-400 individuals for day 43 samples. Results demonstrating how computed values of F_{ST} changed according to these differences in input pool size are reported in Table S4.

2.3.8 Gene identification/ontologies

We next sought to explore the biological pathways that were associated with survivorship in each pH treatment and/or size group during the experiment. To accomplish this, we indexed our list of outlier loci using the annotated transcriptome provided in Moreira *et al.* 2015. Their annotation utilizes NCBI's nucleotide and non-redundant, Swissprot, KEGG, and COG databases, thus providing a thorough survey of potential genes and pathways associated with our candidate SNPs. We generated gene lists for pH-specific outlier loci, which were identified as loci that showed signatures of selection on all sampling days and were unique to each environment. We also generated a candidate gene list for loci that exhibited shared signatures of selection in each treatment. These lists thus only contain robust outlier loci (i.e. containing significant SNPs in multiple independent replicates), with potentially strong effect sizes (i.e. containing significant SNPs at multiple developmental stages). Lastly, we used the Moreira *et al.* annotation to explore the genes that exhibited signatures of selection for shell growth in ambient and low pH conditions, as well as shared signatures of selection for shell size in each treatment.

2.4 Results

2.4.1 Phenotypic trajectories

As expected, shell size was significantly affected by pH treatment throughout the experiment (likelihood ratio test, $p = 0.029$), and shell length of low pH larvae was 8% smaller than that of larvae reared in ambient pH on days 3 and 7. Shell length was affected by the interaction of day and treatment (likelihood ratio test $p < 0.001$), indicating treatment specific growth patterns. From days 7 to 26 the size distributions in each treatment began to converge, with larvae in low pH being only 2.5% smaller than those cultured in the ambient treatment by day 26 (Fig. 2.2). Additionally, treatment-specific patterns of phenotypic variation were observable during this period. Specifically, the coefficient of variation of shell size was

elevated in the low pH treatment on day 3 (ambient pH CV = 3.52; low pH CV = 5.16) and day 7 (ambient pH CV = 3.54; low pH CV = 4.98). This difference in phenotypic variation was reduced on day 14 (ambient pH CV = 8.83; low pH CV = 9.7) and no longer evident by day 26 (ambient pH CV = 11.66; low pH CV = 11.26).

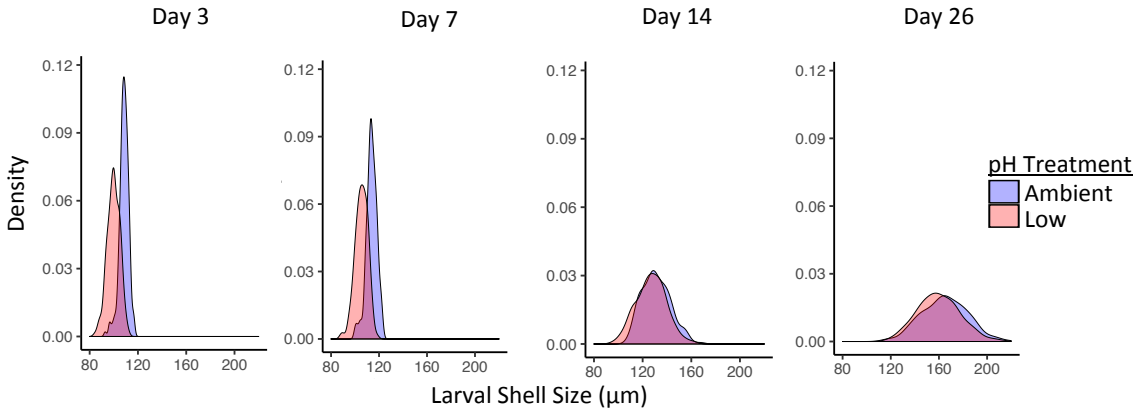

Figure 2.2: Larval size distributions throughout the shell growing period. Blue and red densities correspond to shell size distributions in ambient and low pH treatments, respectively. Larval size was significantly affected by treatment (likelihood ratio test, $p = 0.029$) and the interaction of day and treatment (likelihood ratio test, $p < 0.001$) throughout the shell growing period.

2.4.2 Changes in genetic variation

We identified 29,400 SNPs across the species exome that were present within the larval population across all sampling days and treatments. To link the observed phenotypic trends in each treatment to changes in this variation, we analyzed the SNP's using principal component analysis (PCA), outlier loci identification, and a statistical metric of genomic differentiation (F_{ST}). For both ambient and low pH treatments, all analyses indicated increasing genomic differentiation of the larval cultures away from the day 0 larval population. This trend is visually apparent in the PCA, which incorporated allele frequency data from all

larval samples collected during the pelagic stage and settlement (excluding size-separated groups) (Fig. 2.3). Through time there is an observed increase in Euclidian distance among samples (e.g. days 26 and 43). This may be driven, at least in part, by selection-induced declines in larval survival throughout the pelagic phase, as well as an increase in the influence of allele frequency drift among replicate buckets (i.e. persistent random mortality leading to replicate-specific patterns of selection). Observations of sustained larval mortality throughout the experiment (indicated via empty D-veliger shells in buckets) corroborated these trends, as did our gross estimate of mortality between days 0 and 26 (97.7% and 97.6% in ambient and low pH treatments, respectively).

We identified SNPs that changed significantly in frequency between the day 0 larval population and the larvae sampled on days 6, 26, and 43 in each treatment. Significant SNPs were identified using a rank-based approach and the observed allele frequency shift probabilities generated from the Fisher's Exact and Cochran-Mantel-Haenszel tests. This analysis indicated pervasive signatures of selection in both treatments, with thousands of SNPs significantly changing in frequency throughout the course of the experiment (Figure S9). To identify a list of outlier loci for each treatment, we identified loci containing significant SNPs on all sampling days, thus leveraging independent replicate cultures and multiple sampling days (see Methods for details). This resulted in the identification of 162 and 151 total outlier loci in the ambient and low pH conditions, respectively. We compared the overlap in theses lists to identify pH-specific outliers (loci that were outliers in only one of the pH treatments) and shared outliers (loci that were outliers in both pH treatments). In total, we identified 99 ambient pH-specific outlier loci (31 annotated), 88 low pH-specific outlier loci (29 annotated), and 63 shared loci (24 annotated) based on transcriptome provided in Moreira *et al.* 2015. Therefore, 58% of the outlier identified in the low pH treatment were unique to that environment (i.e. did not display strong signatures of selection in the ambient treatment) (Fig. 2.3C). This finding highlights the potential polygenic nature of low pH adaptation and demonstrates that natural populations currently harbor variation at these putatively

adaptive loci. Another statistical metric of genetic differentiation, F_{ST}, was used to identify changes in the magnitude of selection throughout development. We computed exome-wide estimates of F_{ST} pairwise between the day 0 larval population and each available replicate bucket on all sampling days. The greatest change in F_{ST} occurred between day 0 and 6, before elevating more slowly thereafter, suggesting that the majority of selective mortality in *M. galloprovincialis* larvae occurred prior to day 6 (Fig. 2.3B).

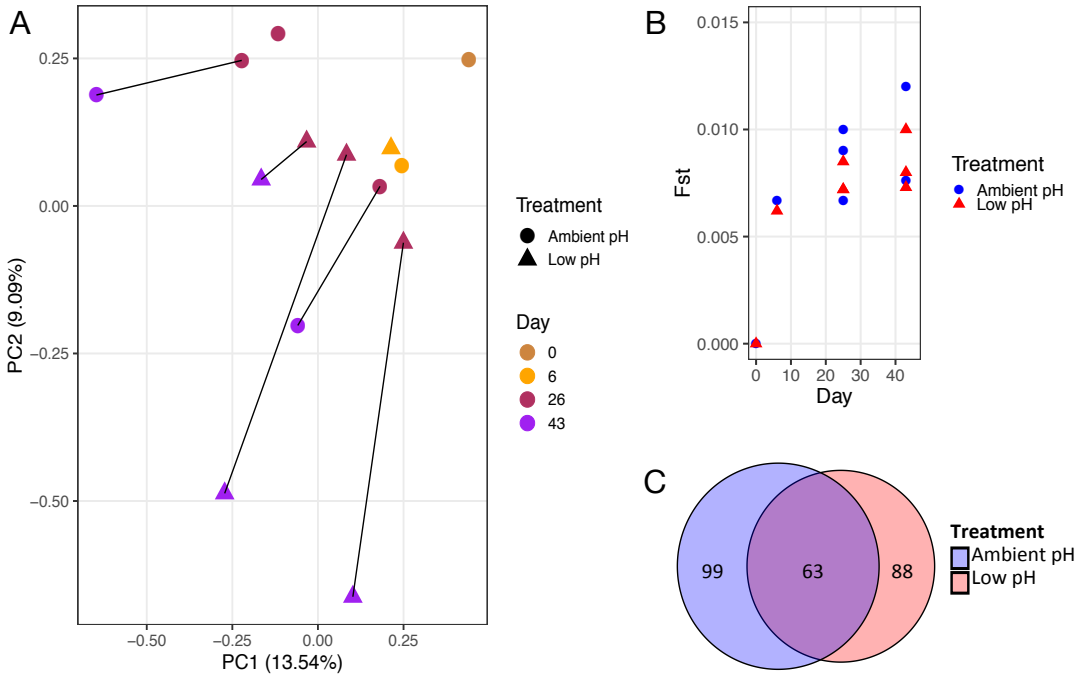

Figure 2.3: Patterns of genomic variation within larval populations throughout development. (A) Principal component analysis of allele frequency data from larval samples collected throughout the course of the experiment. Allele frequency data from 29,400 SNPs were used for PCA. PCA point color corresponds to developmental day, while shape corresponds to treatment condition. (B) F_{ST} between the Day 0 larval population and each larval population treatment replicate throughout development. Blue circles and red triangles correspond to ambient and low pH replicate bucket F_{ST} values, respectively. (C) Venn diagram representing the extent of overlap in outer loci identified in ambient (blue) and low pH (red) treatments.

2.4.3 Signatures of selection on shell growth in ambient and low pH

The size-separation of larvae on day 6 isolated the largest 18% from the smallest 82% of shell growers in the ambient, and the largest 21% from the smallest 79% of shell growers in the low pH treatment (Fig. S10). Hereafter, these groups will be referred to as the fastest and slowest growers, respectively. Shell size on day 6 was significantly affected by treatment and size class (likelihood ratio test, p <0.001). PCA using allele frequency data from the day 0 starting larval population and larval samples collected on day 6 revealed a strong genetic signature of size class (Fig. 2.4A). Specifically, the fastest growers segregated along PC1 from the slowest growers in both treatments, with the day 0 larval population and day 6 larval population samples (from each treatment) falling in between the size-separated groups. The number of significant SNP's differentiating the fastest and slowest growers in each treatment, hereafter referred to as size-selected SNPs, was comparable: 963 significant SNPs were identified in ambient and 846 significant SNPs were identified in the low pH treatment (significance determined using Cochran-Mantel-Haenszel test). This led to the identification of 611 size-selected loci that were unique to the ambient pH treatment (225 annotated), 499 size-selected loci that were unique to the low pH treatment (184 annotated), and 154 size-selected loci (51 annotated) that were shared between environments. Therefore, 76% of loci associated with fast shell growth in low pH were not associated with fast growth in the ambient treatment, indicating unique targets of selection on shell growth in each environment (Fig 2.4C). F_{ST} analysis corroborated this trend, as elevated signatures of differentiation were observed between the fastest growers in ambient and low pH, relative to differentiation between the slowest growers and full larval populations in ambient and low pH treatments (Fig. 2.4B).

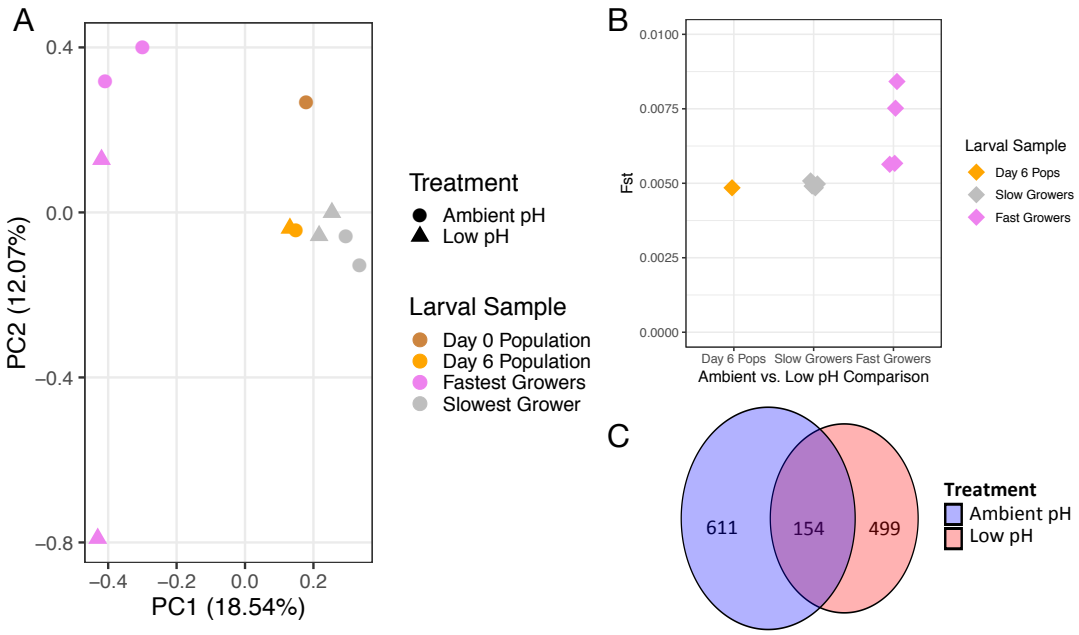

Figure 2.4: Patterns of selection on shell growth in ambient and low pH conditions. (A) Principle component analysis examining genomic signature of size separation in ambient and low pH treatments. Allele frequency data is based on 29,400 SNPs and all samples collected on day 6, as well as the day 0 starting larval population. PCA point color corresponds to developmental day, while shape corresponds to treatment. (B) Exome-wide F_{ST} computed pairwise between ambient and low pH replicate buckets for the entire larval population (Day 6 pops) and the size selected larvae isolated on day 6 (triangle color corresponds to larval sample) (Day 6 Pops: N =1 pairwise comparison; Slowest and Fastest Growers: N = 4 pairwise comparisons). (C) Venn diagram representing extent of overlap in loci displaying signatures of selection for shell growth in ambient (blue) and low pH (red) treatments.

2.5 Discussion

While previous work has shown strong negative effects of low pH on larval development in bivalves (Gazeau *et al.*, 2014b, 2013; Kurihara, 2008; Thomsen *et al.*, 2015b), the results presented here suggest that standing variation within the species could facilitate rapid adapta-

tion to ocean acidification. Observed shell length differences on days 3 and 7 matched expectations for the species based on previous work (-1 μm per 0.1 unit decrease in pH)(Kapsenberg *et al.*, 2018). However, this difference was reduced 50% by day 14. Mechanistically, low pH treatment effects on bivalve larval shell growth are driven by the limited capacity of larvae to regulate carbonate chemistry, specifically aragonite saturation state, in their calcifying space (Melzner *et al.*, 2017; Waldbusser *et al.*, 2015, 2013). Our data show that this physiological limitation is greatest prior to day 7, after which a partial convergence of the size distributions in the ambient and low pH treatments was observed.

It is likely that the partial convergence of shell size distributions observed by day 14 was, at least in part, driven by natural selection for low pH tolerance. We have previously shown that the smallest D-veligers in the low pH treatment display an increased prevalence of morphological abnormalities, which likely become lethal during the shell growth period (Kapsenberg *et al.*, 2018). Directional selection against this phenotypic group would shift the size distribution closer to that of larvae reared in ambient conditions, as we observed. The unique signatures of selection on shell growth after six days of exposure to low pH, as well as the unique outlier loci identified in the low pH environment throughout the larval period, further strengthen the notion that these phenotypic trends were rooted in changes in the larval population's underlying genetic variation.

Documentation of substantial mortality by day 26 and increasing genetic differentiation throughout the experiment, as evidenced by PCA, significant changes in SNP frequencies, and increasing values of F_{ST}, further suggest the process of selection during the shell growth period. The observed trends in F_{ST}, however, highlighted a developmental point of heightened selection occurring before the convergence of the shell size distributions. Specifically, when F_{ST} is scaled by duration of treatment exposure, the genomic differentiation between the day 0 larval population and the larval populations on day 6 was three and five times greater than that observed between the day 0 larval population and the larval populations on days 26 and 43, respectively. This suggests that a largely singular, intense selection event

occurred prior to day 6 and may be responsible for the majority of genetic differentiation that occurs during larval growth and settlement. We recently identified two specific early developmental processes that are sensitive to low pH conditions and occur in this timeframe (Kapsenberg *et al.*, 2018). These processes include the formation of the shell field (early trochophore stage) and the transition between growth of the first and second larval shell (late trochophore stage), both of which occur within 48 hours of fertilization and result in a suite of size-dependent morphological abnormalities that likely become lethal during the shell growth period (Kapsenberg *et al.*, 2018). Traditionally, metamorphosis from the swimming D-veliger to the settled juvenile is regarded as the main genetic bottleneck during the development of marine bivalve larvae (Launey and Hedgecock, 2001). Our sampling from the embryo stage through settlement, however, suggests that there is a major selection event prior to day 6 that may have an even larger effect on shaping genotypes of settled juveniles than any selection thereafter.

Additional factors that may have led to the observed phenotypic dynamics are food-augmented acclimation and selective mortality via food competition. It has been demonstrated that increased energy availability can allow marine invertebrates to withstand pH stress (Pansch *et al.*, 2014) and, in the case of *Mytilus edulis*, food availability can mitigate the negative effects of ocean acidification (Thomsen *et al.*, 2013). This compensation, however, is unlikely in our experiment. Our algal concentrations during the period of phenotypic convergence (days 7-26) fell below optimal concentrations reported for the species (Pettersen *et al.*, 2010; Phillips, 2002). Additionally, settlement was not observed in our experiment until 40 days into development. This falls outside the 3-5 week larval pelagic phase documented in previous work (Carl *et al.*, 2012; Pettersen *et al.*, 2010; Phillips, 2002), and further demonstrates that the larvae were indeed food limited in each treatment. This food limitation may have induced intraspecific competition and facilitated the selective mortality of less fit genotypes, thereby producing the pervasive signatures of selection observed in both treatments starting on day 6. Furthermore, selection may have been concentrated on

the smallest larvae in low pH, thus driving the phenotypic convergence between treatments. ultimately, surviving larvae in the low pH treatment were able to partially compensate for the negative effect of CO_2-acidification on calcification kinetics (Waldbusser *et al.*, 2015). As pH tolerance has been shown to exhibit heritability in *Mytilus* spp. (Thomsen *et al.*, 2017; Kingston *et al.*, 2018), it is possible that multi-generational selection may indeed allow the population to ultimately recover the offset in shell size observed in this experiment.

We identified hundreds of SNPs responding to each pH treatment throughout the larval period and, via stringent filtering techniques, further winnowed these candidates to identify 162 outlier loci in ambient and 151 outlier loci in low pH conditions. Eighty-eight of the low pH outliers (58 %) were statistically unchanged in the ambient conditions. While some of this treatment disparity may be an artifact (i.e. false positives in the low pH or false negatives in the ambient treatment), it is unlikely that this is the case for all the unique outliers identified, given our stringent filtering techniques. These data thus provide evidence that loci that were not critical for fitness in the ambient environment came under strong selection in the low pH environment. The limited amount of overlap in size-selected loci and elevation of F_{ST} differentiation between the fastest growers further indicate novel targets of selection for accelerated shell growth in the low pH environment. As shell growth is a direct proxy for fitness (Allen, 2008; Kapsenberg *et al.*, 2018), these data suggest that the most fit genotypes in ambient conditions may not be the individuals that harbor the adaptive genetic variation necessary to improve fitness in simulated ocean acidification. Furthermore, the near-equal magnitude of mortality observed in each treatment suggests that adaptation to expected declines in seawater pH within this species may proceed via a reshuffling of standing genetic variation, effectively allowing populations to bypass the dramatic declines in population size that are characteristic of rapid evolution to abrupt environmental shifts via fixation of novel mutations (Hoffmann and Sgrò, 2011).

ultimately, these findings contribute to an emerging body of work demonstrating that rapid adaptation can indeed exhibit a polygenic basis (Bergland *et al.*, 2014; Brennan Reid

S. *et al.*, 2019; Campbell-Staton *et al.*, 2017; Rodríguez-Trelles *et al.*, 2013). Variation at functional loci across the genome is likely maintained in populations via multilocus balancing selection between populations spanning environmental gradients (Bay and Palumbi, 2014; Gagnaire *et al.*, 2012; Pespeni and Palumbi, 2013; Silliman, 2019), or within populations experiencing temporally fluctuating selection pressures (Bergland *et al.*, 2014; Wittmann *et al.*, 2017). For example, populations of *Mytilus edulis* inhabiting the Baltic Sea are periodically exposed to the pH conditions used in this study (Thomsen *et al.*, 2017). Given extensive gene flow and hybridization of *Mytilus* populations throughout the Baltic Sea, Atlantic, and Mediterranean, it is possible such gradients could maintain adaptive low pH tolerance throughout these regions, though we lack explicit demonstration of this within the focal population.

The dynamics observed in this study further suggest a potential role of cryptic genetic variation (CGV) in adaptation to climate change. CGV is defined as a subclass of standing variation with a conditional effect, such that it becomes adaptive during evolution to rare or novel environmental conditions (Paaby and Rockman, 2014). This conditional effect may manifest as a genotype-by-genotype interaction, in which an allele's effect is conditional upon the genetic background (resulting from dominance or epistasis), or genotype-by-environment interactions, in which an allele's effect is conditional upon the environment (Paaby and Rockman, 2014). In the context of the present study, the low pH treatment value is indeed rare in the study population's natural habitat (Kapsenberg *et al.*, 2018) and the pH-specific signatures of selection indicate some of the variation that was putatively neutral in the ambient treatment were conditionally beneficial in low pH. Furthermore, a defining characteristic of adaptation via cryptic variation is the release of phenotypic variation in the novel environment (Paaby and Rockman, 2014). Accordingly, we observed elevation of phenotypic variation in the low pH treatment on days 3 and 7, coinciding with the inferred period of heightened selection (between days 0 and 6). Kingston *et al.* similarly showed that stressful conditions (low pH, high temperature, and low food conditions) released phenotypic varia-

tion in calcification rates in two species of Mytilus mussels, and went on to link variation to a number of loci of moderate effect (Kingston *et al.*, 2018). While an important avenue of future research is determining which CGV mechanisms (genotype-by-genotype or genotype-by-environment) may be producing such patterns, the economic and ecological importance of marine mussels, as well as their global exposure to declining seawater pH, highlight the need to conserve standing variation in order to allow the adaptive capacity of natural populations to play out as climate change progresses. Furthermore, exploring the interplay of standing variation maintained by balanced polymorphisms and cryptic variation during adaptation to climate change is an exciting avenue of future research, which may lend fundamental insights into the dynamics of rapid evolutionary processes.

Our list of low-pH outlier loci provide targets of natural selection as ocean acidification progresses. Notably, this list included an *HSPA1A* gene, which encodes heat shock protein 70 (HSP70) (NCBI Accession: XM_022468949), one of a group of gene products whose expression is induced by physiological stressors and generally work to mediate/prevent protein denaturation and folding (Feder and Hofmann, 1999). While substantial evidence has documented the role of HSP70 in the thermal stress response across a range of taxa (Feder and Hofmann, 1999), emerging transcriptomic studies have also demonstrated the protein's role in the physiological response to low pH conditions in marine bivalves (Cummings *et al.*, 2011).

The influence of ocean acidification conditions on the biomineralization process of calcifying marine species has been readily documented (Kroeker *et al.*, 2013). Indeed, two of our candidate low pH outliers mapped to a tyrosinase (NCBI Accession: XM_022487312) and chitinase (NCBI: Accession: MG827131.1) gene, each part of pathways known to be involved in calcium carbonate shell formation in marine bivalves (Arivalagan *et al.*, 2017). Tyrosinase genes most broadly function in the process of sclerotization, the mechanism by which marine bivalves form the shell's periostracum (Zhang *et al.*, 2006), and activity of tyrosinase is heightened during larval shell biogenesis (Huan *et al.*, 2013; Yang *et al.*, n.d.).

The outlier identified in this study mapped to a *tyr3* isoform, which has previously been shown to be upregulated in response to low pH conditions in the Antarctic pteropod (Johnson and Hofmann, 2017) and Mytilus edulis (Hüning *et al.*, 2012). Chitinase genes produce organic scaffolds during shell formation in marine bivalves and have additionally been shown to change expression in response to seawater acidification in Mytilus (Hüning *et al.*, 2012).

While such gene expression-based studies provide insight into the underlying physiological responses to changes in seawater chemistry, our study demonstrates the presence of underlying genetic variation within these putative loci. This provides, to our knowledge, the first documentation of standing genetic variation at functionally relevant loci within marine bivalves, and ultimately offers robust evidence for the species' capacity to adapt to changes in seawater pH. We are currently investigating these candidates more deeply through a combination of comparative transcriptomics, quantitative PCR and *in situ* hybridizations.

Many outlier loci in low pH were also outliers in the ambient treatment (42%). This likely represents the action of selection against recessive homozygotes within the population, termed genetic load (Turner and Williamson, 1968), and selection induced by the laboratory regime. The influence of genetic load has been demonstrated to induce signatures of selection in neutral environments in a range of highly fecund species, such as plants and marine bivalves (Launey and Hedgecock, 2001; Plough *et al.*, 2016). Our crossing scheme likely amplified this signature, as equal proportions of all pairwise crosses were conducted, thereby maximizing the likelihood of lethal, or less fit, homozygotes in the day 0 larval population. These shared signatures of selection could be further associated with selective pressures induced by the laboratory conditions, such as salinity, temperature, or the food resources, which are independent of the pH manipulation, yet still may have favored subset of genetic backgrounds in this genetically diverse species (Romiguier *et al.*, 2014).

Species persistence as global climate change progresses will, in part, hinge upon their ability to evolve in response to the shifting abiotic environment (Hoffmann and Sgrò, 2011). Our data suggest that the economically and ecologically valuable marine mussel, *M. gal-*

loprovincialis, harbors standing variation that would facilitate rapid adaptation to ocean acidification. We have further demonstrated that genotypes exhibiting elevated fitness in current ocean conditions may be distinct from those exhibiting elevated fitness in future oceans. ultimately, these findings support conservation efforts aimed at maintaining variation within natural populations to increase species resilience to future ocean conditions. In a broader evolutionary framework, the substantial levels of genetic variation present in natural populations have historically puzzled evolutionary biologists (Lewontin and Hubby, 1966). Though this study does not address the processes that maintain this variation, we demonstrate its utility in rapid adaptation, thereby advancing our understanding of the mechanisms by which natural populations evolve to abrupt changes in the environment.

2.6 Author Contributions

Mark C. Bitter conceived and designed the experiment with inputs from Lydia Kapsenberg, Jean-Pierre Gattuso, and Catherine A. Pfister. MCB and LK performed the experiment. MCB completed molecular lab work, with exome capture and sequencing assistance from Arbor Biosciences and the University of Chicago Genomics Core. MCB completed all bioinformatics, statistical, and computational analyses. MCB wrote the manuscript with inputs from LK, JPG, and CAP.

CHAPTER 3

THE MOLECULAR BASIS OF ADAPTATION TO OCEAN ACIDIFICATION

3.1 Abstract

Reductions in seawater pH pose extensive threats to marine communities globally. The physiological consequences of this process have become increasingly well characterized across a range of potentially sensitive species. Yet, mechanistic links between how low pH seawater alters organismal physiology and the macroscopic traits upon which selection will ultimately act (e.g. growth, fecundity, etc.) are largely missing from the literature. Additionally, while the impact of expected pH conditions is, on average, detrimental for many species, the extent to which the genes underlying observed physiological responses harbor the variation necessary to evolve as global change progresses is an outstanding question. To resolve these gaps, we leveraged numerous independent approaches to identify candidate genes driving the low pH response in *Mytilus galloprovincialis* larvae, and provide mechanistic links between these candidates and low-pH induced morphological abnormalities. We then used selection coefficient and gene expression analyses to demonstrate that variation at candidate genes impact larval fitness in low pH. In concert, these findings help to explain the broad impacts of changes in seawater pH across a range of marine metazoans, while further suggesting the potential adaptive resilience of marine species as global change progresses.

3.2 Introduction

Observed and projected changes in global oceanic carbonate chemistry have necessitated an understanding of the biological consequences of reductions in seawater pH, a process termed ocean acidification (OA). Seminal research in the field has predominately focused on the average effect of OA on foundational marine species that calcify, such as corals and

phytoplankton (Kleypas *et al.*, 1999; Riebesell *et al.*, 2000). The scope of experimental studies has since expanded and detrimental effects of expected pH on the survival, growth, and abundance in a range of marine taxa are now documented, suggesting dramatic changes to the demographics of natural populations as global change progresses (Kroeker *et al.*, 2013). Such broad impacts may be expected, as maintenance of intracellular pH is fundamental to cellular homeostasis and affects myriad biological processes (Casey *et al.*, 2010). Indeed, evidence for a limited capacity of marine species to regulate intracellular pH under OA conditions has accrued, further suggesting the wide-spread implications of the process across biological traits and species (Melzner *et al.*, 2017; Venn *et al.*, 2013).

The physiological basis of OA sensitivity, which may underlie expected demographic impacts across marine organisms, is additionally becoming resolved. A recent meta-analysis of metazoan transcriptomic-responses to OA identified a strikingly conserved molecular response throughout this diverse group. Specifically, OA conditions consistently elicit shifts in acid-base ion regulation, metabolic processes, calcification, and generalized stress response mechanisms (Strader *et al.*, 2020). While this work provides a generalized characterization for how OA impacts organismal physiology, the candidate genes and pathways driving these broad responses remain largely unknown. Furthermore, though numerous studies note that the impact of seawater pH are, on average, detrimental to a range of marine taxa (Kroeker *et al.* 2013), this viewpoint overlooks the substantial inter-individual variation in sensitivity to global change conditions. Such phenotypic variation, when attributable to underlying differences in the genetic makeup of individuals, will provide the raw material for rapid adaptation to shifts in the pH environment. This process may thus in turn offset many of the expected demographic consequences predicted as a result of OA. The present study utilizes the ecologically and economically important marine bivalve, *Mytilus galloprovincialis*, to both resolve the mechanistic basis of low pH sensitivity and further highlight the substantial adaptive capacity of the species to future ocean acidification.

The effects of OA on *Mytilus* mussels have been explored across all life history-stages.

The impacts on early development, however, have received extensive investigation and are now described in detail. Specifically, OA slows larval development and reduces the saturation state of the calcifying space in the leading shell edge, ultimately depressing D-veliger shell size and integrity (Kapsenberg L. *et al.*, 2018; Melzner *et al.*, 2017). Trochophore larvae exhibit heightened sensitivity to low pH seawater, with OA conditions causing abnormal formation of soft tissue, a process that ultimately induces mortality during the shell growth period (Kapsenberg L. *et al.*, 2018). A recent study by Bitter *et al.* 2019, however, suggests that rapid adaptation may effectively offset the observed phenotypic consequences of OA in the species. Specifically, the study tracked the phenotypic and genetic modifications of a genetically diverse population of *M. galloprovincialis* reared in low pH seawater, throughout larval development and settlement. Patterns of shell size during the pelagic feeding stage indicated that selective mortality allowed the larval population to recover from the impacts of OA on early calcification. Observed patterns of larval survival and genomic variation indicated the vast majority of pH-induced selection occurred during the trochophore to D-veliger transition. Additionally, the study identified signatures of selection that were unique to the low pH environment, suggesting the presence of adaptive variation at putatively functional genes (Bitter *et al.*, 2019). Yet, despite its relevance, the underlying mechanisms by which OA impair trochophore development and drive observed signatures of selection is still unknown. Resolving such mechanistic links will provide key insight into how bivalves will respond to an increasingly acidic ocean.

Here, we identify candidate genes and molecular pathways involved in the *M. galloprovincialis* larval low pH response and provide mechanistic links between these genes and low pH-induced developmental abnormalities. We then assess how individuals from distinct genetic backgrounds vary in their patterns of expression at candidate genes to further elucidate the capacity of such pathways to evolve under OA. We rely on five distinct types of data and analyses to link processes at the gene level with development of larvae under OA conditions – (i) A population-wide transcriptomics study of trochophore larvae reared

in ambient and low pH treatments. (ii) Novel analyses of allele frequency data generated by Bitter *et al.* (2019) to compute the strength of selection at candidate genes exhibiting variation for low pH tolerance. (iii) Functional validation of candidate genes identified in analyses (i) and (ii) using real-time quantitative PCR (qPCR). (iv) *In situ* hybridizations of two candidate genes putatively involved in shell formation to confirm localization of gene expression within the trochophore shell field. (v) A larval low pH exposure experiment from a series of unique male x female crosses to identify the presence of genotype-specific patterns of expression at candidate genes, and link these patterns at the molecular level with differences in a macroscopic trait, larval shell size.

Our transcriptomics and qPCR analyses identified 19 genes involved in the larval physiological response to OA. Leveraging existing annotation and pathway information of these candidates, we demonstrate how the functions of these candidates manifest in the shell and soft-tissue abnormalities observed in mussel larvae reared in low pH. Our selection coefficient analysis demonstrates the capacity for 6 of these loci to rapidly evolve, while differences in gene expression and shell size plasticity across larval families suggests genotype-environment interactions as a fundamental driver of adaptation to global change.

3.3 Methods

3.3.1 Transcriptomic response in trochophore larvae

We quantified transcriptome-wide patterns of gene expression of *M. galloprovincialis* trochophore larvae to identify pathways and genes driving the physiological response of the species during its most sensitive life-history stage. Specifically, larvae from 9 male x female crosses were pooled and reared in a lab system consisting of four pH treatments, with three replicate buckets per treatment, and described in Kapsenberg*et al.* (2018). Briefly, two treatments exposed larvae to low pH ($pH_{Total(T)} = 7.4$) during the trochophore stage and induced phenotypic abnormalities, while the remaining two treatments exposed larvae

to ambient pH conditions (pH_T = 8.1) and resulted in larvae with predominately normal development (Kapsenberg *et al.*, 2018). Approximately 60,000 larvae were sampled at the mid-trochophore stage (33 hours post-fertilization), preserved in trizol, and frozen at -80^oC until RNA extractions. Total RNA was shipped on dry ice from France to the University of Chicago where extract quantity and quality was determined via Bioanalyzer, which demonstrated high quality extracts with RIN scores >9.0. The twelve total RNA samples were sequenced on a single lane of Illumina HiSeq4000, yielding an average of 6.4 Mbases per sample.

Raw RNA sequencing reads were filtered to trim adapters and remove PhiX contamination, low quality reads, and polyA tails. Filtered reads were mapped to the *M. gallo-provincialis* reference transcriptome provided by Moreira *et al.* 2015 using SALMON (Patro *et al.*, 2017). The resulting transcript counts for all samples were analyzed using custom R scripts and the *edgeR* package (Robinson*et al.*, 2010). After filtering, a total of 48,000 transcripts were available for the identification of differentially expressed genes. Data were pooled by larval pH exposure during the trochophore stage, yielding 6 replicates per group. Genes were identified as differentially expressed given an FDR corrected p-value <0.05. Known pathways and networks of differentially expressed genes were explored using the publically available databases UniPROT (https://www.uniprot.org/), Gene Ontology Resource (http://geneontology.org), and STRING (https://string-db.org/) to further gain mechanistic insights into the pathways most altered by low pH seawater. The transcriptomics data was also used to identify gene ontologies overrepresented in the larval low pH physiological response using the goMWU software (Wright *et al.*, 2015). This method leverages observed log-fold change data across all transcripts to identify ontologies that are enriched among either up or down-regulated transcripts using the Mann-Whitney U Test.

3.3.2 Allele frequency analysis and selection coefficient computation

Data from Bitter*et al.* (2019) was used to identify genes that exhibit genetic variation and significant shifts in allele frequency during larval development under an extreme OA-scenario. Briefly, the study reared a genetically diverse larval population of*M. galloprovincialis* at an ambient pH_T level of 8.1 and reduced pH_T level of 7.4 throughout the larval pelagic phase and settlement. The study used a combination of Fisher's Exact test and the Cochran-Mantel-Haenszel test to identify loci with significant deviations in allele frequency between the day 0 larval population and the replicate buckets in each treatment on days 6, 26, and 43 of development. Through this, 29 annotated loci were identified as exhibiting significant shifts in allele frequency on all days of sampling within the low pH treatment. For the present study, existing annotations, ontology, and pathway information were used to further winnow this list to candidate genes putatively involved in the low pH response. These included tyrosinase, chitinase, kinesin, heat shock protein 70, ubiquitin protein ligase, and a thyroid receptor interacting protein. To quantify the strength of selection acting on these loci in the low pH environment, selection coefficients were computed using observed changes in the survival probability of the favored genotype at each candidate gene pre- (day 0) and post-selection (day 26), and in accordance with equations provided by Graham Coop, which are publicly available at: github.com/cooplab/popgen-notes. The frequency of the selected allele was our metric of survival probability and selection coefficients (s) were computed as follows:

$$s = \left| \frac{p_{d0} - p_{d26}}{(p_{d0} - 1)(p_{d26})} \right|$$

where p corresponds to the frequency of the selected allele in the larval population on days 0 (d0) and 26 (d26). In cases in which multiple selected alleles were identified on the same gene, the allele exhibiting the least variation in allele frequency estimates across replicates was used to compute selection coefficients.

3.3.3 Verification of candidate genes by qPCR

qPCR was conducted to provide functional validation of the genes identified via transcriptomics and allele frequency analyses in the larval low pH physiological response. This included all 6 candidate genes identified in the allele frequency analysis and 13 additional, non-overlapping, genes identified as differentially expressed via transcriptomics. qPCR primers were designed for each target and, in some cases, multiple primers were designed using distinct isoforms from the same target gene. Primer pair information, including efficiency testing results, is provided in Table S5. The same total RNA samples isolated for the transcriptomics analyses in (I) were utilized for qPCR. As these samples were generated from an experiment in which larvae from multiple crosses were pooled within each replicate bucket, this assay once again queries the population-wide response at candidate genes.

Total RNA was converted to cDNA using the Applied Biosystems High-Capacity-RNA-to-cDNA kit, as per manufacturer instructions. qPCR reactions were performed on the Applied Biosystems StepOnePlus real-time PCR system, with a total reaction volume of 15 µL consisting of 7.5 µL SYBR Green PCR Master Mix (Applied Biosystems), 1 µL 10 µM primer, 3 µL DNA, and 3 µL DI water per reaction. Six replicates were run per target and treatment. Controls lacking cDNA template were included for each target so as to further validate primer efficiency and identify the presence of non-target contamination. Relative expression of target mRNAs was computed using the comparative CT method and is reported as the $\log_2$-transformed fold change, relative to ambient treatment expression (Schmittgen and Livak, 2008). Significant differences in expression between treatments were determined using a permutational multivariate analysis of variance (PERMANOVA) in R with 999 permutations.

3.3.4 In situ hybridizations

To identify the location of expression within the larval body of two candidate genes likely involved in shell biogenesis, primers for *in situ* hybrization were designed for tyrosinase

and chitinase, following the methods described in Miglioli *et al.* (2019). We additionally conducted hybridizations on a candidate gene not expected to be involved in shell biogenesis, heat shock protein 70, to serve as a control in confirming shell field localization. Larvae for hybridizations were reared in static cultures ($pH_T = 8.0$ at 16.5°C) and sampled at 29 hours post-fertilization. Larvae were preserved in 4% paraformaldehyde and hybridizations were carried out using the methods of Miglioli *et al.* (2019).

3.3.5 Identifying patterns of genotype-environment interactions at candidate genes

We manipulated the genetic background of mussels through controlled crosses to identify genotype-specific patterns of expression at the pH-responsive genes identified above (i.e. genes exhibiting differential expression between treatments and genes both differentially expressed and exhibiting signatures of selection in response to low pH). We additionally connected patterns of expression to a higher-level phenotypic trait correlated with larval fitness, shell size (Allen, 2008; Kapsenberg *et al.*, 2018). Using the same CO_2 manipulation experimental system as previous assays, the offspring of 6 unique male x female crosses were reared in static ambient ($pH_T = 8.1$) and low pH ($pH_T = 7.5$) treatments. Though the low pH treatment for this experiment was higher than that used for the above experiments, it still falls far below contemporary pH values observed in study population's natural habitat and has been shown to induce stress on developing larvae (Kapsenberg *et al.*, 2018). Larvae were reared through the early D-veliger stage (72 hours post-fertilization), homogenized in trizol, and frozen at -80°C. Larvae were shipped frozen on dry ice from France to the University of Chicago, where total RNA was isolated using the EZNA RNA extraction kit for molluscan tissue. Total RNA quantity and quality assessment, cDNA template generation, and qPCR reaction methods were all identical to those described above. Log_2-transformed expression values for each gene were computed for all larval families in the ambient and low pH treatment. This data thus provided a proxy for each family's expression relative to all

others and was used to compare patterns of expression across genes between larvae from distinct genetic backgrounds.

The contributions of treatment and family on observed gene expression patterns were assessed using a linear model, in which the significance of the fixed effects (i.e. treatment and family) was determined using an ANOVA. We quantified the molecular plasticity of each family at candidate genes using a linear regression. Specifically, gene expression was modeled as a function of pH treatment, the linear coefficient of which provided our metric of molecular plasticity. Next, larval shell size for each family was quantified in the ambient and low pH conditions to provide an additional metric for genotype-specific responses to low pH exposure. Larval shell size was determined as the maximum shell length parallel to the hinge using brightfield microscopy and image analysis in ImageJ. The contribution of treatment and family on larval shell size was assessed using a linear mixed effects model, with treatment and family as fixed effects and larval bucket as a random effect (*lme4* package in R). The significance of fixed effects was quantified using a likelihood ratio test. We then quantified differences in shell size plasticity across families in the same manner as for molecular plasticity – shell size was modeled as a function of pH treatment, the linear coefficient provided a metric of shell size plasticity. We identified trait correlations between the gene expression and shell size plasticity data using Pearson's correlation coefficient and the *corr* function in R. Finally, treatment-based differences in the total phenotypic variation of each trait were quantified as the standard deviation of $\log_2$-transformed expression and shell size across families. Through this, we aimed to determine whether exposure to stressful conditions resulted in a release of phenotypic variation.

3.4 Results

3.4.1 Transcriptomics

The transcriptomic analysis revealed 40 differentially expressed genes when larvae were exposed to low pH during the mid-trochophore stage, compared to those exposed to ambient pH (Table S6). Of these, 39 were up-regulated, while only 18 contained annotations in the published transcriptome provided by Moreira *et al.* 2015. The gene ontology (GO) enrichment analysis, however, identified numerous overrepresented gene ontologies altered by the low pH exposure, with 59 and 41 biological processes and molecular function ontologies enriched, respectively. This analysis indicated the effect of low pH exposure on stress response and metabolic pathways (e.g. oxioreductase, antioxidant, ubiquitin protein transferases), cytoskeletal processes (e.g. microtubule motor, myosin heavy chain binding, movement of cell or subcellular component, anatomical structure morphogenesis) and biomineralization pathways (e.g. macromolecule biosynthetic process) (Fig. 3.1). Interestingly, the distribution between up and down-regulated ontologies was similar among enriched ontologies, in contrast to the disproportionate number of up-regulated differentially expressed genes.

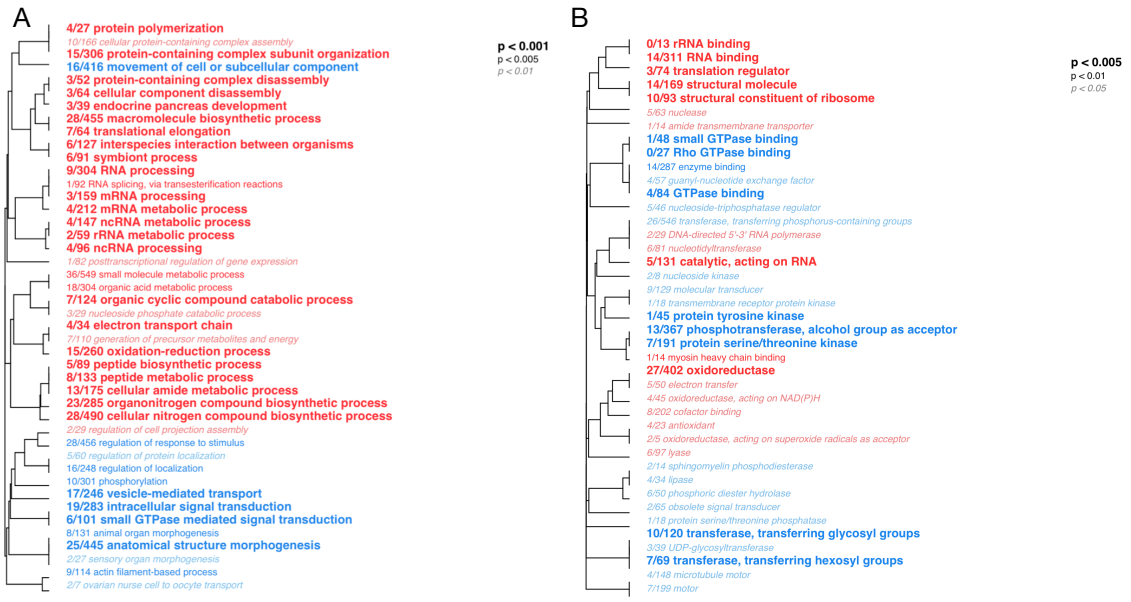

Figure 3.1: Enriched gene ontologies identified during larval low pH response. Hierarchical clustering of overrepresented ontologies involved in biological processes (A) and molecular functions (B). Text size corresponds to ontology p-value significance and text color corresponds to up (red) or down (blue) regulation of ontology. Ratios preceding each ontology correspond to the number of genes within the ontology exhibiting an unadjusted p-value <0.05 relative to the total number of genes within the category.

3.4.2 Allele Frequency, selection coefficient, and qPCR analyses

Selected SNPs at the 6 candidate genes identified in the Bitter *et al.* dataset exhibited dramatic shifts in frequency in the low pH treatment between days 0 and 26 of development, ranging from 5 to nearly 25% (Fig. 3.2). These changes in allele frequency corresponded to selection coefficients ranging between 0.5 and 3.4 (Fig. 3.3). qPCR analysis indicated that all genes displaying signatures of selection after 26 days of treatment exposure exhibited significant increases in expression in the low pH environment 33 hours into development (Fig. 3.2). Furthermore, 11 out of the 13, functionally annotated, differentially expressed genes identified in the transcriptomics analysis, were also confirmed by qPCR to be responsive in

low pH (Fig. S11, Table S5).

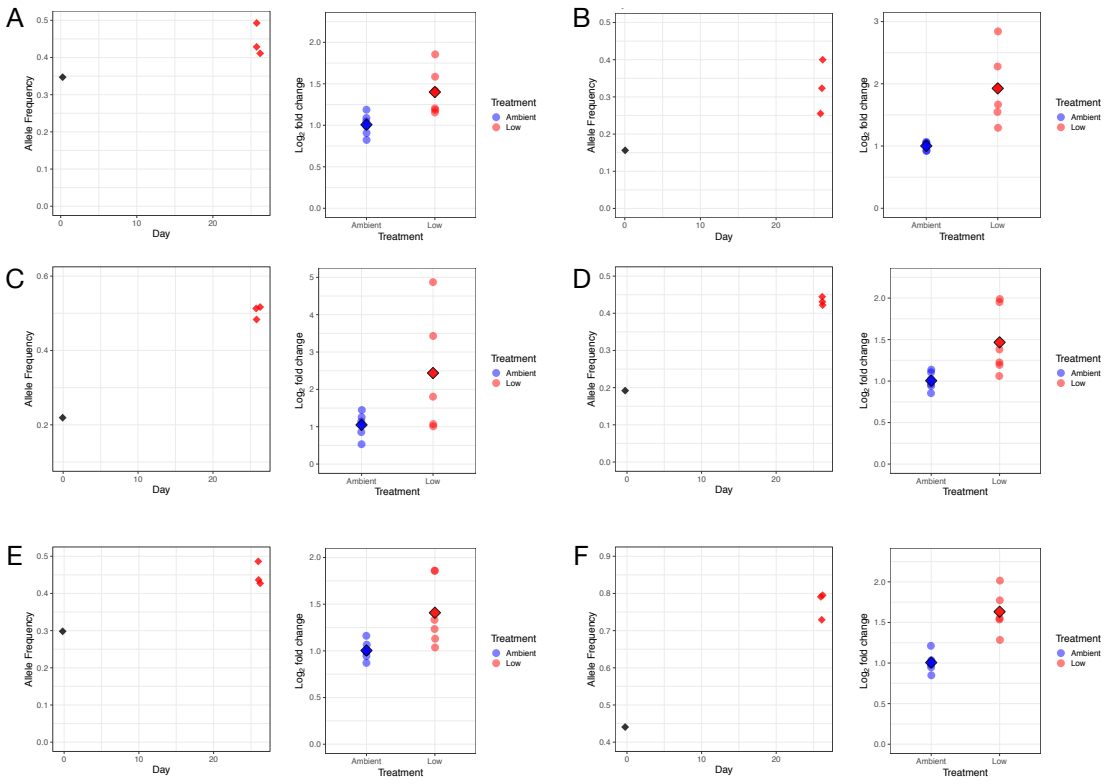

Figure 3.2: Shifts in genetic variation and expression at candidate genes. Observed allele frequency shifts in low pH between days 0 and 26 and log2-fold-expression of larvae sampled 28 hours post-fertilization at (A) heat shock protein 70, (B) tyrosinase, (C) ubiquitin protein ligase, (D) kinesin, (E) thyroid-receptor interacting protein, and (F) chitinase.

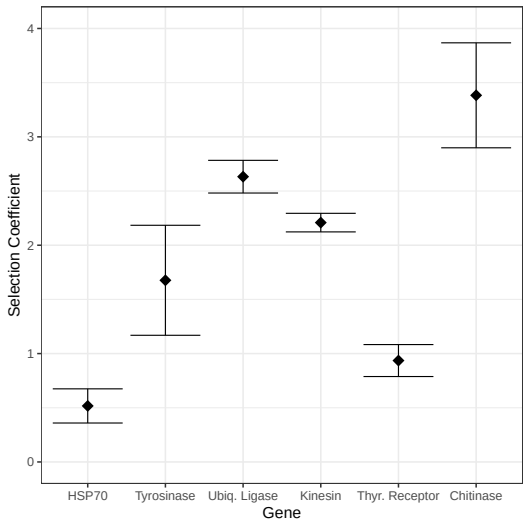

Figure 3.3: Selection coefficients(± SE) at candidate genes.

3.4.3 in situ hybridization of shell biogenesis genes

Tyrosinase and chitinase, our candidate genes with known involvement in biomineralization pathways, each exhibited localized expression in the trochophore shell field, the site of larval calcification and shell growth. Specifically, expression borders the shell field on the right side of the larval body in Figure 3.4.

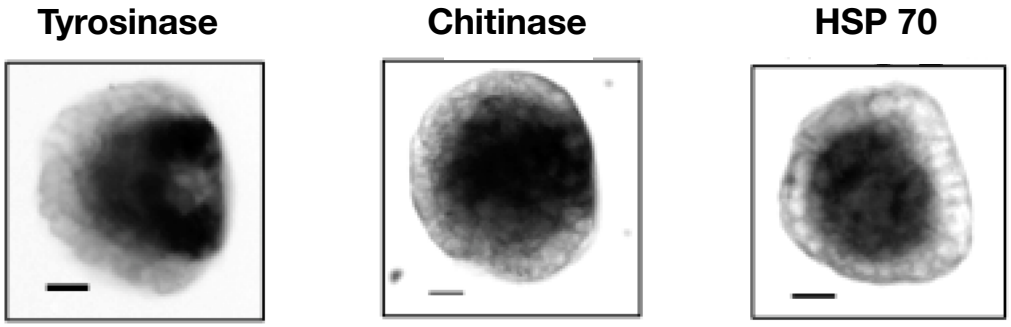

Figure 3.4: *In situ* hybridizations of two candidate genes putatively involved in shell biogenesis, tyrosinase (A) and chitinase (B), and a candidate not expected to exhibit shell field localization, heat shock protein 70 (C). The extension of expression toward the shell field (right side of larval body) can be observed in tyrosinase and chitinase, yet is absent in heat shock protein 70.

3.4.4 Genotype-specific responses to low pH exposure

Genetic background induced a strong effect on the low pH response at both the molecular and morphological-level. Across all male x female crosses, expression at candidate genes was significantly affected by both low pH exposure ($F_1 = 5.3$, $p = 0.02$) and family ($F_5 = 3.0$, $p = 0.01$). Linear regressions of pair-specific patterns in expression across treatments identified order of magnitude differences in molecular plasticity across families, ranging from -1.34 to 0.87 (Fig. 3.5). Significant effects of both treatment ($\chi_1 = 8.9$, $p = 0.003$) and family ($\chi_5 = 114.6$, p) were identified in the larval shell size data. While all larvae exhibited a reduction in shell size between treatments, differences in the magnitude of these changes were again substantial and showed a 14-fold change between families, from 1.7 to 24.4 μm * pH^{-1} (Fig. 3.5). The correlation between gene expression and shell size plasticity was only marginally significant ($t = 2.48$; $p = 0.07$). Finally, a dramatic elevation in the phenotypic variation

in low pH was observed across all families for both log_2-fold-expression (ambient pH SD = 0.77; low pH SD = 1.03) and shell size (ambient pH SD = 6.5; low pH SD = 8.6).

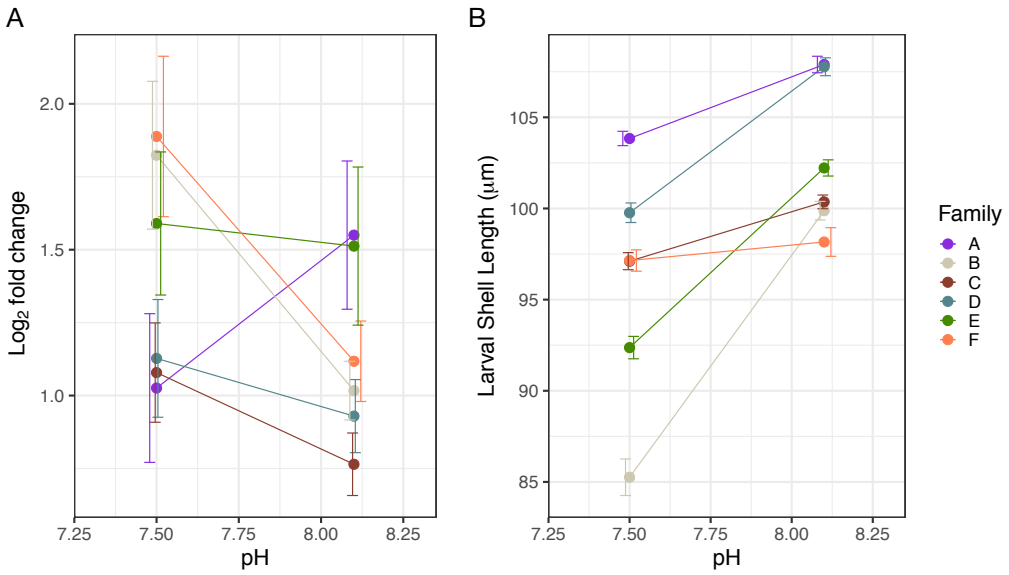

Figure 3.5: Family-based differences in the low pH response. (A) Mean (± SE) log_2-fold expression at candidate genes of larvae from six families reared in ambient and low pH. (B) Mean (± SE) shell size of larvae from the same six families reared in ambient and low pH.

3.5 Discussion

An extensive body of work documenting the phenotypic consequences of OA has accumulated over the past two decades, and the molecular pathways underpinning these responses are now being explored. Here, we combine multiple approaches to effectively identify core molecular pathways and genes involved in the bivalve low pH response, draw mechanistic links between responsive genes and observed phenotypic abnormalities, and elucidate

genotype-environment interactions as a fundamental driver of evolution in changing seas.

3.5.1 The molecular response of M. galloprovincialis to ocean acidification

Results generated from the transcriptomics analyses lend to the growing body of work documenting the broad molecular response of marine taxa to reductions in seawater pH. As with previous studies, overrepresented gene ontologies highlight the importance of generalized stress response and metabolic pathways, ion-homeostasis and cytoskeletal processes, and biomineralization pathways in the bivalve low pH response (Strader *et al.*, 2020). The total number of differentially expressed genes (40) was far fewer than that of overrepresented ontologies/pathways (100), highlighting the limited biological insight gleaned from a analysis in which only annotations and pathway information from genes passing an arbitrary statistical cutoff are considered. The total number of differentially expressed genes identified also falls below that in many previous studies across a range of species (Evans *et al.*, 2017, 2013; Goncalves *et al.*, n.d.; Johnson and Hofmann, 2017; Kaniewska *et al.*, 2015). This discrepancy may in large part be due to statistical artifacts, such as differences in models of gene expression and significance cutoffs, or experimental details, such as treatment exposure time and life-history stage (Evans *et al.*, 2013; Johnson and Hofmann, 2017).

Two of the differentially expressed genes from the transcriptomic analysis, tyrosinase and ubiquitin protein ligase, overlapped with those exhibiting strong signatures of selection in the low pH environment during larval development. Tyrosinase genes are recognized for their role in periostracum formation across marine bivalves (Zhang *et al.*, 2006), and their role in early larval shell formation of *M. galloprovincialis* has recently been described in detail (Miglioli *et al.*, 2019). Unsurprisingly, tyrosinase genes are differentially expressed in response to low pH in a range of calcifying invertebrates, including *Mytilus* mussels (Huning *et al.*, 2012), oysters (Yang *et al.*, 2016), and pteropods (Johnson and Hofmann 2017). Ubiquitin protein ligases play fundamental roles in the cellular stress response, particularly protein folding and degradation (Imai 2000). Though the four remaining genes with strong

signatures of selection were not identified as differentially expressed by our transcriptomics analysis, our qPCR validation demonstrates that these candidates were indeed false negatives in that dataset, highlighting the potential limitations of such 'omics-based approaches in the absence of cross-validation with independent assays. These candidates included chitinase, another gene implicated in larval shell biogenesis (Miglioli *et al.*, 2019), heat shock protein 70, a well-studied gene involved in the metazoan cellular stress responses (Feder and Hofmann 1999), and two genes involved in cellular proliferation, migration and cytoskeletal formation, kinesin and a thyroid receptor-interacting protein. This list of candidate genes provides further evidence of the wide-ranging physiological impacts of OA, yet potentially pinpoints some of the core genes within these pathways driving the larval low pH response. It is important to note that these candidates were identified using only the subset of annotated genes in the transcriptomics (19 out of 40 differentially expressed genes) and allele frequency analysis (29 of 88 outlier loci). This highlights the current limitations of working within the context of non-model species and the potential for further mechanistic insight as molecular resources become increasingly available.

This is the first study to link shifts in expression at genes responding to low pH stress with evidence of selection via allele frequency change during larval development. It is likely that genotype-specific patterns of expression at these loci drive variation in the occurrence of early developmental abnormalities of trochophore larvae, ultimately driving differences in relative fitness and producing the observed signatures of selection at candidate genes in low pH on day 26 of development. Our selection coefficient estimates, ranging from 0.5 to 3.4, indicate strong signatures of selection at these candidate genes during experimental low pH selection. While it is possible that the direction and strength of selection at these candidates may be variable across life-history stages (Schluter *et al.*, 1991), our sampling encompasses the most sensitive life-history stage, suggesting that incorporating data across multiple generations may not have an appreciable impact on these estimates. Our selection coefficients indeed fall within ranges inferred from emerging research on the genomic dynam-

ics of rapid evolutionary processes. For example, inferred selection coefficients for genetic variants under selection in an evolving intra-host HIV population were of similar magnitude (Feder *et al.*, 2019). Theoretical work suggests that adaptation under such strong selection is likely to take place via "soft" selective sweeps, whereby standing variation is rapidly fixed throughout the genome (Hermisson and Pennigs 2005, Messer and Petrov 2010). Thus, the data presented here suggests that favored genotypes could rise rapidly in frequency as global change progresses, potentially offsetting many of the anticipated, and detrimental, phenotypic effects.

3.5.2 Proposed cellular mechanisms of low pH sensitivity and abnormalities

The multiple approaches we have taken here provide the opportunity to draw mechanistic links between our candidate genes and observed phenotypic abnormalities of *M. galloprovincialis* reared in low pH seawater. Kapsenberg *et al.* 2018 first described the direct impact of low pH seawater on calcification-independent processes during the trochophore stage. Specifically, prior to the formation of the larval shell field upon which calcification proceeds, a group of ectoderm cells are invaginated, generating a pore over which the periostracum is secreted. Following this invagination, the pore closes and invaginated cells evaginate to form a flat region beneath the periostracum, which expands via mitotic division. Under low pH conditions, the evagination process is disrupted, precluding the formation of a linear hinge and manifesting in shell deformations during the D-veliger stage (Fig. 3.6).

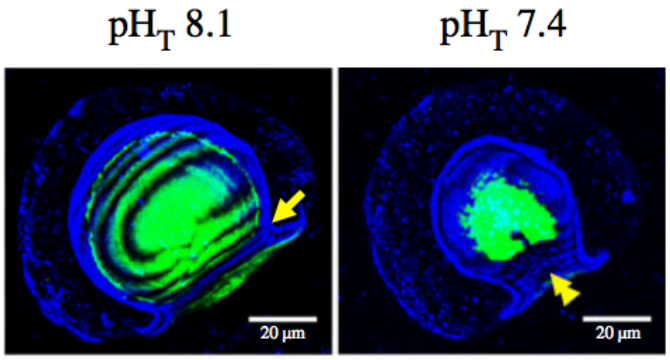

Figure 3.6: Phenotypic consequences of low pH on *M. galloprovincialis* trochophore as presented in Kapenberg *et al.* (2018). Composite confocal images of larvae at 35 hours post-fertilization in which calcium carbonate has been stained green and the organic matrix stained blue. Single arrows in left panel (ambient pH) indicate evaginated pore, while double arrows in right panel (low pH) indicate pore that has failed to evaginate.

Two of our candidate genes, kinesin (Swissprot ID Q9EQW7) and a thyroid receptor interacting protein (Swissprot ID Q15643), likely play key roles in this process. Specifically, kinesins are a superfamily of microtubule motor proteins involved in cytoskeletal formation and mitosis (Dair and Pous 2011), and their activity is inhibited by reductions in intracellular pH (Verhay *et al.*, 2007). Associated ontologies further demonstrate kinesin's role in cell proliferation and include cell cycle (GO:0007049), cell division (GO:0051301), and regulation of cytokinesis (GO:0032465). The thyroid receptor interacting protein we identified is involved in an ArfGAP protein network (STRING database). ArfGAPs are multifunctional proteins regulating membrane traffic and actin remodeling and are involved in cell shape, movement, and migration (Randazzo and Hirsch, 2004). In concert, disruptions to the functions of kinesin and the thyroid receptor interacting protein likely alter the efficacy of cell division and evagination, ultimately reducing the integrity of soft tissue formation of trochophore larvae reared in low pH. Our gene ontology enrichment analysis further indicated alterations to this pathway, as enriched ontologies included anatomical structure morphogenesis, move-

ment of cell or sub-cellular component, actin filament-based process, and microtubule motor (Fig. 3.1). In concert, our candidate genes, as well as enriched ontologies identified using transcriptomics, highlight that the direct impact of low pH seawater on developing bivalve larvae induce pronounced effects on cellular processes, which can manifest as soft tissue abnormalities in developing larvae. Fundamentally, disruptions to such cellular processes may be driven by alterations to intracellular ion concentrations, as mounting evidence suggests a limited capacity of calcifying marine species to regulate intracellular pH during extreme low pH exposure (Melzner *et al.*, 2017; Venn *et al.*, 2013) As observed soft tissue abnormalities are likely lethal, this mechanism may explain the substantial signatures of selection observed by six days into development in low pH seawater (Kapsenberg *et al.*, 2018, Bitter *et al.*, 2019). Furthermore, as these processes are ultimately independent of calcification mechanisms, we suspect this mechanism to drive OA sensitivity across a range of both calcifying and non-calcifying marine species.

The presence of two candidate genes involved in larval shell biogenesis, tyrosinase and chitinase, support the substantial body of work describing the direct impact of low pH seawater on shell formation in marine bivalves. Each gene has been implicated in the formation of the organic shellfield (Miglioli *et al.*, 2019), as was corroborated by our *in situ* hybridization data. Though identification of this mechanism is not novel, this is the first study to identify variation at specific genes involved in this pathway, thus demonstrating that rapid evolution may indeed offset expected declines in the shell development of this foundation species as global change progresses. However, we suggest that the impacts of low pH on biomineralization pathways may be secondary to the calcification-independent process described above, as we lack evidence that delayed development and depression of shell growth produce the magnitude of fitness costs as that induced by soft tissue abnormalities.

3.5.3 Genotype-environment interactions as a driver of evolution to ocean acidification

While many studies documenting the biological effect of expected global change conditions have quantified and reported population or species-wide responses, this approach overlooks potential inter-individual differences in pH sensitivity. Our pair-based analysis of genes responding to changes in seawater pH and shell size plasticity highlight the substantial variation in sensitivity to low pH within a single population of *M. galloprovincialis*. For each trait, the magnitude of responses varied dramatically among families, ultimately producing shifts in the order of trait values (e.g. largest to smallest offspring) between families in each treatment. This corroborates findings of Bitter *et al.* (2019), which used genomic variation data to demonstrate that the fastest growers in ambient pH were of a distinct genetic background to those reared in low pH . Similarly, Campbell *et al.* (2016) documented shifts in the sperm competiveness of different genotypes in ambient and low pH conditions. Such studies highlight the emergence of potential trade-offs under global change, and suggest the importance of maintaining variation to bolster species resilience and adaptive capacity.

The observed correlation between gene expression and shell size plasticity indicates that the genes identified above indeed influence larval growth, a proxy of fitness, in low pH seawater. While the direction of shell size response was identical across families (i.e. all families had a reduction in shell size in low pH), we observed one family exhibiting a net down-regulation of pH-responsive genes, while all other exhibited a net up-regulation. This provides further evidence of genotype-specific patterns of expression at genes influencing larval fitness in low pH. Selection on variation in gene expression is recognized as a fundamental driver of adaptation within and between species (Whitehead and Crawford 2006), and the data presented here demonstrate its potential role in adaptation to OA. Interestingly, the family exhibiting the opposite gene expression response also exhibited the largest shell size in both ambient and low pH treatments. These observations thus provide a novel link between two traits, each acting at distinct levels of biological organization, affected by OA. In concert, these

results suggest that variation in OA sensitivity is underpinned by genotype-environment interactions.

Finally, our quantification of phenotypic variation across families in each treatment indicated a release of variation in the stressful environment, whereby the variance in trait values for both gene expression and shell size across families was elevated. This lends support to a growing body of work demonstrating that novel and/or stressful environments release previously cryptic variation within natural populations, and may ultimately augment rapid adaptation (Paaby and Rockman, 2014). The ubiquity of this phenomenon within the context of OA, and across taxa, may be masked by studies reporting mean effect sizes across groups, and thus presents an important area of future investigation for the field.

3.5.4 Concluding remarks

The consequences of ocean acidification at the species level will be severe across a broad range of species (Kroeker *et al.*, 2013). These single-species effects are expected to reverberate throughout ecological networks, potentially altering the structure and function of marine communities as global change progresses (Pfister *et. al.,* 2014). Identifying candidate pathways disrupted by low pH conditions, however, may provide an efficient means to predict which groups of species may be particularly sensitive, and ultimately augment targeted management efforts to increase the resilience of natural populations as global change progresses. The multiple approaches we adopted here demonstrate the contributions of both shell and soft tissue-based processes on the functional response of marine bivalves to OA. Additionally, these findings highlight the importance of linking responses at the molecular level to macroscopic traits in quantifying organismal sensitivities to global change stressors. Finally, we have shown that metrics of species or population-wide sensitivities may mask the variation available for rapid evolution within natural populations, thus skewing the perceived resilience of species to global change.

3.6 Author Contributions

Mark C. Bitter, Lydia Kapsenberg, and Angelica Miglioli designed and completed the numerous experiments associated with this work. MCB conducted gene ontology, qPCR, and selection coefficient analyses. The transcriptomics dataset was generated by the UC Davis Genome Center and *in situ* hybridizations were conducted by AM. MCB wrote the chapter with input from LK and Catherine A. Pfister.

SUPPLEMENTARY FIGURES

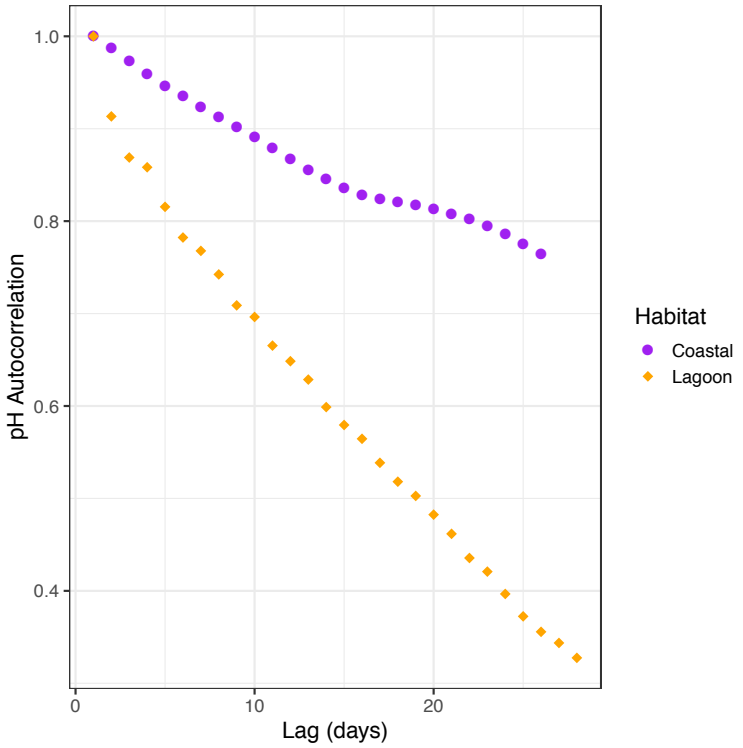

Figure S1: pH autocorrelation across daily lag intervals in the coastal (purple circles) and lagoon (orange diamond) habitats.

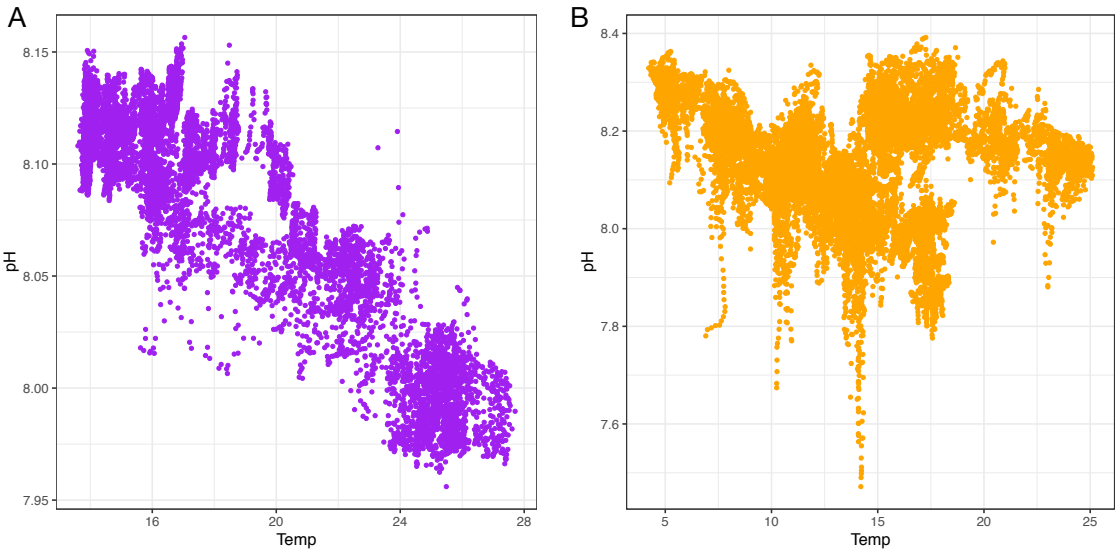

Figure S2: Correlation between temperature and pH in the (A) coastal (R^2 = -0.9, t = -180.86, p <0.001) and (B) lagoon ($R2$ = -0.13, t = -22.63, p <0.001).

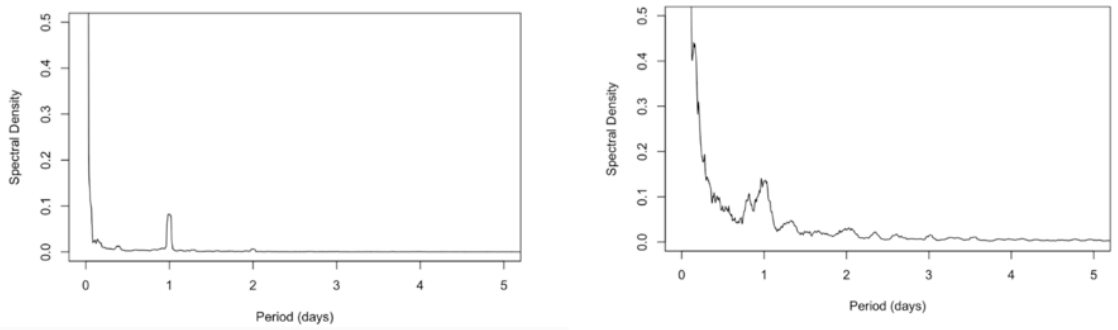

Figure S3: Spectral analysis of pH time-series from the coastal (A) and lagoon (B) sites.

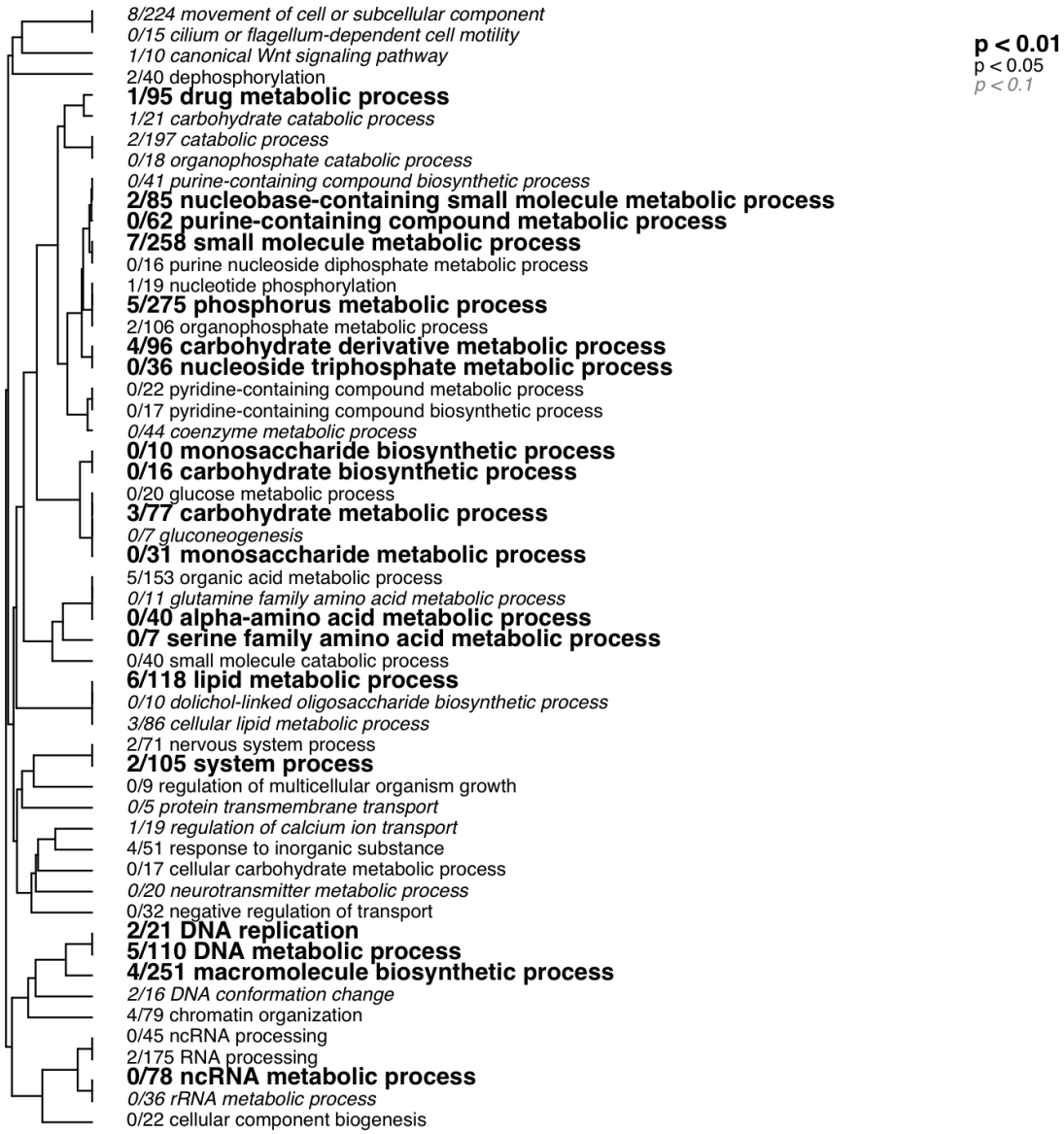

Figure S4: GO enrichment analysis output for population differentiation in ambient conditions, in which the coastal population was used as the reference. Text size indicates FDR-corrected p-value significance. Ratios before each branch indicate how many transcripts within each ontology exhibited a $\log_2$-fold-change >1.

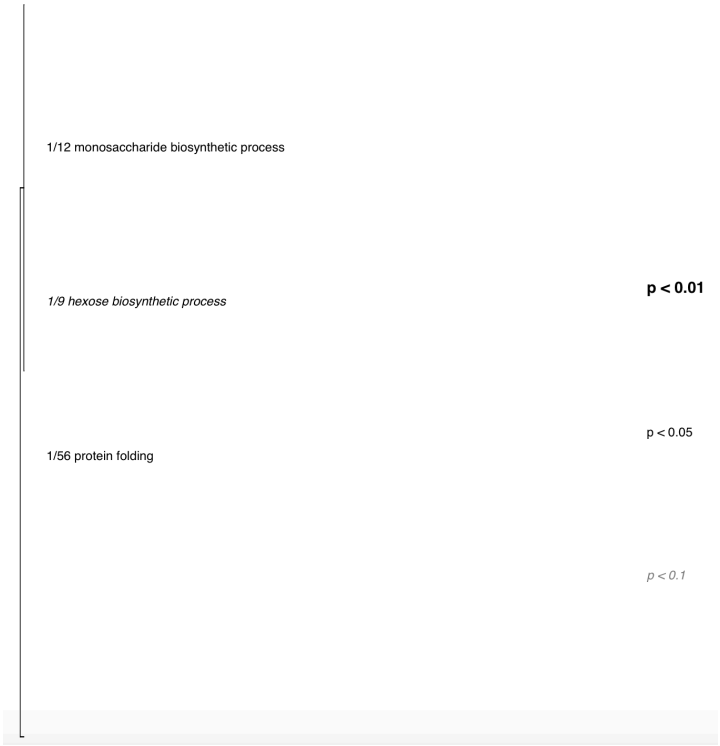

Figure S5: GO enrichment analysis output for population differentiation in low pH conditions, in which the coastal population was used as the reference. Text size indicates p-value significance. Ratios before each branch indicate how many transcripts within each ontology exhibited a $\log_2$-fold-change >1.

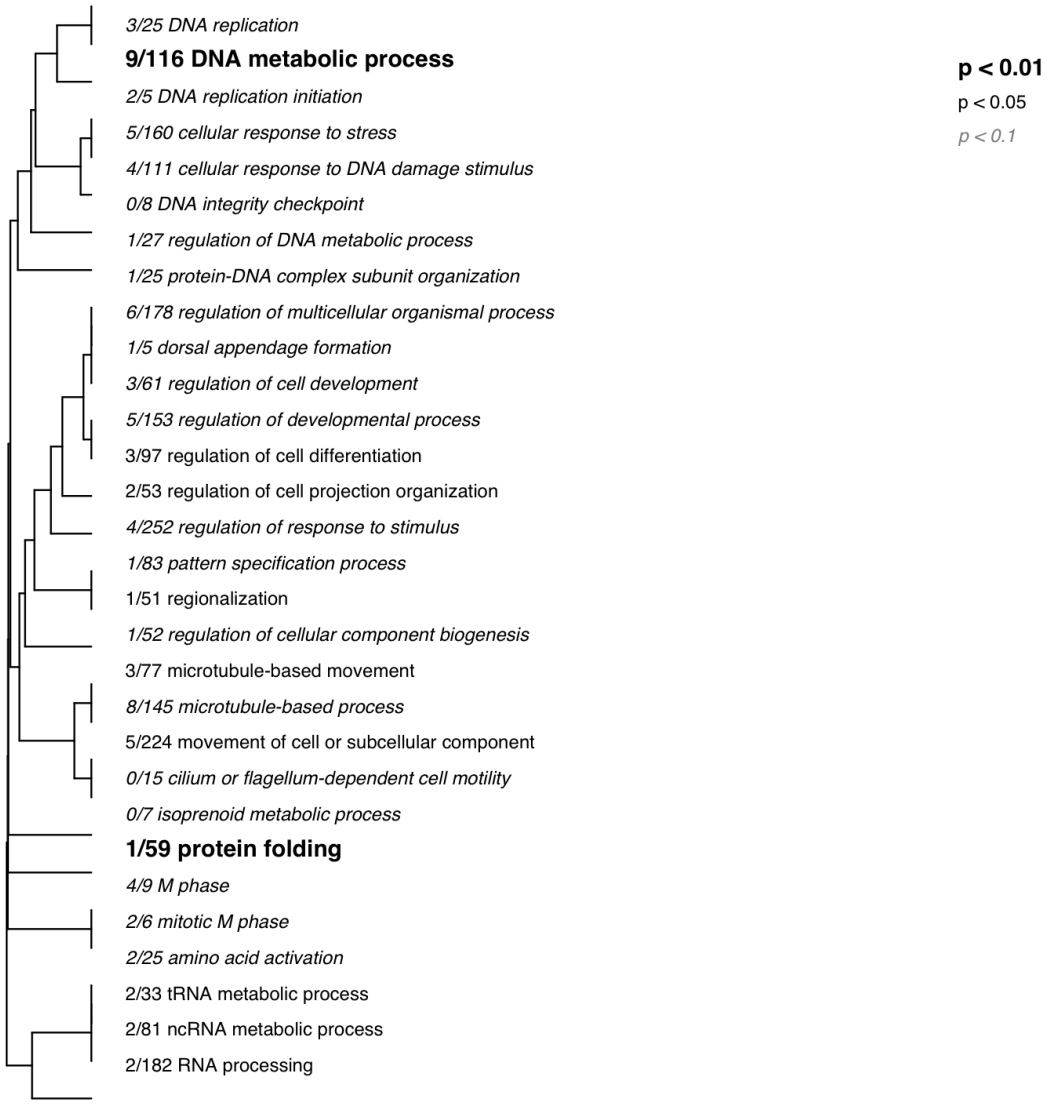

Figure S6: GO enrichment analysis output for coastal population low pH response. Text size indicates FDR-corrected p-value significance. Ratios before each branch indicate how many transcripts within each ontology exhibited a $\log_2$-fold-change >1.

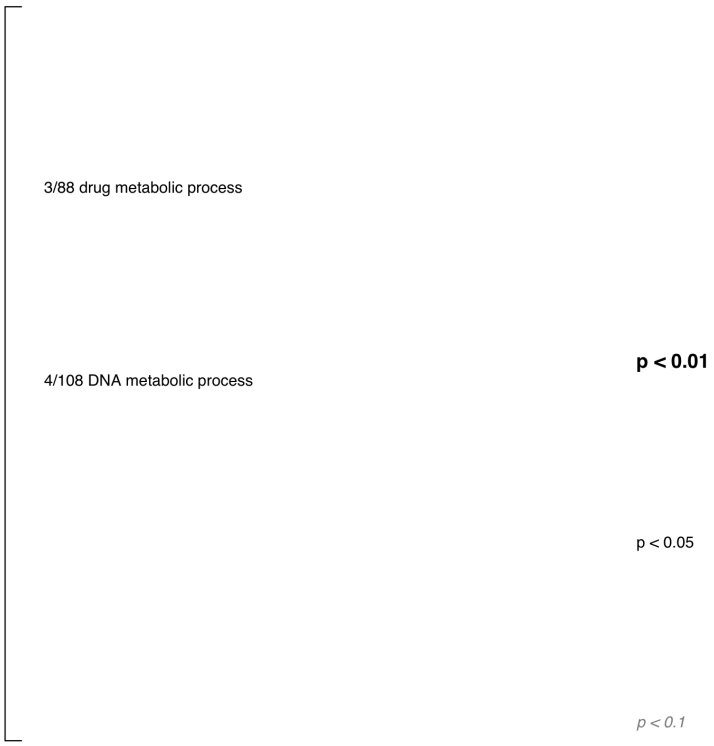

Figure S7: GO enrichment analysis output for lagoon population low pH response. Text size indicates FDR-corrected p-value significance. Ratios before each branch indicate how many transcripts within each ontology exhibited a $\log_2$-fold-change >1.

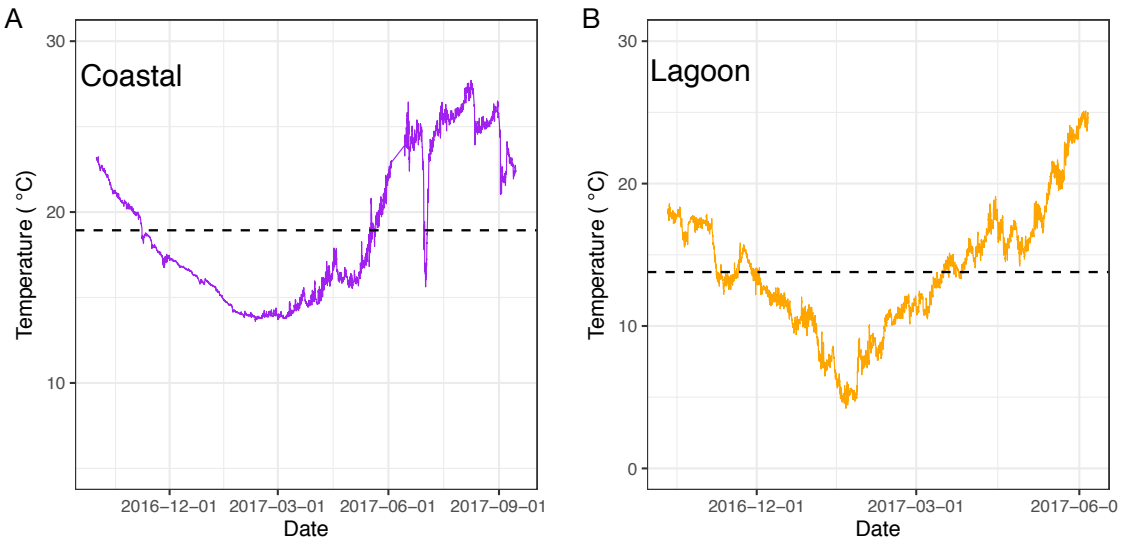

Figure S8: Temperature profiles of the coastal (A) and lagoon (B) habitats throughout the observation windows.

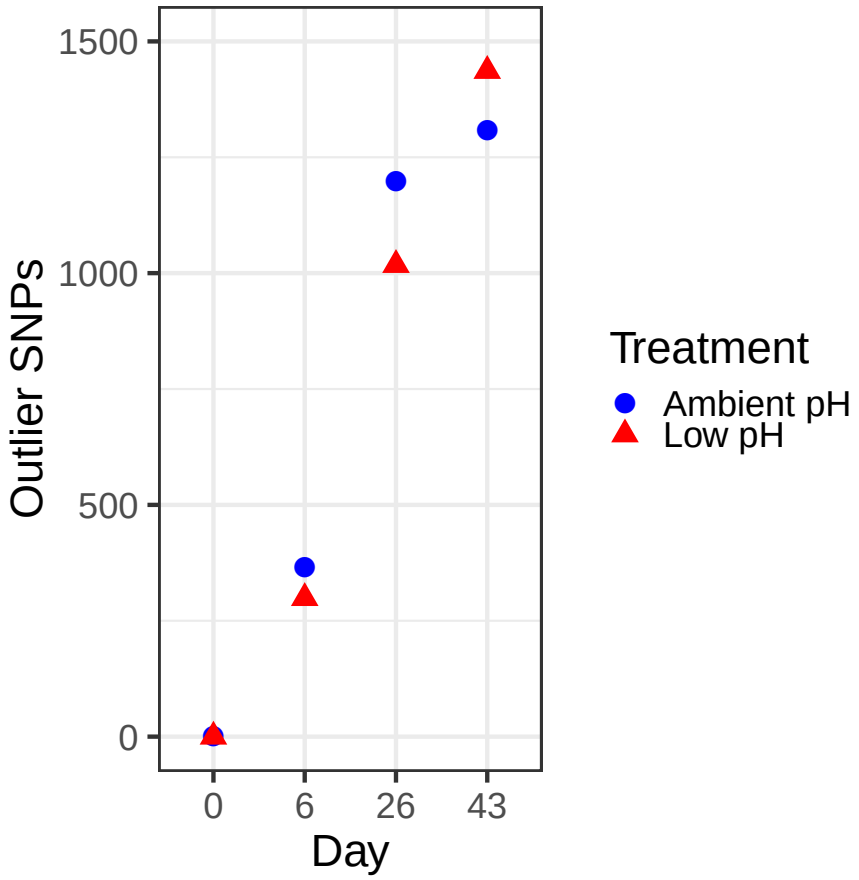

Figure S9: Changes to the number of significant SNPs identified throughout the larval period. Blue circles correspond to ambient and red triangles to low pH treatments) The number of significant SNPs identified reported has been standardized by the number of replicate buckets on each sampling day in order to account for increased power associated with increased replication

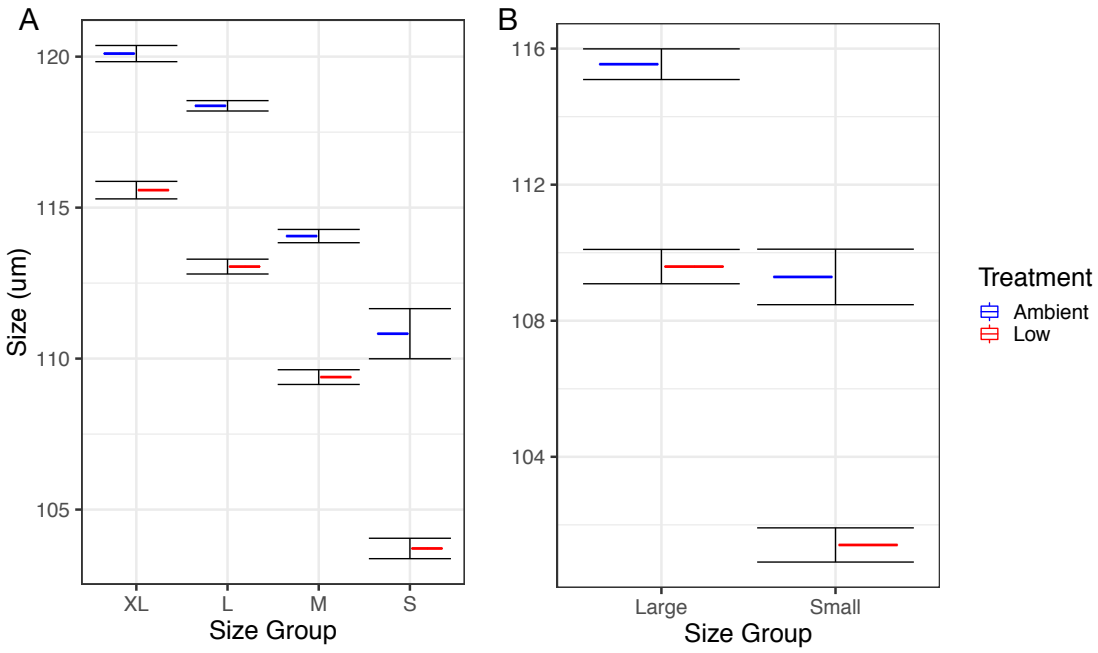

Figure S10: Efficacy of larval size separation method. (A) Pilot data demonstrating the selective isolation of 4 consecutively smaller groups of larvae (mean shell length ± SE) in ambient (blue) and low pH (red) cultured larvae (N = 53-324 per size group; XL = extra large; L = large; M = medium; S = small). (B) Shell length of larvae (mean ± SE) in largest (top 20 %) and smallest (bottom 80 %) individuals in ambient (blue) and low pH (red) conditions from present study (N = 62 – 177 per size group)

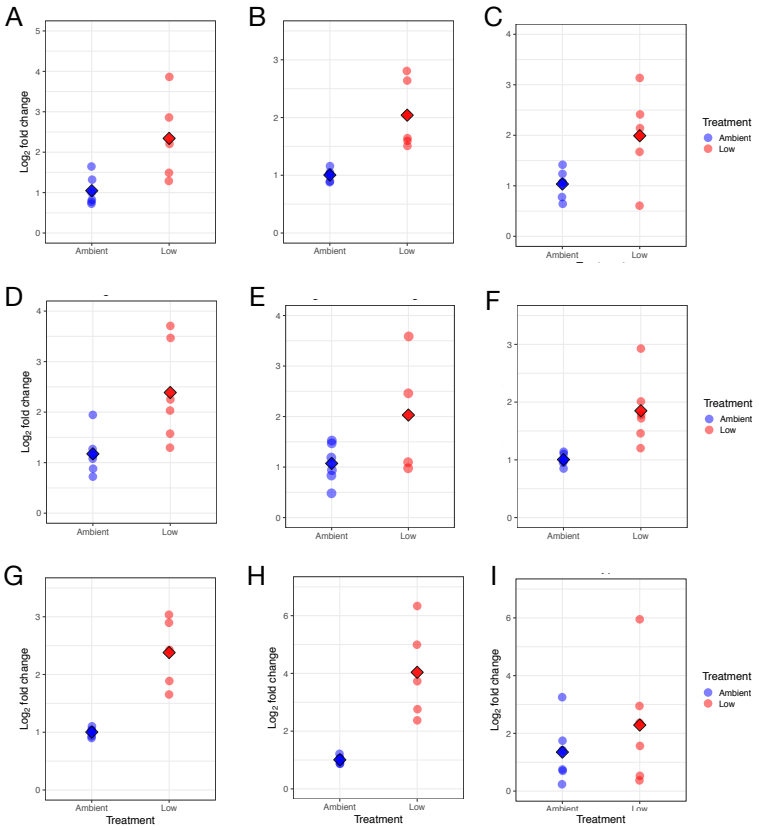

Figure S11: qPCR validation for genes identified as differentially expressed in transcriptomics analysis, but did not exhibit significant shifts in genetic variation during larval low pH selection. (A-I): Alpha protein kinase, IG-like protein, myostatin, ETV-5 protein, elongation factor, metalloreductase, Mgc-protein, a cuticular protein, and a hypothetical protein.

SUPPLEMENTARY TABLES

Table S1: Environment conditions within the common garden and pH manipulation system. Values are reported as mean across all sampling points (±S.D.) and measurement replicates were as follows: pH - N = 12 (Common Garden) N = 1,754 (pH treatments); AT - N = 1 (Common Garden) N = 5 (pH Treatments); Temperature - N = 12 (Common Garden) N = 1,754 (pH Treatments); Salinity - N = 1 (Common Garden) N = 5 (pH Treatments). Aragonite saturation and pCO2 were computed using parameter mean values.

Treatment	pH_T	Ωa	pCO_2	AT (μmol/kg)	T(^oC	SAL (ppt)
Comm. Gard.	7.84 (±0.05)	2.0	770	2585	16.3 (±0.4)	38.4
Stressful pH 1	7.69 (±0.05)	1.4	1116	2554	15.5 (±0.3)	38.2 (±0.1)
Stressful pH 2	7.69 (±0.05)	1.4	1116	2558	15.5 (±0.3)	38.2 (±0.1)
Benign pH 1	8.19 (±0.01)	3.7	292	2556	15.5 (±0.4)	38.2 (±0.1)
Benign pH 2	8.19 (±0.01)	3.6	301	2558	15.4 (±0.4)	38.2 (±0.1)

Table S2: Carbonate chemistry for flow-through experimental system used on days 0-26. Four header tanks (two per treatment) each distributed pH adjusted seawater to three replicate buckets. Low/Ambient 1/2 correspond to treatment replicates drawing water from separate header tanks, thus one replicate bucket per header tank is represented in the table. Time-series pH and temperature data were generated using in autonomous sensor were generated in each representative replicate bucket, and average values (±SD) are presented . Aragonite saturation (Ωa) and pCO2 were computed using average pH and Alkalinity (AT) for each representative replicate. AT and salinity samples (n = 11) were generated from discrete samples taken from each of the four header tanks every other day.

pH treatment	pH_T	Ωa	pCO_2	AT (μmol/kg)	T(^oC	SAL (ppt)
Low 1	7.43(±0.03)	0.85	2127	2565	17.3 (±0.1)	37.6 (±0.1)
Low 2	7.43 (±0.03)	0.85	2130	2569	17.2 (±0.1)	37.6 (±0.1)
Ambient 1	8.01 (±0.01)	3.32	378	2565	17.2 (±0.1)	37.6 (±0.1)
Ambient 2	8.01 (±0.01)	3.31	378	2561	17.2 (±0.1)	37.6 (±0.1)

Table S3: Carbonate chemistry generated from static cultures used to rear larvae from days 27-43. Low/Ambient 1/2/3 correspond to each remaining replicate bucket during this portion of the experiment. Discrete measurements of pH, total alkalinity, temperature, and salinity were taken daily and average values (± SD) are reported. Aragonite saturation (Ωa) and pCO2 were computed using average pH and AT for each replicate.

pH treatment	pH_T	Ωa	pCO_2	AT (µmol/kg)	T(^oC	SAL (ppt)
Low 1	7.53 (±0.10)	1.1	1675	2576 (±13)	17.3(±0.2)	37.4(±0.2)
Low 2	7.53 (±0.09)	1.0	1716	2576 (±13)	17.3(±0.2)	37.4(±0.2)
Low 3	7.54 (±0.10)	1.1	1633	2576 (±13)	17.3(±0.2)	37.4(±0.2)
Ambient 1	8.08 (±0.10)	3.2	403	2579 (±13)	17.3(±0.2)	37.4(±0.2)
Ambient 2	8.01 (±0.07)	2.8	488	2579 (±13)	17.3(±0.2)	37.4(±0.2)
Ambient 3	8.00 (±0.08)	2.8	501	2579 (±13)	17.3(±0.2)	37.4(±0.2)

Table S4: Changes to F_{ST} across ranges of feasible larval population sizes (n). F_{ST} was computed between the Day 0 larval population and the larval population in each treatment using *poolFstat*. Note that in instances where bucket replication (N) >1, the average (± standard deviation) F_{ST} across all replicate buckets is reported, whereas Figure 2.3c depicts F_{ST} values from each independent replicate bucket.

Day	Treatment	N	n	F_{ST} (± SD)
6	Ambient	1	10000	0.0066
6	Ambient	1	25000	0.0067
6	Ambient	1	40000	0.0067
6	Ambient	1	70000	0.0067
6	Ambient	1	90000	0.0067
6	Low	1	10000	0.0062
6	Low	1	25000	0.0062
6	Low	1	40000	0.0062
6	Low	1	70000	0.0062
6	Low	1	90000	0.0062
25	Ambient	3	1000	0.0084 (± 0.0017)
25	Ambient	3	2500	0.0086 (± 0.0017)
25	Ambient	3	4000	0.0087 (± 0.0017)
25	Low	3	1000	0.0074 (± 0.0008)
25	Low	3	2500	0.0076 (± 0.0008)
25	Low	3	4000	0.0077 (± 0.0008)
43	Ambient	2	100	0.0087 (± 0.0033)
43	Ambient	2	250	0.010 (± 0.0033)
43	Ambient	2	400	0.011 (± 0.0033)
43	Low	3	100	0.0073 (± 0.0016)
43	Low	3	250	0.0086 (± 0.0016)
43	Low	3	400	0.0092 (± 0.0016)

Table S5: Primer design information. Transcript ID refers to contig/unigene sequence name from the published transcriptome present in Moreira *et al.* (2015). Primer design denoted with an asterisk was obtained from Miglioli *et al.* (2019).

Gene	Fw (5'-3')	Rv (5'-3')	Efficiency	Transc. ID/Accs.
HSP70	GTAGTCGGTGGCCATTCAGA	GCAAGAGATGGCTGTTTCGG	97%	CL12877.Contig1
Ubiquitin protein ligase	ACTCCGGATGTTTGAAAGCAG	GCCGTGTGTCTCTGTACTGT	91%	CL2533.Contig5
Thyroid receptor protein	TCCTCTTCATCAGCTGTGCA	CCTGATCACGCTGAGATGCT	90%	CL1527.Contig2
Tyrosinase	CCCGAGCATGACATGGAGTT	GATCATGGGCAGCTGTCTCA	93%	CL1145.Contig4
Chitinase	CAAGGGACAGGGTACAGCAG	GTCCAACCACCCTTCTGTCC	93%	MG827131
Kinesin	CAGAAGCATTGGAGAGACGGA	GCTCTCTCACGATCAGCATCA	95%	Unigene35133
Myostatin	GCTCAACTTCCTCCAACGGA	CCCACAGAAAAGCCTTCTCCA	96%	Unigene633
Runt	CACGTATGCCAGACCTTCCA	TCGCCAGAATAACGTTCGGT	95%	XP_021359411.1
ETV5-related protein	GTTCTCGTCTGCAAGCACTG	AACAAAGTGTCCGGAAAACG	87%	Unigene19246
Hypothetial protein	ACGGAACACTTCACCCTGAC	CGGAGAGAAAGCAACGAAAG	97%	CL4139.Contig1
Metalloreduct.	GTTTCGTTCCCATCCATGTC	TCATGGGATCTCCCTACTGG	94%	Unigene41251
Elongation factor	TGGCAAGACCACTCTCACTG	CGTGAGACTCCTCCTTCTGG	93%	Unigene35901
Alpha-protein kinase	GAGGAGGTGATGGACCAGAA	AGGATCGTGACCATTTGGAG	93%	CL7460.Contig2
Slc12	TATTGCGTGTGAAGGATGGA	TTCCGTTGCTAGCATTTTCA	94%	Unigene21137
*Helicase	GCACTCATCAGAAGAAGGTGGG	GCTCTCACTTGTGAAGGGTGAC	NA	DQ158075
MGC69529 protein	GCCCGGAGACTTGTACGTAC	GCTTACGCTCGGACATTTCG	NA	Unigene15921
IG-like protein	TGTCTTCGTGTGCTGTTCCT	AGCGAACGACCGAAGACAAT	NA	Unigene31791
Cuticular protein	TCGAGCCAATTTCCGGTAAGT	TCAACCGGACAATGGACCAA	NA	CL14268.Contig2

Table S6: Transcriptomic Results. Gene name (NA indicates non-annotated transcript), transcript ID (as reported in Moreira *et al.* (2015), expression (Log_2-fold-change), and FDR corrected p-value.

Gene Name	Transcript ID	Expression	P-val.
NA	Unigene94108	2.07	2.81E-07
NA	Unigene11736	1.69	3.96E-06
NA	Unigene97290	2.17	5.26E-06
Chromobox 8	Unigene36491	1.1	1.03E-05
NA	Unigene84909	1.02	1.33E-05
NA	Unigene16595	1.01	1.38E-05
NA	Unigene15921	1.22	4.57E-05
NA	Unigene11735	1.53	4.57E-05
NA	Unigene94115	2.13	4.57E-05
Hypothetical protein	CL15076.Contig2	1.55	0.0001
NA	Unigene31791	0.7	0.0002
NA	Unigene92059	1.94	0.0002
NA	CL12151.Contig2	0.85	0.0002
NA	CL14268.Contig2	1.66	0.0003
NA	Unigene67129	0.95	0.0004
NA	Unigene90028	1.76	0.0004
NA	CL3552.Contig2	0.87	0.0004
NA	Unigene22287	1.17	0.0005
NA	Unigene55968	0.67	0.0013
ARF Gap-like prot.	Unigene26756	0.52	0.0018
Runt	CL14297.Contig2	0.78	0.0026
NA	Unigene87504	0.86	0.0028
NA	Unigene95225	0.5	0.0028
Beta-microseminoprotein-like iso.	Unigene29772	0.77	0.0030
Myostatin	Unigene633	0.97	0.0033
ETV5-related prot.	Unigene19246	0.64	0.0045
Runt	CL14297.Contig1	0.87	0.0059
YbaK/prolyl-tRNA synthetase	CL14751.Contig1	0.660	.0060
NA	Unigene36019	0.67	0.0092
NA	CL2769.Contig2	-0.86	0.0112
NA	CL4139.Contig1	0.44	0.0117
Tyrosinase	CL1145.Contig4	0.76	0.0131
Metalloreductase STEAP4-like	Unigene41251	0.64	0.0179
Hypothetical protein	CL15076.Contig1	1.05	0.0192
Elongation factor 2	Unigene35901	0.71	0.0206
Alpha-protein kinase	CL7460.Contig2	1.25	0.0224
E3 ubiquitin-protein ligase	CL2533.Contig5	0.68	0.0280
Solute carrier family (slc12 like)	Unigene21137	0.58	0.0330
NA	Unigene86350	0.32	0.0484
NA	CL3552.Contig1	0.7	0.0484

REFERENCES

Allen, J.D., 2008. Size-Specific Predation on Marine Invertebrate Larvae. The Biological Bulletin 214, 42–49.

Anestis, A., Lazou, A., Pörtner, H.O., Michaelidis, B., 2007. Behavioral, metabolic, and molecular stress responses of marine bivalve *Mytilus galloprovincialis* during long-term acclimation at increasing ambient temperature. American Journal of Physiology-Regulatory, Integrative and Comparative Physiology 293, 911–921.

Arivalagan, J., Yarra, T., Marie, B., Sleight, V.A., Duvernois-Berthet, E., Clark, M.S., Marie, A., Berland, S., 2017. Insights from the Shell Proteome: Biomineralization to Adaptation. Mol Biol Evol 34, 66–77.

Barrett, R.D.H., Schluter, D., 2008. Adaptation from standing genetic variation. Trends in Ecology Evolution 23, 38–44.

Barshis, D.J., Ladner, J.T., Oliver, T.A., Seneca, F.O., Traylor-Knowles, N., Palumbi, S.R., 2013. Genomic basis for coral resilience to climate change. PNAS 110, 1387–1392.

Bay, R.A., Palumbi, S.R., 2014. Multilocus Adaptation Associated with Heat Resistance in Reef-Building Corals. Current Biology 24, 2952–2956.

Bell, G., 2010. Fluctuating selection: the perpetual renewal of adaptation in variable environments. Philosophical Transactions of the Royal Society B: Biological Sciences 365, 87–97.

Bergland, A.O., Behrman, E.L., O'Brien, K.R., Schmidt, P.S., Petrov, D.A., 2014. Genomic Evidence of Rapid and Stable Adaptive Oscillations over Seasonal Time Scales in Drosophila. PLOS Genetics 10, e1004775.

Berline, L., Rammou, A.-M., Doglioli, A., Molcard, A., Petrenko, A., 2014. A Connectivity-Based Eco-Regionalization Method of the Mediterranean Sea. PLOS ONE 9, e111978.

Bindoff, N.L., Cheung, W.W.L., Kairo, J.G., Arístegui, J., Guinder, V.A., Hallberg, R., Hilmi, N., Jiao, N., O'Donoghue, S., Suga, T., Acar, S., Alava, J.J., Allison, E., Arbic, B., Bambridge, T., Boyd, P.W., Bruggeman, J., Butenschön, M., Chávez, F.P., Cheng, L., Cinar,

M., Costa, D., Defeo, O., Djoundourian, S., Domingues, C., Eddy, T., Endres, S., Fox, A., Free, C., Frölicher, T., Gattuso, J.-P., Gerber, G., Hallegraef, G., Harrison, M., Hennige, S., Hindell, M., Hogg, A., Ito, T., Kenny, T.-A., Kroeker, K., Kwiatkowski, L., Lam, V.W.Y., Laüfkotter, C., LeBillon, P., Bris, N.L., Lotze, H., MacKinnon, J., de Marffy-Mantuano, A., Martel, P., Molinos, J.G., Moseman-Valtierra, S., Motau, A., Mulsow, S., Mutombo, K., Oyinlola, M., Poloczanska, E.S., Pascal, N., Philip, M., Purkey, S., Rathore, S., Rebelo, X., Reygondeau, G., Rice, J., Richardson, A., Riebesell, U., Roach, C., Rocklöv, J., Roberts, M., Sloyan, B., Smith, M., Shurety, A., Wabnitz, C., Whalen, C., 2019. Changing Ocean, Marine Ecosystems, and Dependent Communities. In: IPCC Special Report on the Ocean and Cryosphere in a Changingn Climate 142.

Bitter, M.C., Kapsenberg, L., Gattuso, J.-P., Pfister, C.A., 2019. Standing genetic variation fuels rapid adaptation to ocean acidification. Nat Commun 10, 1–10.

Bolger, A.M., Lohse, M., Usadel, B., 2014. Trimmomatic: a flexible trimmer for Illumina sequence data. Bioinformatics 30, 2114–2120.

Bonamour Suzanne, Chevin Luis-Miguel, Charmantier Anne, Teplitsky Céline, 2019. Phenotypic plasticity in response to climate change: the importance of cue variation. Philosophical Transactions of the Royal Society B: Biological Sciences 374, 20180178.

Botero, C.A., Weissing, F.J., Wright, J., Rubenstein, D.R., 2015. Evolutionary tipping points in the capacity to adapt to environmental change. PNAS 112, 184–189.

Brennan Reid S., Garrett April D., Huber Kaitlin E., Hargarten Heidi, Pespeni Melissa H., 2019. Rare genetic variation and balanced polymorphisms are important for survival in global change conditions. Proceedings of the Royal Society B: Biological Sciences 286, 20190943.

Bresnahan, P.J., Martz, T.R., Takeshita, Y., Johnson, K.S., LaShomb, M., 2014. Best practices for autonomous measurement of seawater pH with the Honeywell Durafet. Methods in Oceanography 9, 44–60.

Campbell-Staton, S.C., Cheviron, Z.A., Rochette, N., Catchen, J., Losos, J.B., Edwards,

S.V., 2017. Winter storms drive rapid phenotypic, regulatory, and genomic shifts in the green anole lizard. Science 357, 495–498.

Carl, C., Poole, A.J., Williams, M.R., Nys, R. de, 2012. Where to Settle—Settlement Preferences of *Mytilus galloprovincialis* and Choice of Habitat at a Micro Spatial Scale. PLOS ONE 7, e52358.

Casey, J.R., Grinstein, S., Orlowski, J., 2010. Sensors and regulators of intracellular pH. Nat. Rev. Mol. Cell Biol. 11, 50–61.

Connor, K.M., Gracey, A.Y., 2011. Circadian cycles are the dominant transcriptional rhythm in the intertidal mussel *Mytilus californianus*. PNAS 108, 16110–16115.

Cosart, T., Beja-Pereira, A., Chen, S., Ng, S.B., Shendure, J., Luikart, G., 2011. Exome-wide DNA capture and next generation sequencing in domestic and wild species. BMC Genomics 12, 347.

Cummings, V., Hewitt, J., Rooyen, A.V., Currie, K., Beard, S., Thrush, S., Norkko, J., Barr, N., Heath, P., Halliday, N.J., Sedcole, R., Gomez, A., McGraw, C., Metcalf, V., 2011. Ocean Acidification at High Latitudes: Potential Effects on Functioning of the Antarctic Bivalve *Laternula elliptica*. PLOS ONE 6, e16069.

Cyronak, T., Takeshita, Y., Courtney, T.A., DeCarlo, E.H., Eyre, B.D., Kline, D.I., Martz, T., Page, H., Price, N.N., Smith, J., Stoltenberg, L., Tresguerres, M., Andersson, A.J., 2019. Diel temperature and pH variability scale with depth across diverse coral reef habitats. Limnology and Oceanography Letters 5, 193-203.

Danecek, P., Auton, A., Abecasis, G., Albers, C.A., Banks, E., DePristo, M.A., Handsaker, R.E., Lunter, G., Marth, G.T., Sherry, S.T., McVean, G., Durbin, R., 2011. The variant call format and VCFtools. Bioinformatics 27, 2156–2158.

De Carlo, E.H., Mousseau, L., Passafiume, O., Drupp, P.S., Gattuso, J.-P., 2013. Carbonate Chemistry and Air–Sea CO2 Flux in a NW Mediterranean Bay Over a Four-Year Period: 2007–2011. Aquat Geochem 19, 399–442.

De Wit, P., Rogers-Bennett, L., Kudela, R.M., Palumbi, S.R., 2014. Forensic genomics

as a novel tool for identifying the causes of mass mortality events. Nat Commun 5, 3652.

DeBiasse, M.B., Kelly, M.W., 2015. Plastic and Evolved Responses to Global Change: What Can We Learn from Comparative Transcriptomics? J Hered esv073.

DeWitt, T.J., Sih, A., Wilson, D.S., 1998. Costs and limits of phenotypic plasticity. Trends in Ecology Evolution 13, 77–81.

Dickson, A.G., 1990. Standard potential of the reaction: AgCl(s) + 12H2(g) = Ag(s) + HCl(aq), and and the standard acidity constant of the ion HSO4 in synthetic sea water from 273.15 to 318.15 K. The Journal of Chemical Thermodynamics 22, 113–127.

Dickson, A.G., Sabine, C.L., Christian, J.R., 2007. Guide to Best Practices for Ocean CO2 Measurements. PICES Special Publication.

Edenhofer, O., Pichs-Madruga, R., Sokona, Y., Farahani, E., Kadner, S., Seyboth, K., Adler, A., Baum, I., Brunner, S., Eickemeier, P., Kriemann, B., Savolainen, J., Schlömer, S., von Stechow, C., Zwickel, T., Minx, J., 2014. IPCC, 2014: Summary for Policymakers. In: Climate Change 2014: MItigation of Climate Change. Contribution of Working-Group III to the Fifth Assessment Report of the Intergovernmental Panel on Climate Change.

Evans, T.G., Chan, F., Menge, B.A., Hofmann, G.E., 2013. Transcriptomic responses to ocean acidification in larval sea urchins from a naturally variable pH environment. Mol Ecol 22, 1609–1625.

Feder, M.E., Hofmann, G.E., 1999. Heat-shock proteins, molecular chaperones, and the stress response: Evolutionary and ecological physiology. Annu. Rev. Physiol. 61, 243–282.

Fotel, F.L., Jensen, N.J., Wittrup, L., Hansen, B.W., 1999. *in situ* and laboratory growth by a population of blue mussel larvae (*Mytilus edulis* L.) from a Danish embayment, Knebel Vig. Journal of Experimental Marine Biology and Ecology 233, 213–230.

Gagnaire, P.-A., Normandeau, E., Côté, C., Hansen, M.M., Bernatchez, L., 2012. The Genetic Consequences of Spatially Varying Selection in the Panmictic American Eel (*Anguilla rostrata*). Genetics 190, 725–736.

Gattuso, J.-P., Epitalon, J.-M., Lavigne, H., 2016. seacarb: Seawater Carbonate Chem-

istry. R package version 3.2.2.

Gazeau, F., Alliouane, S., Bock, C., Bramanti, L., López Correa, M., Gentile, M., Hirse, T., Pörtner, H.-O., Ziveri, P., 2014a. Impact of ocean acidification and warming on the Mediterranean mussel (*Mytilus galloprovincialis*). Front. Mar. Sci. 1.

Gazeau, F., Parker, L.M., Comeau, S., Gattuso, J.-P., O'Connor, W.A., Martin, S., Pörtner, H.-O., Ross, P.M., 2013. Impacts of ocean acidification on marine shelled molluscs. Mar Biol 160, 2207–2245.

Gomulkiewicz, R., Kirkpatrick, M., 1992. Quantitative genetics and the evolution of reaction norms. Evolution 46, 390–411.

Goncalves, P., Jones, D.B., Thompson, E.L., Parker, L.M., Ross, P.M., Raftos, D.A., 2017. Transcriptomic profiling of adaptive responses to ocean acidification. Molecular Ecology 26, 5977-5988.

Hoegh-Guldberg, O., Cai, R., Poloczanksa, E.S., Brewer, P.G., Sundby, S., Hilmi, K., Fabry, V.J., Jung, S., 2014. In: Climate Change 2014: Impacts, Adaptation, and Vulnerability. Part B: Regional Aspects. Contribution of Working Group II to the Fifth Assessment Report of the Intergovernmental Panel on Climate Change. Cambridge University Press, Cambridge, United Kingdom and New York, NY, USA, pp. 1655-1733.

Hoffmann, A.A., Sgrò, C.M., 2011. Climate change and evolutionary adaptation. Nature 470, 479–485.

Hofmann, G.E., Evans, T.G., Kelly, M.W., Padilla-Gamiño, J.L., Blanchette, C.A., Washburn, L., Chan, F., McManus, M.A., Menge, B.A., Gaylord, B., Hill, T.M., Sanford, E., LaVigne, M., Rose, J.M., Kapsenberg, L., Dutton, J.M., 2014. Exploring local adaptation and the ocean acidification seascape – studies in the California Current Large Marine Ecosystem. Biogeosciences 11, 1053–1064.

Hofmann, G.E., Smith, J.E., Johnson, K.S., Send, U., Levin, L.A., Micheli, F., Paytan, A., Price, N.N., Peterson, B., Takeshita, Y., Matson, P.G., Crook, E.D., Kroeker, K.J., Gambi, M.C., Rivest, E.B., Frieder, C.A., Yu, P.C., Martz, T.R., 2011. High-Frequency

Dynamics of Ocean pH: A Multi-Ecosystem Comparison. PLoS ONE 6, e28983.

Hönisch, B., Ridgwell, A., Schmidt, D.N., Thomas, E., Gibbs, S.J., Sluijs, A., Zeebe, R., Kump, L., Martindale, R.C., Greene, S.E., Kiessling, W., Ries, J., Zachos, J.C., Royer, D.L., Barker, S., Marchitto, T.M., Moyer, R., Pelejero, C., Ziveri, P., Foster, G.L., Williams, B., 2012. The Geological Record of Ocean Acidification. Science 335, 1058–1063.

Huan, P., Liu, G., Wang, H., Liu, B., 2013. Identification of a tyrosinase gene potentially involved in early larval shell biogenesis of the Pacific oyster *Crassostrea gigas*. Dev Genes Evol 223, 389–394.

Hüning, A.K., Lange, S.M., Ramesh, K., Jacob, D.E., Jackson, D.J., Panknin, U., Gutowska, M.A., Philipp, E.E.R., Rosenstiel, P., Lucassen, M., Melzner, F., 2016. A shell regeneration assay to identify biomineralization candidate genes in mytilid mussels. Marine Genomics, Cells to Shells: The genomics of mollusc exoskeletons 27, 57–67.

Hüning, A.K., Melzner, F., Thomsen, J., Gutowska, M.A., Krämer, L., Frickenhaus, S., Rosenstiel, P., Pörtner, H.-O., Philipp, E.E.R., Lucassen, M., 2012. Impacts of seawater acidification on mantle gene expression patterns of the Baltic Sea blue mussel: implications for shell formation and energy metabolism. Mar Biol 160, 1845–1861.

Johnson, K.M., Hofmann, G.E., 2017b. Transcriptomic response of the Antarctic pteropod *Limacina helicina antarctica* to ocean acidification. BMC Genomics 18, 812.

Kaniewska, P., Chan, C.-K.K., Kline, D., Ling, E.Y.S., Rosic, N., Edwards, D., Hoegh-Guldberg, O., Dove, S., 2015. Transcriptomic Changes in Coral Holobionts Provide Insights into Physiological Challenges of Future Climate and Ocean Change. PLoS One 10, e0139223.

Kapsenberg, L., Alliouane, S., Gazeau, F., Mousseau, L., Gattuso, J.-P., 2017. Coastal ocean acidification and increasing total alkalinity in the northwestern Mediterranean Sea. Ocean Sci. 13, 411–426.

Kapsenberg, L., Bockmon, E.E., Bresnahan, P.J., Kroeker, K.J., Gattuso, J.-P., Martz, T.R., 2017a. Advancing Ocean Acidification Biology Using Durafet® pH Electrodes. Front. Mar. Sci. 4.

Kapsenberg, L., Cyronak, T., 2019. Ocean acidification refugia in variable environments. Global Change Biology 25, 3201–3214.

Kapsenberg, L., Hofmann, G.E., 2016. Ocean pH time-series and drivers of variability along the northern Channel Islands, California, USA. Limnol. Oceanogr. 61, 953–968.

Kapsenberg L., Miglioli A., Bitter M. C., Tambutté E., Dumollard R., Gattuso J.-P., 2018. Ocean pH fluctuations affect mussel larvae at key developmental transitions. Proceedings of the Royal Society B: Biological Sciences 285, 20182381.

Kapsenberg, Lydia, Okamoto, D.K., Dutton, J.M., Hofmann, G.E., 2017b. Sensitivity of sea urchin fertilization to pH varies across a natural pH mosaic. Ecology and Evolution 7, 1737-1750.

Kellermann, V., Hoffmann, A.A., Kristensen, T.N., Moghadam, N.N., Loeschcke, V., 2015. Experimental Evolution under Fluctuating Thermal Conditions Does Not Reproduce Patterns of Adaptive Clinal Differentiation in Drosophila melanogaster. The American Naturalist 186, 582–593.

Kelly, M.W., Hofmann, G.E., 2013. Adaptation and the physiology of ocean acidification. Funct Ecol 27, 980–990.

Kelly, M.W., Pankey, M.S., DeBiasse, M.B., Plachetzki, D.C., 2017. Adaptation to heat stress reduces phenotypic and transcriptional plasticity in a marine copepod. Funct Ecol 31, 398–406.

Kenkel, C.D., Matz, M.V., 2017. Gene expression plasticity as a mechanism of coral adaptation to a variable environment. Nature Ecology Evolution 1, 0014.

Kingsolver, J.G., Huey, R.B., 1998. Evolutionary Analyses of Morphological and Physiological Plasticity in Thermally Variable Environments. Integr Comp Biol 38, 545–560.

Kingsolver, J.G., Wiernasz, D.C., 1991. Seasonal Polyphenism in Wing-Melanin Pattern and Thermoregulatory Adaptation in Pieris Butterflies. The American Naturalist 137, 816–830.

Kingston, S.E., Martino, P., Melendy, M., Reed, F.A., Carlon, D.B., 2018. Linking

genotype to phenotype in a changing ocean: inferring the genomic architecture of a blue mussel stress response with genome-wide association. Journal of Evolutionary Biology 31, 346–361.

Kleypas, J.A., Buddemeier, R.W., Archer, D., Gattuso, J.-P., Langdon, C., Opdyke, B.N., 1999. Geochemical Consequences of Increased Atmospheric Carbon Dioxide on Coral Reefs. Science 284, 118–120.

Kofler, R., Orozco-terWengel, P., Maio, N.D., Pandey, R.V., Nolte, V., Futschik, A., Kosiol, C., Schlötterer, C., 2011. PoPoolation: A Toolbox for Population Genetic Analysis of Next Generation Sequencing Data from Pooled Individuals. PLOS ONE 6, e15925.

Kroeker, K.J., Kordas, R.L., Crim, R., Hendriks, I.E., Ramajo, L., Singh, G.S., Duarte, C.M., Gattuso, J.-P., 2013. Impacts of ocean acidification on marine organisms: quantifying sensitivities and interaction with warming. Global Change Biology 19, 1884–1896.

Kurihara, H., 2008. Effects of CO2-driven ocean acidification on the early developmental stages of invertebrates. Marine Ecology Progress Series 373, 275–284.

Kurihara, H., Asai, T., Kato, S., Ishimatsu, A., 2008. Effects of elevated pCO2 on early development in the mussel *Mytilus galloprovincialis*. Aquat Biol 4, 225–233.

Langmead, B., Salzberg, S.L., 2012. Fast gapped-read alignment with Bowtie 2. Nat Methods 9, 357–359.

Lannan, J.E., 1980. Broodstock management of *Crassostrea gigas*: I. Genetic and environmental variation in survival in the larval rearing system. Aquaculture 21, 323–336.

Launey, S., Hedgecock, D., 2001. High Genetic Load in the Pacific Oyster *Crassostrea gigas*. Genetics 159, 255–265.

Lewontin, R.C., Cohen, D., 1969. On Population Growth in a Randomly Varying Environment. PNAS 62, 1056–1060.

Lewontin, R.C., Hubby, J.L., 1966. A Molecular Approach to the Study of Genic Heterozygosity in Natural Populations. II. Amount of Variation and Degree of Heterozygosity in Natural Populations of *Drosophila pseudoobscura*. Genetics 54, 595–609.

Li H., Handsaker B., Wysoker A., Fennel T., *et al.,* 2009. The sequency alignment/map format and SAMtools. Bioinformatics 25, 2078-2079.

Lockwood, B.L., Somero, G.N., 2011. Transcriptomic responses to salinity stress in invasive and native blue mussels (genus Mytilus). Molecular Ecology 20, 517–529.

Lohman, B.K., Weber, J.N., Bolnick, D.I., 2016. Evaluation of TagSeq, a reliable low-cost alternative for RNAseq. Molecular Ecology Resources 16, 1315–1321.

López-Maury, L., Marguerat, S., Bähler, J., 2008. Tuning gene expression to changing environments: from rapid responses to evolutionary adaptation. Nat. Rev. Genet. 9, 583–593.

Love, M.I., Huber, W., Anders, S., 2014. Moderated estimation of fold change and dispersion for RNA-seq data with DESeq2. Genome Biology 15, 550.

Lueker, T.J., Dickson, A.G., Keeling, C.D., 2000. Ocean pCO2 calculated from dissolved inorganic carbon, alkalinity, and equations for K1 and K2: validation based on laboratory measurements of CO2 in gas and seawater at equilibrium. Marine Chemistry 70, 105–119.

Mallet, A.L., Zouros, E., Gartner-Kepkay, K.E., Freeman, K.R., Dickie, L.M., 1985. Larval viability and heterozygote deficiency in populations of marine bivalves: evidence from pair matings of mussels. Mar. Biol. 87, 165–172.

Martz, T.R., Connery, J.G., Johnson, K.S., 2010. Testing the Honeywell Durafet (R) for seawater pH applications. Limnol. Oceanogr. Meth. 8, 172–184.

Maynard, A., Bible, J.M., Pespeni, M.H., Sanford, E., Evans, T.G., 2018. Transcriptomic responses to extreme low salinity among locally adapted populations of Olympia oyster (*Ostrea lurida*). Mol. Ecol. 27, 4225–4240.

Melzner, F., Thomsen, J., Koeve, W., Oschlies, A., Gutowska, M.A., Bange, H.W., Hansen, H.P., Körtzinger, A., 2013. Future ocean acidification will be amplified by hypoxia in coastal habitats. Mar Biol 160, 1875–1888.

Melzner, F., Thomsen, J., Ramesh, K., Hu, M.Y., Bleich, M., 2017. Mussel larvae modify calcifying fluid carbonate chemistry to promote calcification. Nature Communications 8,

1709.

Messer, P.W., Ellner, S.P., Hairston, N.G., 2016. Can Population Genetics Adapt to Rapid Evolution? Trends in Genetics 32, 408–418.

Miglioli, A., Dumollard, R., Balbi, T., Besnardeau, L., Canesi, L., 2019. Characterization of the main steps in first shell formation in *Mytilus galloprovincialis*: possible role of tyrosinase. Proceedings of the Royal Society B: Biological Sciences 286, 20192043.

Moll, P., Ante, M., Seitz, A., Reda, T., 2014. QuantSeq 3 mRNA sequencing for RNA quantification. Nat Methods 11, 1-3.

Moran, N.A., 1992. The Evolutionary Maintenance of Alternative Phenotypes. The American Naturalist 139, 971–989.

Moreira, R., Pereiro, P., Canchaya, C., Posada, D., Figueras, A., Novoa, B., 2015. RNA-Seq in *Mytilus galloprovincialis*: comparative transcriptomics and expression profiles among different tissues. BMC Genomics 16, 728.

Paaby, A.B., Rockman, M.V., 2014. Cryptic genetic variation: evolution's hidden substrate. Nature Reviews Genetics 15, 247–258.

Pansch, C., Schaub, I., Havenhand, J., Wahl, M., 2014. Habitat traits and food availability determine the response of marine invertebrates to ocean acidification. Global Change Biology 20, 765–777.

Patro, R., Duggal, G., Love, M.I., Irizarry, R.A., Kingsford, C., 2017. Salmon provides fast and bias-aware quantification of transcript expression. Nature Methods 14, 417–419.

Perez, F.F., Fraga, F., 1987. The pH measurements in seawater on the NBS scale. Marine Chemistry 21, 315–327.

Pespeni, M.H., Palumbi, S.R., 2013. Signals of selection in outlier loci in a widely dispersing species across an environmental mosaic. Mol Ecol 22, 3580–3597.

Pettersen, A.K., Turchini, G.M., Jahangard, S., Ingram, B.A., Sherman, C.D.H., 2010. Effects of different dietary microalgae on survival, growth, settlement and fatty acid composition of blue mussel (*Mytilus galloprovincialis*) larvae. Aquaculture 309, 115–124.

Pfister, C.A., Esbaugh, A.J., Frieder, C.A., Baumann, H., *et. al.*, 2014. Detecting the unexpected: A research framework for ocean acidification. Environmental Science Technology 48, 9982-9994.

Phillips, N.E., 2002. Effects of Nutrition-Mediated Larval Condition on Juvenile Performance in a Marine Mussel. Ecology 83, 2562–2574.

Plough, L.V., Shin, G., Hedgecock, D., 2016. Genetic inviability is a major driver of type III survivorship in experimental families of a highly fecund marine bivalve. Molecular Ecology 25, 895–910.

Plus, M., Chapelle, A., Lazure, P., Auby, I., Levavasseur, G., Verlaque, M., Belsher, T., Deslous-Paoli, J.-M., Zaldıvar, J.-M., Murray, C.N., 2003. Modelling of oxygen and nitrogen cycling as a function of macrophyte community in the Thau lagoon. Continental Shelf Research, European Land-Ocean Interaction 23, 1877–1898.

Quesada, H., Zapata, C., Alvarez, G., 1995. A multilocus allozyme discontinuity in the mussel *Mytilus galloprovincialis*: the interaction of ecological and life-history factors. Oceanographic Literature Review 9, 769–770.

Randazzo, P.A. and Hirsch, D.A., 2004. Arf GAPs: multifunctional proteins that regulate membrane traffic and actin remodelling. Cellular Signalling 16, 401-413.

Reed, T.E., Waples, R.S., Schindler, D.E., Hard, J.J., Kinnison, M.T., 2010. Phenotypic plasticity and population viability: the importance of environmental predictability. Proceedings of the Royal Society B: Biological Sciences 277, 3391–3400.

Riebesell, U., Zondervan, I., Rost, B., Tortell, P.D., Zeebe, R.E., Morel, F.M.M., 2000. Reduced calcification of marine plankton in response to increased atmospheric CO 2. Nature 407, 364–367.

Robinson, M.D., McCarthy, D.J., Smyth, G.K., 2010. edgeR: a Bioconductor package for differential expression analysis of digital gene expression data. Bioinformatics 26, 139–140.

Rodríguez-Trelles, F., Tarrío, R., Santos, M., 2013. Genome-wide evolutionary response to a heat wave in Drosophila. Biology Letters 9, 20130228.

Romiguier, J., Gayral, P., Ballenghien, M., Bernard, A., Cahais, V., Chenuil, A., Chiari, Y., Dernat, R., Duret, L., Faivre, N., Loire, E., Lourenco, J.M., Nabholz, B., Roux, C., Tsagkogeorga, G., Weber, A. a.-T., Weinert, L.A., Belkhir, K., Bierne, N., Glémin, S., Galtier, N., 2014. Comparative population genomics in animals uncovers the determinants of genetic diversity. Nature 515, 261–263.

Sanford, E., Kelly, M.W., 2011. Local Adaptation in Marine Invertebrates. Annual Review of Marine Science 3, 509–535.

Satuito, C.G., Natoyama, K., Yamazaki, M., Fusetani, N., 1994. Larval development of the mussel *Mytilus edulis* galloprovincialis cultured under laboratory conditions. Fisheries science 60, 65–68.

Schaum, E., Rost, B., Millar, A.J., Collins, S., 2013. Variation in plastic responses of a globally distributed picoplankton species to ocean acidification. Nature Clim. Change 3, 298–302.

Scheiner, S.M., 1993. Genetics and Evolution of Phenotypic Plasticity. Annu. Rev. Ecol. Syst. 24, 35–68.

Scheiner, S.M., Holt, R.D., 2012. The genetics of phenotypic plasticity. X. Variation versus uncertainty. Ecology and Evolution 2, 751–767.

Schiebelhut, L.M., Puritz, J.B., Dawson, M.N., 2018. Decimation by sea star wasting disease and rapid genetic change in a keystone species, *Pisaster ochraceus*. PNAS 115, 7069–7074.

Schluter, D., Price, T.D., Rowe, L., 1991. Conflicting selection pressures and life history trade-offs. Proc. R. Soc. Lond. B 246, 11–17.

Schmittgen, T.D., Livak, K.J., 2008. Analyzing real-time PCR data by the comparative CT method. Nature Protocols 3, 1101–1108.

Seebacher, F., White, C.R., Franklin, C.E., 2015. Physiological plasticity increases resilience of ectothermic animals to climate change. Nature Clim. Change 5, 61–66.

Silliman, K., 2019. Population structure, genetic connectivity, and adaptation in the

Olympia oyster (*Ostrea lurida*) along the west coast of North America. Evolutionary Applications 12, 923–939.

Stillman, J.H., 2003. Acclimation Capacity Underlies Susceptibility to Climate Change. Science 301, 65–65.

Storey, J.D., Bass, A.J., Dabney, A., Robinson, D., 2019. qvalue: Q-value estimation for false discovery rate control. R package version 3.2.2.

Strader, M.E., Wong, J.M., Hofmann, G.E., 2020. Ocean acidification promotes broad transcriptomic responses in marine metazoans: a literature survey. Front Zool 17, 7.

Sunday, J.M., Calosi, P., Dupont, S., Munday, P.L., Stillman, J.H., Reusch, T.B.H., 2014. Evolution in an acidifying ocean. Trends in Ecology Evolution 29, 117–125.

Thompson, E.L., Taylor, D.A., Nair, S.V., Birch, G., Coleman, R., Raftos, D.A., 2012. Optimal acclimation periods for oysters in laboratory-based experiments. J Molluscan Stud 78, 304–307.

Thomsen, J., Casties, I., Pansch, C., Körtzinger, A., Melzner, F., 2013. Food availability outweighs ocean acidification effects in juvenile *Mytilus edulis*: laboratory and field experiments. Glob Change Biol 19, 1017–1027.

Thomsen, J., Haynert, K., Wegner, K.M., Melzner, F., 2015a. Impact of seawater carbonate chemistry on the calcification of marine bivalves. Biogeosciences 12, 4209–4220.

Thomsen, J., Stapp, L.S., Haynert, K., Schade, H., Danelli, M., Lannig, G., Wegner, K.M., Melzner, F., 2017. Naturally acidified habitat selects for ocean acidification–tolerant mussels. Science Advances 3, e1602411.

Tufto, J., 2015. Genetic evolution, plasticity, and bet-hedging as adaptive responses to temporally autocorrelated fluctuating selection: A quantitative genetic model. Evolution 69, 2034–2049.

Tufto, J., 2000. The Evolution of Plasticity and Nonplastic Spatial and Temporal Adaptations in the Presence of Imperfect Environmental Cues. The American Naturalist 156, 121–130.

Turner, J.R.G., Williamson, M.H., 1968. Population Size, Natural Selection and the Genetic Load. Nature 218, 700.

Umina, P.A., Weeks, A.R., Kearney, M.R., McKechnie, S.W., Hoffmann, A.A., 2005. A Rapid Shift in a Classic Clinal Pattern in Drosophila Reflecting Climate Change. Science 308, 691–693.

Van der Auwera, G.A., Carneiro, M.O., Hartl, C., Poplin, R., Del Angel, G., Levy-Moonshine, A., Jordan, T., Shakir, K., Roazen, D., Thibault, J., Banks, E., Garimella, K.V., Altshuler, D., Gabriel, S., DePristo, M.A., 2013. From FastQ data to high confidence variant calls: the Genome Analysis Toolkit best practices pipeline. Curr Protoc Bioinformatics 43, 11.10.1-33.

Vargas, C.A., Lagos, N.A., Lardies, M.A., Duarte, C., Manríquez, P.H., Aguilera, V.M., Broitman, B., Widdicombe, S., Dupont, S., 2017. Species-specific responses to ocean acidification should account for local adaptation and adaptive plasticity. Nature Ecology Evolution 1, 0084.

Venn, A.A., Tambutte, E., Holcomb, M., Laurent, J., Allemand, D., Tambutte, S., 2013. Impact of seawater acidification on pH at the tissue-skeleton interface and calcification in reef corals. Proceedings of the National Academy of Sciences 110, 1634–1639.

Ventura, A., Schulz, S., Dupont, S., 2016. Maintained larval growth in mussel larvae exposed to acidified under-saturated seawater. Scientific Reports 6, 23728.

Via, S., Lande, R., 1985. Genotype-Environment Interaction and the Evolution of Phenotypic Plasticity. Evolution 39, 505–522.

Waldbusser, G.G., Brunner, E.L., Haley, B.A., Hales, B., Langdon, C.J., Prahl, F.G., 2013. A developmental and energetic basis linking larval oyster shell formation to acidification sensitivity. Geophysical Research Letters 40, 2171–2176.

Waldbusser, G.G., Hales, B., Langdon, C.J., Haley, B.A., Schrader, P., Brunner, E.L., Gray, M.W., Miller, C.A., Gimenez, I., 2015. Saturation-state sensitivity of marine bivalve larvae to ocean acidification. Nature Climate Change 5, 273–280.

Waldbusser, G.G., Salisbury, J.E., 2014. Ocean Acidification in the Coastal Zone from an Organism's Perspective: Multiple System Parameters, Frequency Domains, and Habitats. Annual Review of Marine Science 6, 221–247.

Whitehead, A., Crawford, D.L., 2006. Variation within and among species in gene expression: raw material for evolution. Molecular Ecology 15, 1197–1211.

Whitlock, M.C. and Lotterhos K.E. 2015. Reliable detection of loci responsible for local adaptation: Inference of a null model through trimming the distribution of F_{ST}. The American Naturalist 186, 24-36.

Wieczynski, D.J., Turner, P.E., Vasseur, D.A., 2018. Temporally Autocorrelated Environmental Fluctuations Inhibit the Evolution of Stress Tolerance. The American Naturalist 191, 195–207.

Williams, J.W., Jackson, S.T., Kutzbach, J.E., 2007. Projected distributions of novel and disappearing climates by 2100 AD. Proc. Natl. Acad. Sci. U.S.A. 104, 5738–5742.

Wittmann, M.J., Bergland, A.O., Feldman, M.W., Schmidt, P.S., Petrov, D.A., 2017. Seasonally fluctuating selection can maintain polymorphism at many loci via segregation lift. PNAS 114, 9932–9941.

Wootton, J.T., Pfister, C.A., 2012. Carbon System Measurements and Potential Climatic Drivers at a Site of Rapidly Declining Ocean pH. PLOS ONE 7, e53396.

Wootton, J.T., Pfister, C.A., Forester, J.D., 2008. Dynamic patterns and ecological impacts of declining ocean pH in a high-resolution multi-year dataset. PNAS 105, 18848-18853.

Wright, R.M., Aglyamova, G.V., Meyer, E., Matz, M.V., 2015. Gene expression associated with white syndromes in a reef building coral, Acropora hyacinthus. BMC Genomics 16, 371.

Yang, B., Pu, F., Li, L., You, W., Ke, C., Feng, D., n.d. Functional analysis of a tyrosinase gene involved in early larval shell biogenesis in *Crassostrea angulata* and its response to ocean acidification. Comparative Biochemistry and Physiology Part B: Biochemistry and

Molecular Biology.

Zhang, C., Xie, L., Huang, J., Chen, L., Zhang, R., 2006. A novel putative tyrosinase involved in periostracum formation from the pearl oyster (*Pinctada fucata*). Biochemical and Biophysical Research Communications 342, 632–639.